Bethe strings in the spin dynamical structure factor of the Mott-Hubbard phase in the one-dimensional fermionic Hubbard model

José M. P. Carmelo[1,2,3,*] and Tilen Čadež[4,*]

[1]*Center of Physics of University of Minho and University of Porto, P-4169-007 Oporto, Portugal*

[2]*Department of Physics, University of Minho, Campus Gualtar, P-4710-057 Braga, Portugal*

[3]*Boston University, Department of Physics, 590 Commonwealth Avenue, Boston, Massachusetts 02215, USA*

[4]*Center for Theoretical Physics of Complex Systems, Institute for Basic Science (IBS), Daejeon 34126, Republic of Korea*

(Received 6 August 2020; revised 9 October 2020; accepted 24 December 2020; published 15 January 2021)

The spectra and role in the spin dynamical properties of bound states of elementary magnetic excitations named Bethe strings that occur in some integrable spin and electronic one-dimensional models have recently been identified and realized in several materials by experiments. Corresponding theoretical studies have usually relied on the one-dimensional spin-1/2 Heisenberg antiferromagnet in a magnetic field. At the isotropic point, it describes the large onsite repulsion U limit of the spin degrees of freedom of the one-dimensional fermionic Hubbard model with one electron per site in a magnetic field h. In this paper we consider the thermodynamic limit and study the effects of lowering the latter quantum problem ratio $u = U/4t$, where t is the first-neighbor transfer integral, on the line-shape singularities in (k, ω)-plane regions at and just above the lower thresholds of the transverse and longitudinal spin dynamical structure factors. The most significant spectral weight contribution from Bethe strings leads to a gapped continuum in the spectrum of the spin dynamical structure factor $S^{+-}(k, \omega)$. Our study focuses on the line shape singularities at and just above the gapped lower threshold of that continuum, which have been identified in experiments. Our results are consistent with the contribution of Bethe strings to $S^{zz}(k, \omega)$ being small at low spin densities and becoming negligible upon increasing that density. Our results provide physically important information about how electron itinerancy affects the spin dynamics.

DOI: 10.1103/PhysRevB.103.045118

I. INTRODUCTION

Recently, there has been a renewed interest in the experimental identification and realization of bound states of elementary magnetic excitations named Bethe strings in materials whose magnetic properties are described by the one-dimensional (1D) spin-1/2 Heisenberg antiferromagnet in magnetic fields [1–5]. This applies to that model isotropic point in the case of experimental studies of $CuCl_2 2N(C_5D_5)$ and $Cu(C_4H_4N_2)(NO_3)_2$ [4–6].

The isotropic spin-1/2 Heisenberg XXX chain describes the spin degrees of freedom of the 1D fermionic Hubbard model's Mott-Hubbard insulator phase in the limit of large onsite repulsion U. That phase is reached at a density of one electron per site. Interesting related physical questions are whether lowering the ratio $u = U/4t$ leads to a description of the spin dynamical properties suitable to spin-chain compounds and how electron itinerancy affects the spin dynamics. Here t is the model first-neighbor transfer integral.

In the case of the 1D fermionic Hubbard model, there are in its exact solution [7–9] two types of Bethe strings described by complex nonreal Bethe-ansatz rapidities. They refer to the model spin and charge degrees of freedom, respectively [10–12]. Here we call them charge and spin n-strings. The nature of their configurations becomes clearer in terms of the *rotated electrons* that are generated from the electrons by a unitary transformation. It is such that $\sigma = \uparrow, \downarrow$ rotated-electron single-site occupancy, rotated-electron double-site occupancy, and rotated-electron no site occupancy are good quantum numbers for the whole $u > 0$ range. (For electrons they are good quantum numbers only for large u.) The corresponding electron - rotated-electron unitary operator is uniquely defined in Ref. [13] by its set of $4^L \times 4^L = 4^{2L}$ matrix elements between *all* 4^L energy eigenstates that span the model's Hilbert space. Here L is the number of sites and lattice length in units of lattice spacing one.

The spin n-strings are for $n > 1$ bound states of a number n of spin-singlet pairs of rotated electrons with opposite spin projection that singly occupy sites. The charge n-strings are for $n > 1$ bound states of n charge η-spin singlet pairs of rotated-electron doubly and unoccupied sites [11,12]. However, energy eigenstates described by only real Bethe-ansatz rapidities do not contain $n > 1$ charge and spin n-strings and are populated by unbound spin-singlet pairs and unbound charge η-spin singlet pairs [11,12]. Ground states are not populated by the latter type of pairs.

Previous studies focused on contributions to the spin dynamical structure factors of the 1D fermionic Hubbard model with one electron per site from excited energy eigenstates described by real Bethe-anstaz rapidities at zero magnetic field [14–16] and in a finite magnetic field [17]. There were also studies of structure factors of the 1D Hubbard model in a magnetic field in the limit of low excitation energy ω [18].

[*]These authors contributed equally to this work.

Our study addresses the 1D Hubbard model with one electron per site in the spin subspace spanned by energy eigenstates without charge η-spin singlet pairs. Some of these energy eigenstates are described by complex nonreal spin Bethe-ansatz rapidities and thus are populated by spin n-strings.

The general goal of this paper is the study of the contribution from spin n-string states to the spin dynamical structure factors of the 1D Hubbard model with one electron per site in a magnetic field h. Our study relies on the dynamical theory introduced for the 1D Hubbard model in Ref. [19]. It has been adapted to the 1D Hubbard model with one electron per site in a spin subspace spanned by energy eigenstates described by real Bethe-ansatz rapidities in Ref. [17]. The studies of this paper use the latter dynamical theory in an extended spin subspace spanned by two classes of energy eigenstates, populated and not populated by spin n-strings, respectively.

In the case of integrable models, the general dynamical theory of Refs. [17,19,20] reaches the same finite-energy dynamical correlation functions expressions as the mobile quantum impurity model scheme of Refs. [21,22]. Such expressions apply at and in the (k, ω)-plane vicinity of the corresponding spectra's lower thresholds'. That for the former dynamical theory and the mobile quantum impurity model scheme such dynamical correlation functions expressions are for arbitrary finite values of the excitation energy indeed the same and account for the same microscopic processes is an issue discussed and confirmed in Appendix A of Ref. [11] and in Ref. [23] for a representative integrable model and several dynamical correlation functions.

The dynamical theory of Refs. [17,19,20] is a generalization to the whole $u = U/4t > 0$ range of the approach used in the $u \rightarrow \infty$ limit in Refs. [24,25]. Momentum dependent exponents in the expressions of spectral functions have also been obtained in Refs. [26,27].

Beyond the studies of Ref. [17], here the application of the dynamical theory is extended to the contribution to the spin dynamical structure factors from excited energy eigenstates populated by spin n-strings.

The theory refers to the thermodynamic limit, in which the expression of the square of the matrix elements of the dynamical structure factors between the ground state and the excited states behind most spectral weight has the general form given in Eq. (D7). It does not provide the precise values of the u and m dependent constant $0 < B_s \leqslant 1$ and u dependent constants $0 < f_l < 1$ where $l = 0, 2, 4$ in that expression. In spite of this limitation, our results provide important physical information on the dynamical structure factors under study.

In the case of the related isotropic spin 1/2 Heisenberg chain in a magnetic field, it is known [4] that the only contribution from excited energy eigenstates populated by spin n-strings that leads to a (k, ω)-plane gapped continuum with a significant amount of spectral wight refers to $S^{+-}(k, \omega)$.

Based on a relation between the level of negativity of the momentum dependent exponents that control the spin dynamical structure factors (k, ω)-plane singularities and the amount of spectral weight existing near them, we confirm that that result applies to the whole $u > 0$ range of the 1D Hubbard model with one electron per site in a magnetic field. However, the contribution of spin n-strings states to $S^{zz}(k, \omega)$ is found to be small at low spin densities and to become negligible upon increasing it beyond a spin density $\tilde{m}$ that decreases upon decreasing u, reading $\tilde{m} = 0$ for $u \rightarrow \infty$ and $\tilde{m} \approx 0.317$ for $u \gg 1$. Finally, the contribution of these states to $S^{-+}(k, \omega)$ is found to be negligible at finite magnetic fields.

The main aim of this paper is the study of the line shape singularities of $S^{+-}(k, \omega)$, $S^{xx}(k, \omega)$, and $S^{zz}(k, \omega)$ at and just above the (k, ω)-plane gapped lower threshold of the spectra associated with spin n-string states. The corresponding singularity peaks have been identified in neutron scattering experiments [4–6].

As a side result, we address the more general problem of the line-shape of the transverse and longitudinal spin dynamical structure factors at finite magnetic field h in the (k, ω)-plane vicinity of singularities at and above the lower thresholds of the spectra of the excited energy eigenstates of the 1D Hubbard model with one electron per site that produce a significant amount of spectral weight. This includes both excited states with and without spin n-strings. The contribution from the latter states leads to the largest amount of spin dynamical structure factors' spectral weight [17].

Our secondary goal is to provide an overall physical picture that includes the relative (k, ω)-plane location of all spectra with a significant amount of spectral weight and accounting for the contributions of different types of states to *both* the gapped and gapless lower threshold singularities that emerge in the spin dynamical structure factors.

The paper is organized as follows. The model and the spin dynamical structure factors are the issues addressed in Sec. II. In Sec. III the (k, ω)-plane spectra of the excited states that lead to most dynamical structure factors' spectral weight are studied, with emphasis on those of the spin n-string states. The line shape at and above the gapped lower thresholds of the n-string states' dynamical structure factors spectra is the main subject of Sec. IV. As a side result, in that section the problem is revisited at and above the lower thresholds of the (k, ω)-plane continua associated with excited states described by real Bethe-anstaz rapidities. In Sec. V the limiting behaviors of the spin dynamical structure factors are addressed. Finally, the discussion and concluding remarks are presented in Sec. VI.

A set of useful results needed for our studies are presented in five Appendices. This includes the selection rules and sum rule provided in Appendix A. In Appendix B the gapless transverse and longitudinal continuum spectra are revisited. The energy gaps between the gapped lower thresholds of the spin n-string states' spectra and the lower (k, ω)-plane continua is the issue addressed in Appendix C. In Appendix D the number and current number deviations and the spectral functionals that control the momentum dependent exponents in the spin dynamical structure factors' expressions are given. Some useful quantities also needed for our studies are defined and provided in Appendix E.

II. THE MODEL AND THE SPIN DYNAMICAL STRUCTURE FACTORS

In this paper we use in general units of lattice constant and Planck constant one. Our study refers to spin subspaces spanned by energy eigenstates for which the number of lattice

sites N_a equals that of electrons $N = N_\uparrow + N_\downarrow$, of which $N_\uparrow$ and $N_\downarrow$ have up- and down-spin projection, respectively.

The Hubbard model with one electron per site at vanishing chemical potential in a magnetic field h under periodic boundary conditions on a 1D lattice of length $L \to \infty$ is given by

$$\hat{H} = t\,\hat{T} + U\,\hat{V}_D + 2\mu_B h\,\hat{S}^z. \tag{1}$$

Here μ_B is the Bohr magneton and for simplicity in $g\mu_B$ we have taken $g = 2$. The operators read

$$\hat{T} = -\sum_{\sigma=\uparrow,\downarrow}\sum_{j=1}^{N}(c^\dagger_{j,\sigma}\,c_{j+1,\sigma} + c^\dagger_{j+1,\sigma}\,c_{j,\sigma}) \quad \text{and}$$

$$\hat{V}_D = \sum_{j=1}^{N}\hat{\rho}_{j,\uparrow}\hat{\rho}_{j,\downarrow} \quad \text{where} \quad \hat{\rho}_{j,\sigma} = c^\dagger_{j,\sigma}\,c_{j,\sigma} - 1/2, \tag{2}$$

where $\hat{T}$ is the kinetic-energy operator in units of t, $\hat{V}_D$ is the electron (or spin $1/2$ atom) on-site repulsion operator in units of U, the operator $c^\dagger_{j,\sigma}$ (and $c_{j,\sigma}$) creates (and annihilates) a spin-projection $\sigma = \uparrow, \downarrow$ electron at lattice site $j = 1, ..., N$, and the electron number operators read $\hat{N} = \sum_{\sigma=\uparrow,\downarrow}\hat{N}_\sigma$ and $\hat{N}_\sigma = \sum_{j=1}^{N}\hat{n}_{j,\sigma} = \sum_{j=1}^{N}c^\dagger_{j,\sigma}\,c_{j,\sigma}$. Moreover, $\hat{S}^z = \sum_{j=1}^{N}\hat{S}^z_j$ is the diagonal generator of the global spin $SU(2)$ symmetry algebra. We denote the energy eigenstate's spin projection by $S^z = -(N_\uparrow - N_\downarrow)/2 \in [-S, S]$, where $S \in [0, N/2]$ denotes their spin.

Our results refer to magnetic fields $0 < h < h_c$ and corresponding spin densities $0 < m < 1$. Here $m = (N_\uparrow - N_\downarrow)/N_a$ and h_c is the critical magnetic field above which there is fully polarized ferromagnetism. The corresponding spin-density curve that relates h and m is given by

$$h(m) = -\frac{\varepsilon^0_s(k_{F\downarrow})}{2\mu_B}\bigg|_{m=1-2k_{F\downarrow}/\pi} \in [0, h_c], \quad \text{where}$$

$$2\mu_B\,h_c = 2\mu_B\,h(m)|_{m=1} = \sqrt{(4t)^2 + U^2} - U, \tag{3}$$

$\varepsilon^0_s(q)$ is the s band energy dispersion, Eq. (E21), whose zero-energy level is shifted relative to that in Eq. (E8), such that $\varepsilon_s(k_{F\downarrow}) = 0$, and the magnetic energy scale $2\mu_B\,h_c$ is associated with the quantum phase transition from the Mott-Hubbard insulator phase to fully polarized ferromagnetism. It defines the corresponding critical magnetic field, $h_c = (\sqrt{(4t)^2 + U^2} - U)/2\mu_B$.

The spin dynamical structure factors studied in this paper in the (k, ω)-plane vicinity of well defined singularities are quantities of both theoretical interest and of interest for comparison with experimentally measurable quantities. They can be written as

$$S^{aa}(k,\omega) = \sum_{j=1}^{N}e^{-ikj}\int_{-\infty}^{\infty}dt\,e^{-i\omega t}\,\langle GS|\hat{S}^a_j(t)\hat{S}^a_j(0)|GS\rangle$$
$$= \sum_{\nu}\left|\langle\nu|\hat{S}^a_k|GS\rangle\right|^2\delta\big(\omega - \omega^{aa}_\nu(k)\big). \tag{4}$$

Here $a = x, y, z$, the spectra read $\omega^{aa}_\nu(k) = (E^{aa}_\nu - E_{GS})$, E^{aa}_ν refers to the energies of the excited energy eigenstates that contribute to the $aa = xx, yy, zz$ dynamical structure factors, E_{GS} is the initial ground state energy, and $\hat{S}^a_k$ are for $a = x, y, z$ the Fourier transforms of the usual local $a = x, y, z$ spin operators $\hat{S}^a_j$, respectively.

Due to the rotational symmetry in spin space, off-diagonal components of the spin dynamical structure factor vanish, $S^{aa'}(k,\omega) = 0$ for $a \neq a'$, and the two transverse components are identical, $S^{xx}(k,\omega) = S^{yy}(k,\omega)$. At zero and finite magnetic field, one has that $S^{zz}(k,\omega) = S^{xx}(k,\omega)$ and $S^{zz}(k,\omega) \neq S^{xx}(k,\omega)$, respectively.

In the transverse case, we often address the problem in terms of the dynamical structure factors $S^{+-}(k,\omega)$ and $S^{-+}(k,\omega)$ in $S^{xx}(k,\omega) = \frac{1}{4}[S^{+-}(k,\omega) + S^{-+}(k,\omega)]$. We rely on the symmetry that exists for the problems under study between the spin density intervals $m \in]-1, 0]$ and $m \in]0, 1[$, such that

$$S^{-+}(k,\omega)|_m = S^{+-}(k,\omega)|_{-m} \quad \text{and}$$
$$S^{+-}(k,\omega)|_m = S^{-+}(k,\omega)|_{-m}$$
$$\text{for} \quad m \in]0, 1[. \tag{5}$$

Hence, we only consider explicitly the spin density interval $m \in]0, 1[$. Since $S^{aa}(k,\omega) = S^{aa}(-k,\omega)$ and the same applies to $S^{+-}(k,\omega)$ and $S^{-+}(k,\omega)$, for simplicity the results of this paper refer to $k > 0$ momenta in the first Brillouin zone, $k \in [0, \pi]$.

Some useful selection rules tell us which classes of energy eigenstates have nonzero matrix elements with the ground state [28]. Such selection rules as well as some useful sum rules are given in Appendix A.

The selection rules in Eq. (A1) reveal that at $h = 0$ and thus $m = 0$ when $S^{zz}(k,\omega) = S^{xx}(k,\omega)$, the longitudinal dynamical structure factor is fully controlled by transitions from the ground state for which $S^z = S = 0$ to excited states with spin numbers $S^z = 0$ and $S = 1$. However, following such rules the transverse dynamical structure factors are controlled by transitions from that ground state to excited states with spin numbers $S^z = \pm 1$ and $S = 1$.

This is different from the case for magnetic fields $0 < h < h_c$ considered in this paper. According to the selection rules, Eq. (A2), the longitudinal dynamical structure factor $S^{zz}(k,\omega) \neq S^{xx}(k,\omega)$ is controlled by transitions from the ground state with spin numbers $S^z = -S$ to excited states with the same spin numbers $S^z = -S$. According to the same selection rules, the dynamical structure factors $S^{+-}(k,\omega)$ and $S^{-+}(k,\omega)$ are controlled by transitions from the ground state with spin numbers $S^z = -S$ to excited states with spin numbers $S^z = -S \pm 1$.

III. DYNAMICAL STRUCTURE FACTORS SPECTRA

Our study of the spin dynamical structure factors relies on the representation of the energy eigenstates suitable to the dynamical theory used in this paper [17]. It involves "quasiparticles" that in this paper we call *sn* particles. Here $n = 1, ..., \infty$ is the number of spin-singlet pairs that describes their internal degrees of freedom.

For $n > 1$ a *sn* particle contains n bound spin-singlet pairs, the integer n being also the length of the corresponding spin n-string. For simplicity, we denote the $s1$ particles by s particles. Their internal degrees of freedom correspond to a single singlet pair. Energy eigenstates that are not populated

and are populated by sn particles with $n > 1$ pairs are described by real and complex nonreal Bethe-anstaz rapidities, respectively.

As mentioned in Sec. I and confirmed in Appendix D, there is a direct relation between the values of the momentum dependent exponents that within the dynamical theory used here control the line shape in the (k, ω)-plane vicinity of the spin dynamical structure factors spectral features and the amount of spectral weight located near them: Negative exponents imply the occurrence of singularities associated with a significant amount of spectral weight in their (k, ω)-plane vicinity.

The use of this criterion reveals that in the present thermodynamic limit and for magnetic fields $0 < h < h_c$, the only significant contribution to $S^{+-}(k, \omega)$ from energy eigenstates populated by sn particles refers to those populated by $N_\downarrow - 2$ s particles and one $s2$ particle. Here $N_\downarrow = N_\downarrow^0 + 1 \in [2, N/2]$ is the excited energy eigenstate's number of down-spin electrons in the case of initial ground states with $N_\downarrow^0 \in [1, N/2 - 1]$.

There is as well a much weaker contribution at small spin densities from states populated by $N_\downarrow - 3$ s particles and one $s3$ particle. Here $N_\downarrow = N_\downarrow^0 + 1 \in [3, N/2]$ for the excited energy eigenstate in the case of initial ground states with $N_\downarrow^0 \in [2, N/2 - 1]$.

In the case of $S^{zz}(k, \omega)$, this refers only to energy eigenstates populated by $N_\downarrow - 2$ s particles and one $s2$ particle. Here $N_\downarrow = N_\downarrow^0 \in [2, N/2]$ both for the excited energy eigenstate and initial ground states. The contribution from such states to $S^{-+}(k, \omega)$ is found to be negligible, since all relevant exponents are both positive and large.

The contribution to $S^{+-}(k, \omega)$ from energy eigenstates populated by $N_\downarrow - 3$ s particles and one $s3$ particle that occurs for small values of the spin density is very weak and is negligible near the (k, ω)-plane singularities to which the analytical expressions obtained in our study refer to. In addition, the latter very weak contributions occur in (k, ω)-plane regions above the gapped lower threshold of the spectrum continuum associated with energy eigenstates populated by $N_\downarrow - 2$ s particles and one $s2$ particle. [The expression of that spectrum is given below in Eq. (6).]

Hence, the energy eigenstates described by complex nonreal Bethe ansatz rapidities considered in our study are populated by $N_\downarrow - 2$ s particles and one $s2$ particle. Such states contain thus a single spin n-string of length $n = 2$. In addition, we account for the contribution from energy eigenstates populated by $N_\downarrow$ s particles that are described by real Bethe ansatz rapidities.

The goal of this section is to introduce the spectra associated with (k, ω)-plane regions that contain most spectral weight of the spin dynamical structure factors. The (k, ω)-plane distribution of such spectra is represented for $S^{+-}(k, \omega)$, $S^{xx}(k, \omega)$, and $S^{zz}(k, \omega)$ in Figs. 1–6, respectively. [In these figures, the spectra of the branch lines studied below are such that the $s2$ and $s2'$ branch lines are represented by blue lines and the $\bar{s}$ and $\bar{s}'$ branch lines by red and green lines, respectively; The $U = 0$ electronic Fermi points $k_{F\downarrow} = \frac{\pi}{2}(1 - m)$ and $k_{F\uparrow} = \frac{\pi}{2}(1 + m)$ define at $u > 0$ the ground-state s band Fermi points $\pm k_{F\downarrow}$ and the s band limiting momentum values $\pm k_{F\uparrow}$.] The spectra displayed in Figs. 1, 3, and 5 refer to spin densities (a)–(c) $m = 0.1$ and (d)–(f) $m = 0.3$ and $u = 0.4, 1.0, 15.0$. In Figs. 2, 4, and 6 they correspond to spin densities (a)–(c) $m = 0.5$ and (d)–(f) $m = 0.8$ and the same set $u = 0.4, 1.0, 15.0$ of u values.

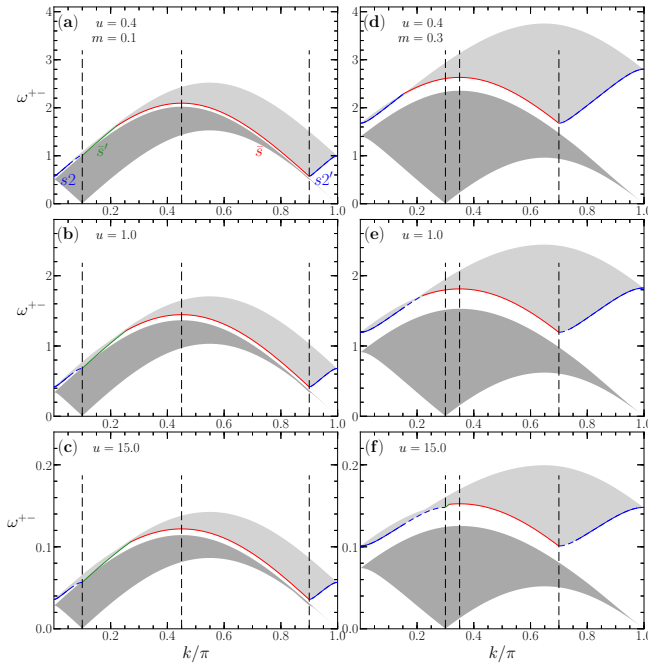

FIG. 1. The two (k, ω)-plane lower and upper continuum regions where for spin densities (a)–(c) $m = 0.1$ and (d)–(f) $m = 0.3$ and $u = 0.4, 1.0, 15.0$ there is in the thermodynamic limit more spectral weight in $S^{+-}(k, \omega)$. The sketch of the (k, ω)-plane distributions represented here and in Figs. 2–6 does not provide information on the relative amount of spectral weight contained within each spectrum's gray continuum. [The three reference vertical lines mark the momenta (a)–(c) $k = k_{F\uparrow} - k_{F\downarrow} = \pi/10$, $k = k_{F\downarrow} = 9\pi/20$, and $k = 2k_{F\downarrow} = 9\pi/10$ and (d)–(f) $k = k_{F\uparrow} - k_{F\downarrow} = 3\pi/10$, $k = k_{F\downarrow} = 7\pi/20$, and $k = 2k_{F\downarrow} = 7\pi/10$, where $k_{F\downarrow} = \frac{\pi}{2}(1 - m)$ and $k_{F\uparrow} = \frac{\pi}{2}(1 + m)$, Eq. (E7).] The lower and upper continuum spectra are associated with excited energy eigenstates without and with spin n-strings, respectively. In the thermodynamic limit, the (k, ω)-plane region between the upper threshold of the lower continuum and the gapped lower threshold of the upper n-string continuum has nearly no spectral weight. In the case of the gapped lower threshold of the spin n-string continuum, the analytical expressions given in this paper refer to near and just above that threshold whose subintervals correspond to branch lines parts represented in the figure by solid and dashed lines. The latter refer to k intervals where the momentum dependent exponents plotted in Figs. 7–10 are negative and positive, respectively. In the former intervals, $S^{+-}(k, \omega)$ displays singularity peaks, seen also in experimental studies of $CuCl_2{\cdot}2N(C_5D_5)$ and $Cu(C_4H_4N_2)(NO_3)_2$ [4–6].

In the cases of $S^{+-}(k, \omega)$ and $S^{xx}(k, \omega)$, the figures show both a lower continuum (k, ω)-plane region whose spectral weight is associated with excited states without spin n-strings and an upper continuum whose spectral weight stems from excited states populated by spin n-strings. In the case of $S^{zz}(k, \omega)$, the contribution to the spectral weight from excited states containing spin n-strings is much weaker than for $S^{+-}(k, \omega)$ and $S^{xx}(k, \omega)$ and does not lead to an upper

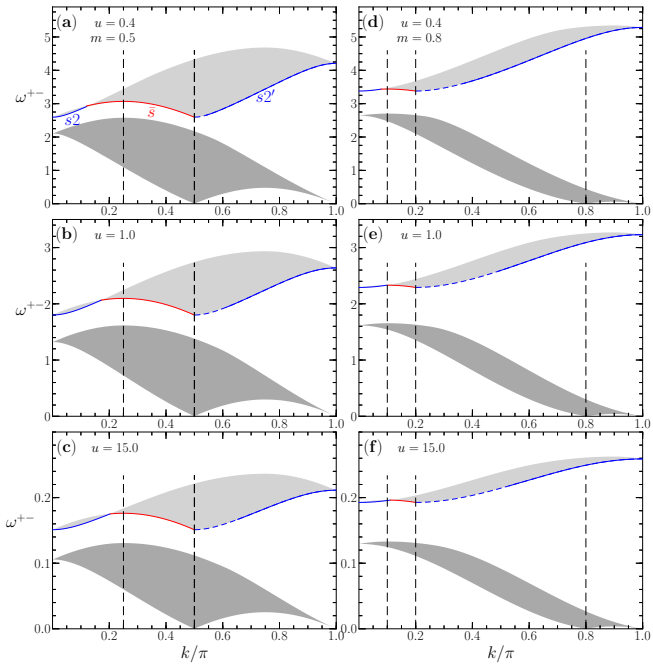

FIG. 2. The same continuum spectra as in Fig. 1 for spin densities (a)–(c) $m = 0.5$ and (d)–(f) $m = 0.8$ and $u = 0.4, 1.0, 15.0$. [The three reference vertical lines mark the momenta (a)–(c) $k = k_{F\downarrow} = \pi/4$ and $k = k_{F\uparrow} - k_{F\downarrow} = 2k_{F\downarrow} = \pi/2$ and (d)–(f) $k = k_{F\downarrow} = \pi/10$, $k = 2k_{F\downarrow} = \pi/5$, and $k = k_{F\uparrow} - k_{F\downarrow} = 4\pi/5$, where $k_{F\downarrow} = \frac{\pi}{2}(1 - m)$ and $k_{F\uparrow} = \frac{\pi}{2}(1 + m)$, Eq. (E7).]

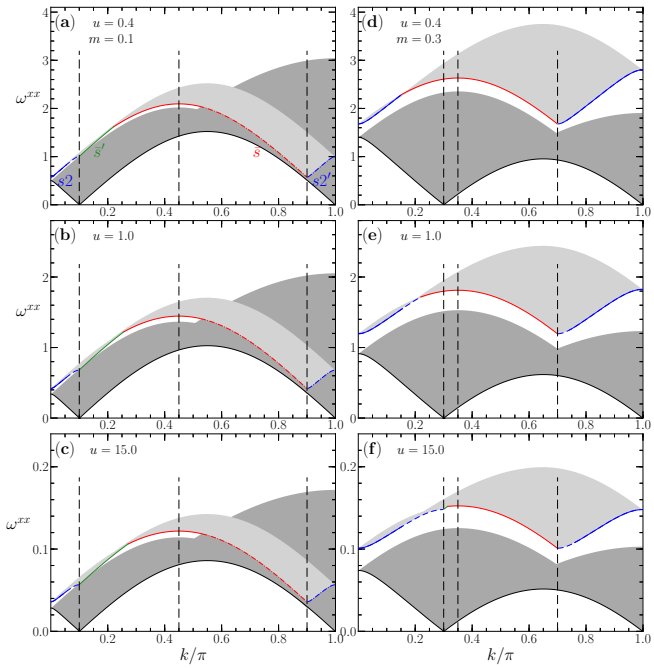

FIG. 3. The two (k, ω)-plane lower and upper continuum regions where for spin densities (a)–(c) $m = 0.1$ and (d)–(f) $m = 0.3$ and $u = 0.4, 1.0, 15.0$ there is in the thermodynamic limit more spectral weight in $S^{xx}(k, \omega)$. The notations are the same as in Fig. 1. [The three reference vertical lines mark the momenta (a)-(c) $k = k_{F\uparrow} - k_{F\downarrow} = \pi/10$, $k = k_{F\downarrow} = 9\pi/20$, and $k = 2k_{F\downarrow} = 9\pi/10$ and (d)–(f) $k = k_{F\uparrow} - k_{F\downarrow} = 3\pi/10$, $k = k_{F\downarrow} = 7\pi/20$, and $k = 2k_{F\downarrow} = 7\pi/10$, where $k_{F\downarrow} = \frac{\pi}{2}(1 - m)$ and $k_{F\uparrow} = \frac{\pi}{2}(1 + m)$, Eq. (E7).] The additional part of the lower continuum relative to that of $S^{+-}(k, \omega)$ in Figs. 1 and 2 stems from the contributions of $S^{-+}(k, \omega)$. As a result, for some k intervals the upper spin n-string continuum overlaps with the lower continuum.

continuum. The gapped lower threshold of such states' spectrum is represented in Figs. 5 and 6 by a (k, ω)-plane line.

Since at finite magnetic fields the contribution to the spectral weight from excited states containing spin n-strings is negligible in the case of $S^{-+}(k, \omega)$ and their lower continuum spectrum was previously studied [17], its (k, ω)-plane spectrum distribution is not shown here. Note though that in Figs. 3 and 4 for $S^{xx}(k, \omega)$, the additional part of the lower continuum relative to that of $S^{+-}(k, \omega)$ represented in Figs. 1 and 2 stems from contributions of $S^{-+}(k, \omega)$. As a result, for small spin densities and some k intervals the upper spin n-string continuum of $S^{xx}(k, \omega)$ overlaps with its lower continuum.

In the case of both $S^{+-}(k, \omega)$ and $S^{zz}(k, \omega)$, there is in the present thermodynamic limit for spin densities $0 < m < 1$ and thus finite magnetic fields $0 < h < h_c$ very little spectral weight between the upper threshold of the lower continuum associated with spin n-string-less excited states and the gapped lower threshold of the spin n-string states' spectra in Figs. 1, 2, 5, and 6, respectively. The same applies to $S^{xx}(k, \omega)$ in the k intervals of Figs. 3 and 4 for which there is a gap between the upper continuum associated with spin n-string states and the lower continuum.

Indeed, in the thermodynamic limit nearly all the small amount of spectral weight associated with the spin n-string-less excited energy eigenstates named in the literature four-spinon states, is contained inside the lower continuum in such figures. This also applies to large finite systems. In the large u limit, in which the spin degrees of freedom of the present model with one electron per site are described by the isotropic spin-1/2 Heisenberg chain, this is so for the latter model both at the isotropic point $\Delta = 1$ (see Fig. 4 of Ref. [29]) and for anisotropy $\Delta < 1$ (see Fig. 1 of Ref. [30]).

Concerning this key issue for our study that the amount of spectral weight in the (k, ω)-plane gap regions shown in Figs. 1–6 is negligible, let us consider the more involved case of $S^{+-}(k, \omega)$. Similar conclusions apply to the simpler problems of the other spin dynamical structure factors. The behavior of spin operators matrix elements between energy eigenstates in the selection rules valid for $u > 0$ and magnetic fields $0 < h < h_c$, Eq. (A2) of Appendix A, has important physical consequences. It implies that the spectral weight stemming from excited energy eigenstates described by only real Bethe-ansatz rapidities existing in finite systems in a (k, ω)-plane region corresponding to the momentum interval $k \in [2k_{F\downarrow}, \pi]$ and excitation energy values ω above the upper threshold of the lower continuum in Figs. 1 and 2, whose spectrum's expression is given in Eq. (B2) of Appendix B, becomes negligible in the present thermodynamic limit for a macroscopic system.

Our thermodynamic limit's study is complementary to and consistent with results obtained by completely different methods for finite-size systems and small yet finite t^2/U [4,28]. The spectral weight located in that (k, ω)-plane region is

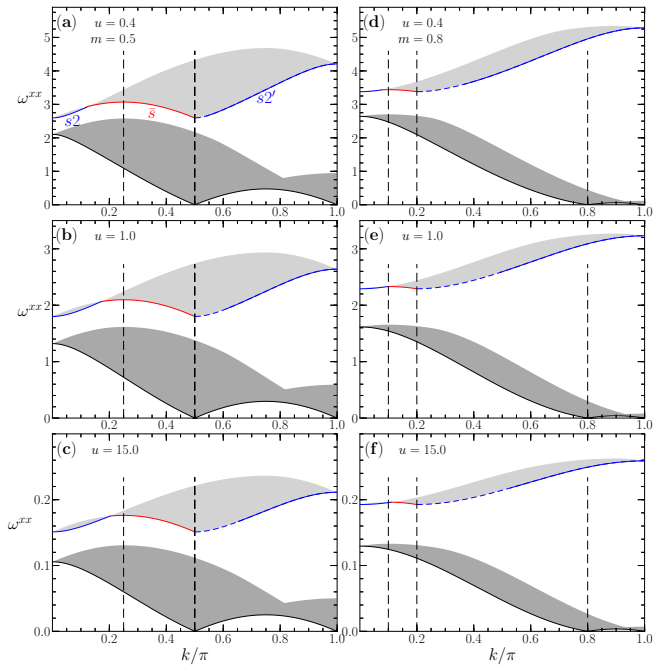

FIG. 4. The same continuum spectra as in Fig. 3 for spin densities (a)–(c) $m = 0.5$ and (d)–(f) $m = 0.8$ and $u = 0.4, 1.0, 15.0$. For such spin densities, there is no overlap between the upper spin n-string continuum and the lower continuum. [The three reference vertical lines mark the momenta (a)–(c) $k = k_{F\downarrow} = \pi/4$ and $k = k_{F\uparrow} - k_{F\downarrow} = 2k_{F\downarrow} = \pi/2$ and (d)–(f) $k = k_{F\downarrow} = \pi/10$, $k = 2k_{F\downarrow} = \pi/5$, and $k = k_{F\uparrow} - k_{F\downarrow} = 4\pi/5$, where $k_{F\downarrow} = \frac{\pi}{2}(1-m)$ and $k_{F\uparrow} = \frac{\pi}{2}(1+m)$, Eq. (E7).]

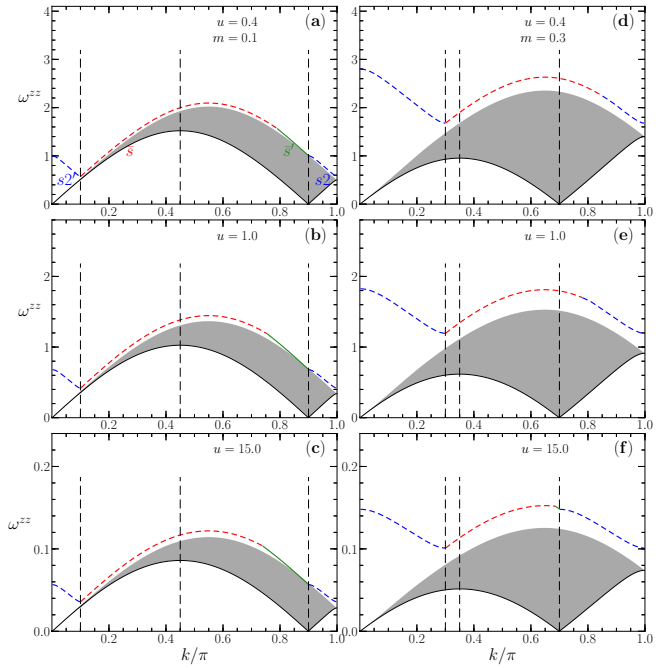

FIG. 5. The (k, ω)-plane continuum region where for spin densities (a)–(c) $m = 0.1$ and (d)–(f) $m = 0.3$ and $u = 0.4, 1.0, 15.0$ there is in the thermodynamic limit more spectral weight in $S^{zz}(k, \omega)$. [The three reference vertical lines mark the momenta (a)–(c) $k = k_{F\uparrow} - k_{F\downarrow} = \pi/10$, $k = k_{F\downarrow} = 9\pi/20$, and $k = 2k_{F\downarrow} = 9\pi/10$ and (d)–(f) $k = k_{F\uparrow} - k_{F\downarrow} = 3\pi/10$, $k = k_{F\downarrow} = 7\pi/20$, and $k = 2k_{F\downarrow} = 7\pi/10$ where $k_{F\downarrow} = \frac{\pi}{2}(1-m)$ and $k_{F\uparrow} = \frac{\pi}{2}(1+m)$, Eq. (E7).] Contributions from excited states containing spin n-strings are much smaller than for $S^{+-}(k, \omega)$ and $S^{xx}(k, \omega)$ and do not lead to an upper continuum. The gapped lower threshold of such states is though displayed. Only when for spin densities $0 < m < \tilde{m}$ where $\tilde{m} = 0$ for $u \to 0$ and $\tilde{m} \approx 0.317$ for $u \gg 1$ that threshold coincides with the $\bar{s}'$ branch line, singularities occur near and just above it. That line is represented as a solid (green) line. In the remaining parts of the gapped lower threshold, which for spin densities $\tilde{m} < m < 1$ means all of it, the momentum dependent exponents are positive and there are no singularities. This reveals there is a negligible amount of spectral weight near such lines.

found to decrease upon increasing the system size [4]. This is confirmed by comparing the spectra represented in the first row frames of Figs. 3(a) and 3(b) of Ref. [4] for two finite-size systems with $N = 320$ and $N = 2240$ spins, respectively, in the case under consideration of the spin dynamical structure factor $S^{+-}(k, \omega)$.

More generally, the selection rules in Eqs. (A1) and (A2) valid for $u > 0$ are behind in the thermodynamic limit nearly all spectral weight generated by transitions to excited energy eigenstates described only by real Bethe-ansatz rapidities being contained in the (k, ω)-plane lower continuum shown in Figs. 1 and 2, whose spectrum is given in Eq. (B2).

Let us consider the (k, ω)-plane spectral weight distributions shown in Fig. 18 of Ref. [28] for $S^{+-}(k, \omega)$, which apply to the half-filled 1D Hubbard model for small yet finite t^2/U. As reported in that reference, due to the interplay of the selections rules given in Eqs. (A1) and (A2) for $h = 0$ and $0 < h < h_c$, respectively, the spectral weight existing between the continuous lower boundary ϵ_{4L} and the upper boundary ϵ_{4U} at $h = 0$ becomes negligible for finite magnetic fields $0 < h < h_c$. In addition, the spectral weight existing between the continuous lower boundary ϵ_{5L} and the upper boundary ϵ_{5U} for small finite-size systems, becomes negligible in the thermodynamic limit for a macroscopic system. This is indeed due to the selection rules, Eq. (A2), as discussed in that reference, which for the 1D Hubbard model with one fermion per site are valid for $u > 0$. As also reported in Ref. [28], only the spectral weight below the continuous lower boundary $\epsilon_{5L}(q)$, located in the (k, ω)-plane between the lower boundary ϵ_{6L} and the upper boundary ϵ_{6U} has a significant amount of spectral weight.

This refers to the (k, ω)-plane region where, according to the analysis of Ref. [28], for magnetic fields $0 < h < h_c$ a macroscopic system has nearly the whole spectral weight stemming from transitions to excited energy eigenstates described by only real Bethe-ansatz rapidities. Consistently with the spectral weight in the present gap region being negligible, the (k, ω)-plane between the continuous lower boundary ϵ_{6L} and the upper boundary ϵ_{6U} in Fig. 18 of that reference corresponds precisely to the lower continuum shown in Figs. 1 and 2, whose spectrum is provided in Eq. (B2).

Besides the s and $s2$ particles, there is in the present spin subspace a c particle branch of Bethe ansatz quantum numbers associated with the charge degrees of freedom [17,19]. However, it refers to a corresponding full c momentum band

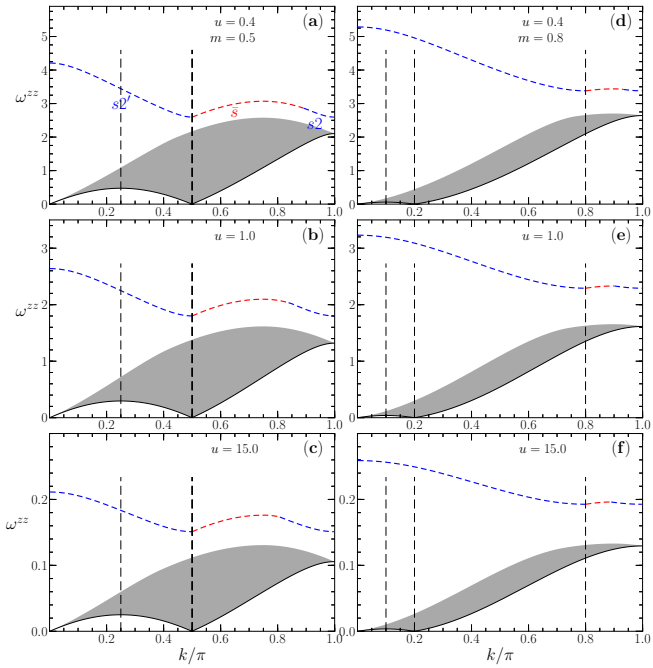

FIG. 6. The same continuum spectra as in Fig. 5 for spin densities (a)–(c) $m = 0.5$ and (d)–(f) $m = 0.8$ and $u = 0.4, 1.0, 15.0$. For these spin densities, there are no singularities near the gapped lower threshold of the spin n-string excited states. For these spin densities the contribution of such states to $S^{zz}(k,\omega)$ are actually negligible over the whole (k,ω) plane. [The three reference vertical lines mark the momenta (a)–(c) $k = k_{F\downarrow} = \pi/4$ and $k = k_{F\uparrow} - k_{F\downarrow} = 2k_{F\downarrow} = \pi/2$ and (d)–(f) $k = k_{F\downarrow} = \pi/10$, $k = 2k_{F\downarrow} = \pi/5$, and $k = k_{F\uparrow} - k_{F\downarrow} = 4\pi/5$, where $k_{F\downarrow} = \frac{\pi}{2}(1-m)$ and $k_{F\uparrow} = \frac{\pi}{2}(1+m)$, Eq. (E7).]

that does not contribute to the spin dynamical properties. Its only contribution to the spin problem studied in this paper stems from microscopic momentum shifts $-\frac{\pi}{L}$ or $\frac{\pi}{L}$ of all the corresponding c band N discrete momentum values $q_j = \frac{2\pi}{L} I^c_j$. Here $I^c_j = 0, \pm 1, \pm 2, ...$ for $N_s + N_{s2}$ even and $I^c_j = \pm 1/2, \pm 3/2, \pm 5/2, ...$ for $N_s + N_{s2}$ odd are the Bethe-ansatz c band quantum numbers in Eq. (E6). Those lead to macroscopic momentum variations $-\pi$ or π, respectively, upon changes in the value of the numbers of s and $s2$ particles, according to the boundary conditions given in Eq. (E6).

The line shape near the gapped lower threshold of the $S^{+-}(k,\omega)$'s continuum spectrum represented in Figs. 1 and 2 is controlled by the above class of excited states that are generated by the occupancy configurations of both $N_s = N_\downarrow - 2s$ particles over $N_\uparrow$ discrete momentum values $q_j = \frac{2\pi}{L} I^s_j$ and one $s2$ particle over $N_\uparrow - N_\uparrow + 1$ discrete momentum values $q_j = \frac{2\pi}{L} I^{s2}_j$. Here (i) $I^s_j = 0, \pm 1, \pm 2, ...$ for $N_\uparrow$ odd and $I^s_j = \pm 1/2, \pm 3/2, \pm 5/2, ...$ for $N_\uparrow$ even and (ii) $I^{s2}_j = 0, \pm 1, \pm 2, ...$ for $N_{s2} = 1$ are the Bethe-ansatz s and $s2$ band quantum numbers, respectively, in Eq. (E6). However, the line shape in the vicinity of the lower threshold of the $S^{+-}(k,\omega)$'s lower continuum spectrum in the same figures is controlled by excited energy eigenstates described by real Bethe ansatz rapidities. Those are described by occupancy configurations of $N_s = N_\downarrow$ s particles over $N_\uparrow$ discrete momentum values $q_j = \frac{2\pi}{L} I^s_j$.

The Bethe-ansatz equations and quantum numbers whose occupancy configurations generate the energy eigenstates that span the spin subspaces used in our studies are given in Eqs. (E1) and (E2) in functional form, in terms of s and $s2$ bands momentum distributions. Those describe the momentum occupancy configurations that generate such states.

As further discussed in Appendix D, ground states are for spin densities $0 < m < 1$ only populated by the $N_c = N$ nondynamical c particles and $N_s = N_\downarrow s$ particles that symmetrically or quasi-symmetrically occupy the s band, which also contains $N^h_s = N_\uparrow - N_\downarrow$ holes.

The gapped upper spectrum in Figs. 1 and 2 associated with the (k,ω)-plane continuum of $S^{+-}(k,\omega)$ that stems from transitions from the ground state to excited energy eigenstates populated by $N_s = N_\downarrow - 2$ s particles and one $s2$ particle is given by

$$\omega^{+-}_\Delta(k) = -\varepsilon_s(q_1) + \varepsilon_{s2}(q_2),$$
$$\text{where} \quad k = \iota k_{F\downarrow} - q_1 + q_2 \quad \text{and} \quad \iota = \pm 1$$
$$\text{for} \quad q_1 \in [-k_{F\downarrow}, k_{F\downarrow}] \quad \text{and}$$
$$q_2 \in [0, (k_{F\uparrow} - k_{F\downarrow})] \quad \text{for} \quad \iota = 1$$
$$q_2 \in [-(k_{F\uparrow} - k_{F\downarrow}), 0] \quad \text{for} \quad \iota = -1. \qquad (6)$$

This spectrum has two branches corresponding to $\iota = \pm 1$ such that,

$$k = k_{F\downarrow} - q_1 + q_2 \in [0, \pi]$$
$$k = -k_{F\downarrow} - q_1 + q_2 \in [-\pi, 0]. \qquad (7)$$

In Eq. (6) and other expressions of spin dynamical structure factors' spectra given below and in Appendices B and C, $\varepsilon_s(q)$ and $\varepsilon_{s2}(q)$ are the s and $s2$ band energy dispersions, respectively, defined by Eqs. (E8), (E9), and (E11)–(E20). Limiting behaviors of such dispersions and corresponding s and $s2$ group velocities that provide useful information on the corresponding spin dynamical structure factors' spectra momentum, spin density, and interaction dependencies are provided in Eqs. (E22)–(E38).

We denote by $\Delta^{ab}(k)$ where $ab = +-, xx, zz$ the spectra of the spin n-string excited states' gapped lower thresholds of $S^{ab}(k,\omega)$. They play an important role in our study, since for some k intervals there are singularities at and just above them.

For $S^{+-}(k,\omega)$, $S^{xx}(k,\omega)$, and $S^{zz}(k,\omega)$ such gapped thresholds have a different form for two spin density intervals $m \in]0, \tilde{m}]$ and $m \in [\tilde{m}, 1[$, respectively. Here $\tilde{m}$ is a u dependent spin density at which the following equality holds:

$$W_{s2}|_{m=\tilde{m}} = -\varepsilon_s(2k_{F\downarrow} - k_{F\uparrow})|_{m=\tilde{m}}. \qquad (8)$$

From the use of the $\varepsilon_{s2}(0)$'s expression given in Eq. (E24), the $s2$ energy bandwidth W_{s2} appearing here can be expressed as $W_{s2} = 4\mu_B h - \varepsilon_{s2}(0)$. The spin density $\tilde{m}$ is a continuous increasing function of u that in the $u \to 0$ and $u \gg 1$ limits reads

$$\lim_{u\to 0} \tilde{m} = 0 \quad \text{and} \quad \lim_{u\gg 1} \tilde{m} \approx 0.317. \qquad (9)$$

Momenta involving a related momentum $\tilde{k}$ separate parts of the gapped lower threshold spectra of $S^{+-}(k,\omega)$, $S^{xx}(k,\omega)$, and $S^{zz}(k,\omega)$ that refer to different types of k dependencies.

At $k = \tilde{k}$ the following relations that define it hold:

$$\begin{aligned} W_{s2} &= \varepsilon_s(k_{F\uparrow} - \tilde{k}) - \varepsilon_s(k_{F\downarrow} - \tilde{k}) \\ &\quad \text{for} \quad \tilde{k} \geqslant (k_{F\uparrow} - k_{F\downarrow}) \quad \text{and} \quad m \in [0, \tilde{m}], \\ W_{s2} &= 4\mu_B\, h - \varepsilon_{s2}(\tilde{k}) - \varepsilon_s(k_{F\downarrow} - \tilde{k}) \\ &\quad \text{for} \quad \tilde{k} \leqslant (k_{F\uparrow} - k_{F\downarrow}) \quad \text{and} \quad m \in [\tilde{m}, 1[. \end{aligned} \tag{10}$$

The momentum $\tilde{k}$ is given by $\tilde{k} = (k_{F\uparrow} - k_{F\downarrow})$ at $m = \tilde{m}$.

The spectra of the transverse gapped lower thresholds are such that

$$\Delta^{xx}(k) = \Delta^{+-}(k) \quad \text{for} \quad k \in [0, \pi]. \tag{11}$$

(The equality $\Delta^{-+}(k) = \Delta^{+-}(k)$ also holds, yet as reported above the amount of $S^{-+}(k, \omega)$'s spectral weight produced by excited n-string states is negligible in the thermodynamic limit and finite magnetic fields.) The spectrum of the longitudinal gapped lower threshold is also related to $\Delta^{+-}(k)$ as follows:

$$\Delta^{zz}(k) = \Delta^{+-}(\pi - k) \quad \text{for} \quad k \in [0, \pi]. \tag{12}$$

For smaller spin densities $m \in [0, \tilde{m}]$, the spectrum $\Delta^{+-}(k)$ is given by

$$\begin{aligned} \Delta^{+-}(k) &= \varepsilon_{s2}(k) \quad \text{for} \quad k \in [0, (k_{F\uparrow} - k_{F\downarrow})] \\ &= 4\mu_B\, h - \varepsilon_s(k_{F\uparrow} - k) \quad \text{for} \quad k \in [(k_{F\uparrow} - k_{F\downarrow}), \tilde{k}] \\ &= 4\mu_B\, h - W_{s2} - \varepsilon_s(k_{F\downarrow} - k) \quad \text{for} \quad k \in [\tilde{k}, 2k_{F\downarrow}] \\ &= \varepsilon_{s2}(k - 2k_{F\downarrow}) \quad \text{for} \quad k \in [2k_{F\downarrow}, \pi]. \end{aligned} \tag{13}$$

For larger spin densities $m \in [\tilde{m}, 1[$, that spectrum is slightly different and reads

$$\begin{aligned} \Delta^{+-}(k) &= \varepsilon_{s2}(k) \quad \text{for} \quad k \in [0, \tilde{k}[\\ &= 4\mu_B\, h - W_{s2} - \varepsilon_s(k_{F\downarrow} - k) \\ &\quad \text{for} \quad k \in]\tilde{k}, 2k_{F\downarrow}] \\ &= \varepsilon_{s2}(k - 2k_{F\downarrow}) \quad \text{for} \quad k \in [2k_{F\downarrow}, \pi]. \end{aligned} \tag{14}$$

The expressions of the previously studied two-parametric transverse gapless spectra [17] $\omega^{-+}(k)$ and $\omega^{+-}(k)$, whose superposition gives $\omega^{xx}(k)$, and that of the longitudinal gapless spectrum $\omega^{zz}(k)$ that [except for $\omega^{-+}(k)$] refer to the lower continua in Figs. 1–6, are given in Eqs. (B1)–(B3). The corresponding excited energy eigenstates are described by real Bethe-ansatz rapidities. The expressions of the one-parametric spectra of their upper thresholds $\omega_{ut}^{-+}(k)$, $\omega_{ut}^{+-}(k)$, $\omega_{ut}^{xx}(k)$, and $\omega_{ut}^{zz}(k)$ and lower thresholds $\omega_{lt}^{-+}(k)$, $\omega_{lt}^{+-}(k)$, $\omega_{lt}^{xx}(k)$, and $\omega_{lt}^{zz}(k)$ are also provided in Appendix B.

We consider the following energy gaps:

$$\begin{aligned} \Delta_{\rm gap}^{+-}(k) &= \Delta^{+-}(k) - \omega_{ut}^{+-}(k) \geqslant 0, \\ \Delta_{\rm gap}^{xx}(k) &= \Delta^{xx}(k) - \omega_{ut}^{xx}(k), \\ \Delta_{\rm gap}^{zz}(k) &= \Delta^{zz}(k) - \omega_{ut}^{zz}(k) \geqslant 0, \end{aligned} \tag{15}$$

where

$$\begin{aligned} \Delta_{\rm gap}^{xx}(k) &= \Delta^{+-}(k) - \omega_{ut}^{+-}(k) \quad \text{for} \quad k \in \left[0, k_{ut}^{xx}\right], \\ \Delta_{\rm gap}^{xx}(k) &= \Delta^{+-}(k) - \omega_{ut}^{-+}(k) \quad \text{for} \quad k \in \left[k_{ut}^{xx}, \pi\right], \end{aligned} \tag{16}$$

and

$$\Delta_{\rm gap}^{zz}(k) = \Delta_{\rm gap}^{+-}(\pi - k) \quad \text{for} \quad k \in [0, \pi]. \tag{17}$$

The momentum $k_{ut}^{xx} > k_{F\uparrow} - k_{F\downarrow}$ in Eq. (16) is that at which the equality $\omega_{ut}^{-+}(k_{ut}^{xx}) = \omega_{ut}^{+-}(k_{ut}^{xx})$ holds. In the thermodynamic limit and for the k intervals for which such energy gaps are positive, there is a negligible amount of spectral weight in their corresponding (k, ω)-plane regions. This justifies why here we named them gaps.

The upper threshold spectra $\omega_{ut}^{-+}(k)$, $\omega_{ut}^{+-}(k)$, $\omega_{ut}^{xx}(k)$, $\omega_{ut}^{zz}(k)$ in Eqs. (15)–(17) are given in Eqs. (B4)–(B7). The spectra $\omega_{ut}^{+-}(k)$, $\omega_{ut}^{xx}(k)$, and $\omega_{ut}^{zz}(k)$ refer to the upper thresholds of the lower continua in Figs. 1–6, respectively.

As confirmed from analysis of Figs. 1–6, one has that $\Delta_{\rm gap}^{+-}(k) \geqslant 0$ and $\Delta_{\rm gap}^{zz}(k) \geqslant 0$, whereas $\Delta_{\rm gap}^{xx}(k)$ is negative for some k intervals. Specifically,

$$\begin{aligned} \Delta_{\rm gap}^{xx}(k) \leqslant 0 \quad &\text{for} \\ k \in [\bar{k}_0, \pi] \quad &\text{for} \quad m \in]0, \bar{m}_0], \\ k \in [\bar{k}_0, \bar{k}_1] \quad &\text{for} \quad m \in]\bar{m}_0, \bar{m}]. \end{aligned} \tag{18}$$

The values of the spin densities $\bar{m}_0$ and $\bar{m} > \bar{m}_0$ increase and decrease upon increasing u, their limiting values being

$$\begin{aligned} \lim_{u\to 0} \bar{m}_0 &= \frac{2}{\pi} \arcsin\left(\frac{1}{3}\right) \approx 0.216, \\ \lim_{u\to 0} \bar{m} &= \frac{2}{\pi} \arctan\left(\frac{1}{2}\right) \approx 0.295, \\ \lim_{u\gg 1} \bar{m}_0 &\approx 0.239 \quad \text{and} \quad \lim_{u\gg 1} \bar{m} \approx 0.276. \end{aligned} \tag{19}$$

The momenta $\bar{k}_0$ and $\bar{k}_1$ also appearing in Eq. (18) are such $k_{ut}^{xx} \leqslant \bar{k}_0 \leqslant \bar{k}_1$, and $\bar{k}_0 \leqslant \bar{k}_1 \leqslant \pi$. The equality, $\bar{k}_0 = \bar{k}_1$, holds at $m = \bar{m}$. At that spin density the momentum $\bar{k}_0 = \bar{k}_1$ is very little u dependent. It is given by $\bar{k}_0 = \bar{k}_1 = 2k_{F\downarrow}$ in the $\lim_{u\to 0}$ limit and for $u \gg 1$ it reaches a value very near and just above $2k_{F\downarrow}$.

For $m \in]0, \bar{m}]$ and the k intervals in Eq. (18), the $S^{xx}(k, \omega)$'s expressions in the vicinity of that factor gapped lower threshold obtained in this paper are not valid because $\Delta_{\rm gap}^{xx}(k) < 0$. However, the $S^{+-}(k, \omega)$ and $S^{zz}(k, \omega)$'s expressions in the vicinity of their gapped lower thresholds considered in the following are valid for all k intervals, since the energy gaps $\Delta_{\rm gap}^{+-}(k)$ and $\Delta_{\rm gap}^{zz}(k)$ are finite and positive for $0 < m < 1$ and $u > 0$.

In Appendix C, limiting values of the energy gaps considered here and their values at some specific momenta are provided.

IV. THE LINE SHAPE AT AND NEAR THE SPIN DYNAMICAL STRUCTURE FACTORS' SINGULARITIES

The spin dynamical structure factors' singularities studied in this paper occur at and just above spectral lines that within the dynamical theory of Refs. [17,19] are called branch lines. Such lines coincide with well defined k intervals of the (k, ω)-plane lower thresholds of both the spectra of excited states populated and not populated by spin n-strings, respectively, plotted in Figs. 1–6.

In the case of the contribution from spin n-string states, the dynamical theory line shape expressions are valid provided there is no or nearly no spectral weight just below the corresponding gapped lower thresholds. In the present

thermodynamic limit, the amount of spectral weight just below such thresholds either vanishes or is extremely small. In the latter case, the very weak coupling to it leads to a higher order contribution to the line shape expressions given in the following that can be neglected in that limit.

In the case of the lower (k, ω)-plane spectrum continua in Figs. 1–6 of excited states not populated by spin n-strings and thus described by real Bethe-ansatz rapidities, there is no spectral weight below the corresponding lower thresholds. This ensures that the expressions of the spin dynamical structure factors at and just above such thresholds are exact.

The momentum interval $k \in [0, \pi]$ of the gapped lower thresholds of spectra of spin n-string states is divided in several subintervals that refer to a set of branch lines called $s2$, $\bar{s}$, $\bar{s}'$, and $s2'$ branch line. The corresponding excited states are populated by $N_\downarrow - 2$ s particles and one $s2$ particle. The lower thresholds of the spectra associated with excited states populated by $N_\downarrow$ s particles, either correspond to a single s branch line or to two sections of such a line.

The $\bar{s}$, $\bar{s}'$, and s branch lines refer to k ranges corresponding to a maximum s band q interval $q \in [-(k_{F\downarrow} - \delta q_s), (k_{F\downarrow} - \delta q_s)]$ in the case of s hole creation and to a maximum s band q interval such that $|q| \in [(k_{F\downarrow} + \delta q_s), k_{F\uparrow}]$ in case of s particle creation. Here δq_s such that $\delta q_s / k_{F\uparrow} \ll 1$ for $0 < m < 1$ is for the different branch lines either very small or vanishes in the thermodynamic limit.

In the very small k intervals corresponding to the s band intervals $q \in [-k_{F\downarrow}, -(k_{F\downarrow} - \delta q_s)]$ and $q \in [(k_{F\downarrow} - \delta q_s), k_{F\downarrow}]$ the line shape of the spin dynamical structure factors is different, as given in Ref. [17]. (See Eqs. (128)–(133) of Ref. [17].)

Similarly, in the case of the (k, ω)-plane vicinity of the $s2$ and $s2'$ branch lines, which are part of the gapped lower thresholds, the line shape expressions obtained in this paper are valid in k ranges corresponding to $s2$ band maximum intervals $q \in [-(k_{F\uparrow} - k_{F\downarrow} - \delta q_{s2}), 0]$ or $q \in [0, (k_{F\uparrow} - k_{F\downarrow} - \delta q_{s2})]$. Here δq_{s2} such that $\delta q_{s2}/(k_{F\uparrow} - k_{F\downarrow}) \ll 1$ is for $0 < m < 1$ very small and may vanish in the thermodynamic limit. (And again, the spin dynamical structure factors expressions are different and known for $q \in [-(k_{F\uparrow} - k_{F\downarrow}), -(k_{F\uparrow} - k_{F\downarrow} - \delta q_{s2})]$ and $q \in [(k_{F\uparrow} - k_{F\downarrow} - \delta q_{s2}), (k_{F\uparrow} - k_{F\downarrow})]$ yet are not of interest for this study.)

In the present thermodynamic limit, the above s band momentum intervals are thus represented in the following as $q \in]-k_{F\downarrow}, k_{F\downarrow}[$ and $|q| \in]k_{F\downarrow}, k_{F\uparrow}]$ and the $s2$ band momentum intervals by $q \in]-(k_{F\uparrow} - k_{F\downarrow}), 0]$ or $q \in [0, (k_{F\uparrow} - k_{F\downarrow})[$.

Around the specific momentum values where along a gapped lower threshold or a lower threshold two neighboring branch lines or branch line sections cross, there are small momentum widths where the corresponding lower threshold refers to a boundary line that connects the two branch lines or branch line sections under consideration.

In the thermodynamic limit, such momentum intervals are in general negligible and the corresponding small spectra deviations are not visible in the spectra plotted in Figs. 1–6. In the cases they are small yet more extended, the two branch lines or branch line sections run very near the lower threshold and there is very little spectral weight between it and such lines. In this case, the singularities on the two branch lines or branch line sections remain the dominant spectral feature.

We again account for such negligible effects by replacing [and] by]and[, respectively, at the k limiting values that separate lower thresholds' k intervals associated with two neighboring branch lines or branch line sections.

A. The line shape near the $s2$, $\bar{s}$, $\bar{s}'$, and $s2'$ branch lines (gapped lower thresholds)

Here we study the line shape at and just above the gapped lower thresholds of the spectra plotted in Figs. 1–6 of the transverse and longitudinal structure factors. In the case of $S^{xx}(k, \omega)$, this refers to k intervals for which $\Delta^{xx}_{\rm gap}(k) > 0$ and thus different from those given in Eq. (18). In Appendix D, the number and current number deviations as well as the spectral functionals that control the expressions of the spin dynamical structure factors given below are provided.

The line shape near the gapped lower thresholds has the following general form,

$$S^{ab}(k, \omega) = C^{\Delta}_{ab}\big[\omega - \Delta^{ab}_{\beta}(k)\big]^{\zeta^{ab}_{\beta}(k)} \quad \text{for} \quad [\omega - \Delta^{ab}_{\beta}(k)] \geqslant 0, \quad \text{where} \quad \beta = s2, \bar{s}, \bar{s}', s2', \quad \text{and} \quad ab = +-, xx, zz \quad \big(\text{valid when } \Delta^{ab}_{\rm gap} > 0\big). \tag{20}$$

Here C^{Δ}_{ab} is a constant that has a fixed value for the k and ω ranges associated with small values of the energy deviation $[\omega - \Delta^{ab}_{\beta}(k)] \geqslant 0$, the gapped lower threshold spectra $\Delta^{ab}_{\beta}(k)$ are given in Eqs. (11)–(14) and the index $\beta = s2, \bar{s}, \bar{s}', s2'$ labels branch lines or branch line sections that are part of the gapped lower thresholds in some specific k intervals defined in the following.

The branch-line exponents that appear in Eq. (20) have the following general form:

$$\zeta^{aa}_{\beta}(k) = -1 + \sum_{\iota=\pm 1} \Phi^2_{\iota}(q) \quad \text{for} \quad \beta = s2, \bar{s}, \bar{s}', s2', s, \tag{21}$$

where the spectral functionals $\Phi_\iota(q)$ suitable to each type of branch line are given in Eqs. (D9)–(D12). [This also includes the s branch lines that define the lower thresholds of the lower continua in Figs. 1–6. Their exponents are also of form, Eq. (21), and appear in the spin dynamical structure factors' general expression provided below in Eq. (33).]

As mentioned above, the amount of spectral weight below the gapped thresholds either vanishes or is very small. In the latter case, the very weak coupling to it leads to a higher order contribution to the line shapes given in Eqs. (20) and (21) that can be neglected in the present thermodynamic limit.

The relation of the excitation momentum k to the s band momentum q or $s2$ band momentum q that appear in the Φ_ι's argument in the general exponent expression, Eq. (21), is branch-line dependent. Hence, it is useful to revisit the expressions of the spectra of the gapped lower thresholds, Eqs. (11)–(14) and (12), for each of their branch lines or branch line sections, including information on the relation between the physical excitation momentum k and the s or $s2$ bands momenta q. The corresponding expressions are given for the k intervals for which the dynamical structure factor's expression is of the form, Eq. (20), which implies

replacements of [and] by]and[, respectively, in the limits of such intervals.

In the case of $S^{+-}(k,\omega)$, the gapped lower threshold spectrum $\Delta^{+-}(k)$ is divided in the following branch-line intervals,

$$\begin{aligned}
&\Delta^{+-}_{s2}(k) = \varepsilon_{s2}(k) \quad \text{and} \quad k = q, \\
&\text{where} \quad k \in]0, (k_{F\uparrow} - k_{F\downarrow})[\text{and} \\
&\qquad q \in]0, (k_{F\uparrow} - k_{F\downarrow})[\\
&\qquad \text{for} \quad m \in]0, \tilde{m}] \\
&\quad \text{and} \quad k \in]0, \tilde{k}[\text{and} \quad q \in [0, \tilde{k}[\\
&\qquad \text{for} \quad m \in [\tilde{m}, 1[, \qquad (22)
\end{aligned}$$

$$\begin{aligned}
&\Delta^{+-}_{\bar{s}'}(k) = 4\mu_B\, h - \varepsilon_s(k_{F\uparrow} - k) \quad \text{and} \\
&\qquad k = k_{F\uparrow} - q, \\
&\text{where} \quad k \in](k_{F\uparrow} - k_{F\downarrow}), \tilde{k}[\text{and} \\
&\qquad q \in](k_{F\uparrow} - \tilde{k}), k_{F\downarrow}[\\
&\qquad \text{for} \quad m \in]0, \tilde{m}], \qquad (23)
\end{aligned}$$

$$\begin{aligned}
&\Delta^{+-}_{\bar{s}}(k) = 4\mu_B\, h - W_{s2} - \varepsilon_s(k_{F\downarrow} - k) \\
&\quad \text{and} \quad k = k_{F\downarrow} - q, \\
&\text{where} \quad k \in [\tilde{k}, 2k_{F\downarrow}[\text{and} \\
&\qquad q \in] - k_{F\downarrow}, (k_{F\downarrow} - \tilde{k})[\\
&\qquad \text{for} \quad m \in]0, \tilde{m}] \\
&\quad \text{and} \quad k \in]\tilde{k}, 2k_{F\downarrow}[\text{and} \\
&\qquad q \in] - k_{F\downarrow}, (k_{F\downarrow} - \tilde{k})[\\
&\qquad \text{for} \quad m \in [\tilde{m}, 1[, \qquad (24)
\end{aligned}$$

and

$$\begin{aligned}
&\Delta^{+-}_{s2'}(k) = \varepsilon_{s2}(k - 2k_{F\downarrow}) \quad \text{and} \quad k = 2k_{F\downarrow} + q \\
&\text{where} \quad k \in]2k_{F\downarrow}, \pi[\text{and} \\
&\qquad q \in]0, (k_{F\uparrow} - k_{F\downarrow})[\\
&\qquad \text{for} \quad m \in]0, 1[. \qquad (25)
\end{aligned}$$

The corresponding k dependent exponents of general form, Eq. (21), that appear in the expression, $S^{+-}(k,\omega) = C^{\Delta}_{+-}[\omega - \Delta^{+-}_{\beta}(k)]^{\zeta^{+-}_{\beta}(k)}$, Eq. (20) for $ab = +-$ and $\beta = s2, \bar{s}', \bar{s}, s2'$, are given by

$$\begin{aligned}
&\zeta^{+-}_{s2}(k) = -1 + \sum_{\iota=\pm 1}\left[-\frac{\iota}{2\xi^1_{ss}} + \Phi_{s,s2}(\iota k_{F\downarrow}, q)\right]^2 \\
&\qquad \text{for} \quad q = k \quad \text{and} \\
&\quad k \in]0, (k_{F\uparrow} - k_{F\downarrow})[\quad \text{for} \quad m \in]0, \tilde{m}] \\
&\quad k \in]0, \tilde{k}[\quad \text{for} \quad m \in [\tilde{m}, 1[, \\
&\zeta^{+-}_{\bar{s}'}(k) = -1 + \sum_{\iota=\pm 1}\left[-\frac{\xi^1_{ss}}{2} - \Phi_{s,s}(\iota k_{F\downarrow}, q)\right]^2 \\
&\qquad \text{for} \quad q = k_{F\uparrow} - k \quad \text{and} \\
&\quad k \in](k_{F\uparrow} - k_{F\downarrow}), \tilde{k}[\quad \text{for} \quad m \in]0, \tilde{m}],
\end{aligned}$$

TABLE I. The momentum $k > 0$ and s and $s2$ bands number and current number deviations defined in Appendix D for $+-$ transverse spin excitations populated by one $s2$ particle and thus described by both real and complex nonreal rapidities in the case of the $s2$ branch line, $\bar{s}'$ branch line, $\bar{s}$ branch line, and $s2'$ branch line that for the momentum intervals given in the text are part of the corresponding gapped lower threshold.

Branch line	k in terms of q	δN^F_s	δJ^F_s	δN^{NF}_s	δJ_{s2}	δN_{s2}
$s2$	$k = q$	-1	0	0	0	1
$\bar{s}'$	$k = k_{F\uparrow} - q$	0	1/2	-1	1/2	1
$\bar{s}$	$k = k_{F\downarrow} - q$	0	1/2	-1	0	1
$s2'$	$k = 2k_{F\downarrow} + q$	-1	1	0	0	1

$$\begin{aligned}
&\zeta^{+-}_{\bar{s}}(k) = -1 + \sum_{\iota=\pm 1}\left[\iota\frac{\xi^0_{ss2}}{2} + \frac{\xi^1_{ss}}{2} - \Phi_{s,s}(\iota k_{F\downarrow}, q)\right]^2 \\
&\qquad \text{for} \quad q = k_{F\downarrow} - k \quad \text{and} \\
&\quad k \in]\tilde{k}, 2k_{F\downarrow}[\quad \text{for} \quad m \in]0, \tilde{m}] \\
&\quad k \in]\tilde{k}, 2k_{F\downarrow}[\quad \text{for} \quad m \in]0, \tilde{m}], \\
&\zeta^{+-}_{s2'}(k) = -1 + \sum_{\iota=\pm 1}\left[-\frac{\iota}{2\xi^1_{ss}} + \xi^1_{ss} + \Phi_{s,s2}(\iota k_{F\downarrow}, q)\right]^2 \\
&\qquad \text{for} \quad q = k - 2k_{F\downarrow} \quad \text{and} \quad k \in]2k_{F\downarrow}, \pi[. \qquad (26)
\end{aligned}$$

The phase shifts in units of 2π, $\Phi_{s,s}(\iota k_{F\downarrow}, q)$ and $\Phi_{s,s2}(\iota k_{F\downarrow}, q)$ where $\iota = \pm 1$, appearing in this equation and in other exponents' expressions provided in the following are defined by Eqs. (E39)–(E43). Limiting behaviors of such phase shifts are provided in Eqs. (E44)–(E48). The phase-shifts related parameters $\xi^1_{ss} = 1/\xi^0_{ss}$ and ξ^0_{ss2} also appearing in the above exponents' expressions are defined by Eqs. (E49)–(E53) and (E54)–(E55), respectively.

Physically, $\pm 2\pi\,\Phi_{s,s}(\pm k_{F\downarrow}, q)$ is the phase shift acquired by a s particle of momentum $\pm k_{F\downarrow}$ upon creation of one s band hole $(-2\pi\,\Phi_{s,s})$ and one s particle $(+2\pi\,\Phi_{s,s})$ at a momentum q in the s band interval $q \in] - k_{F\downarrow}, k_{F\downarrow}[$ and such that $|q| \in]k_{F\downarrow}, k_{F\uparrow}]$, respectively. However, $2\pi\,\Phi_{s,s2}(\pm k_{F\downarrow}, q)$ is the phase shift acquired by a s particle of momentum $\pm k_{F\downarrow}$ upon creation of one $s2$ particle at a momentum q in the $s2$ band subinterval $q \in [0, (k_{F\uparrow} - k_{F\downarrow}$ [or $q \in](k_{F\uparrow} - k_{F\downarrow}, 0]$.

The three functionals $\Phi_\iota(q)$ in the general expression, Eq. (21), specific to the exponents given in Eq. (26) for the $S^{+-}(k,\omega)$'s $s2$, $s2'$ branch lines, $\bar{s}$ branch line, and $\bar{s}'$ branch line are provided in Eqs. (D9), (D10), and (D11), respectively. The corresponding suitable specific values of the number and current number deviations used in such functionals are for the present branch lines given in Table I.

The $S^{+-}(k,\omega)$'s $s2$, $\bar{s}'$, $\bar{s}$, and $s2'$ branch line exponents whose expressions are given in Eq. (26) are plotted as a function of k in Figs. 7, 8, 9, and 10, respectively. In the k intervals of the gapped lower threshold of the spin n-string continuum in Figs. 1 and 2 for which they are negative, which are represented by solid lines in these figures, there are singularities at and just above the corresponding $\beta = s2, \bar{s}', \bar{s}, s2'$ branch lines in the expression $S^{+-}(k,\omega) = C^{\Delta}_{+-}(\omega - \Delta^{+-}_{\beta}(k))^{\zeta^{+-}_{\beta}(k)}$, Eq. (20) for $ab = +-$.

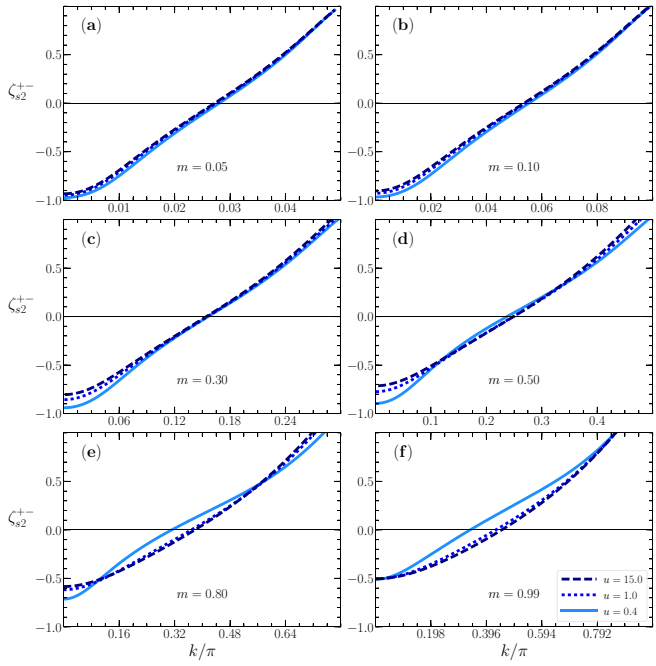

FIG. 7. The momentum dependence of the exponent that in the k intervals for which it is negative controls the $S^{+-}(k,\omega)$ line shape near and just above the $s2$ branch line for spin densities m (a) 0.05, (b) 0.1, (c) 0.3, (d) 0.5, (e) 0.8, and (f) 0.99 and $u = 0.4, 1.0, 15.0$. The $s2$ branch line is part of the gapped lower threshold of the spin n-strings continuum displayed in Figs. 1 and 2. The same exponent, in the k intervals for which it is negative, also controls the $S^{xx}(k,\omega)$'s line shape near and just above the $s2$ branch line in the spin n-strings continuum displayed in Figs. 3 and 4.

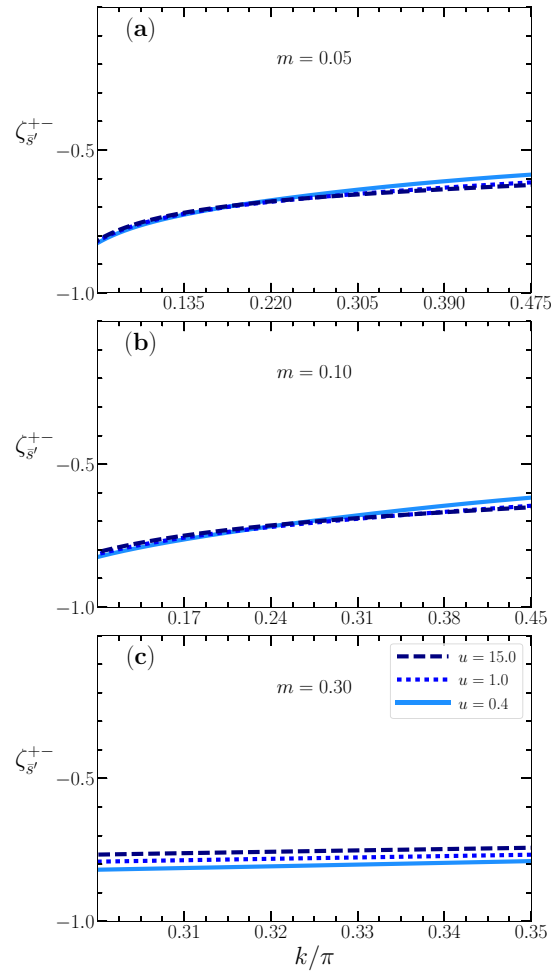

FIG. 8. The same as in Fig. 7 for the $\bar{s}'$ branch line. That line coincides with the gapped lower threshold of the spin n-strings continuum for small k intervals and only for spin densities $0 < m < \tilde{m}$ where $\tilde{m}$ continuously increases from $\tilde{m} = 0$ for $u \to 0$ to $\tilde{m} \approx 0.317$ for $u \gg 1$. The corresponding exponent plotted here is negative for such k intervals.

The related $S^{xx}(k,\omega)$'s expression, Eq. (20) for $ab = xx$, in the vicinity and just above the gapped lower threshold of the spin n-string continuum in Figs. 3 and 4 is similar to that of $S^{+-}(k,\omega)$ for the k intervals for which there is no overlap with the lower continuum spectrum associated with excited states described by real Bethe-ansatz rapidities. This thus excludes the low-m k intervals considered in Eq. (18).

Concerning again the relation between the physical excitation momentum k and the s and $s2$ bands momenta q, it is useful to provide the $S^{zz}(k,\omega)$'s expressions of the gapped lower threshold spectrum $\Delta^{zz}(k)$, Eqs. (15) and (17), for each of its branch-line parts as,

$$\begin{aligned}\Delta^{zz}_{s2}(k) &= \varepsilon_{s2}(k-(k_{F\uparrow}-k_{F\downarrow})) \quad \text{and}\\ &\quad k = (k_{F\uparrow}-k_{F\downarrow})+q\\ \text{where}\quad &k \in]0,(k_{F\uparrow}-k_{F\downarrow})[\text{and}\\ &q \in]-(k_{F\uparrow}-k_{F\downarrow}),0[\\ &\text{for}\quad m \in]0,1[,\end{aligned} \tag{27}$$

$$\begin{aligned}\Delta^{zz}_{\bar{s}}(k) &= 4\mu_B\, h - W_{s2} - \varepsilon_s(k_{F\uparrow}-k) \quad \text{and}\\ &\quad k = k_{F\uparrow}-q,\\ \text{where}\quad &k \in](k_{F\uparrow}-k_{F\downarrow}),(\pi-\tilde{k})[\quad \text{and}\\ &q \in]-(k_{F\downarrow}-\tilde{k}),k_{F\downarrow}[\\ &\text{for}\quad m \in]0,\tilde{m}]\\ \text{and}\quad &k \in](k_{F\uparrow}-k_{F\downarrow}),(\pi-\tilde{k})[\text{and}\\ &q \in]-(k_{F\downarrow}-\tilde{k}),k_{F\downarrow}[\\ &\text{for}\quad m \in [\tilde{m},1[,\end{aligned} \tag{28}$$

$$\begin{aligned}\Delta^{zz}_{\bar{s}'}(k) &= 4\mu_B\, h - \varepsilon_s(k_{F\downarrow}-k) \quad \text{and}\quad k = k_{F\downarrow}-q,\\ \text{where}\quad &k \in](\pi-\tilde{k}),2k_{F\downarrow}[\quad \text{and}\\ &q \in]-k_{F\downarrow},-(k_{F\uparrow}-\tilde{k})[\\ &\text{for}\quad m \in]0,\tilde{m}],\end{aligned} \tag{29}$$

and

$$\begin{aligned}\Delta^{zz}_{s2'}(k) &= \varepsilon_{s2}(k-\pi) \quad \text{and}\quad k = \pi+q,\\ \text{where}\quad &k \in]2k_{F\downarrow},\pi[\text{and}\\ &q \in]-(k_{F\uparrow}-k_{F\downarrow}),0[\\ &\text{for}\quad m \in]0,\tilde{m}]\end{aligned}$$

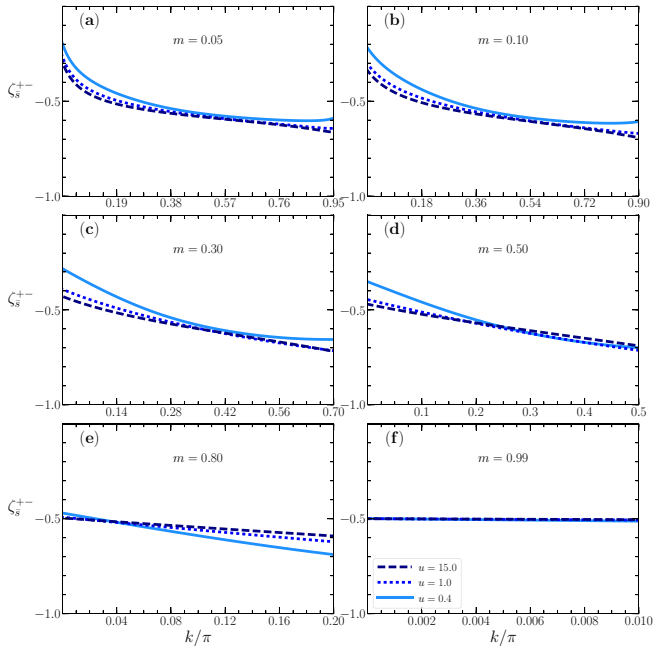

FIG. 9. The same as in Fig. 7 for the $\bar{s}$ branch line, which refers to subintervals of the gapped lower threshold of the spin n-string continuum of both $S^{+-}(k,\omega)$ and $S^{xx}(k,\omega)$. In the case of $S^{xx}(k,\omega)$, the momentum dependent exponent plotted here is valid only for the k intervals of the $\bar{s}$ branch line in Figs. 3 and 4 for which there is a gap between it and the upper threshold of the lower continuum.

$$\text{and} \quad k \in](\pi - \tilde{k}), \pi[\quad \text{and} \quad q \in]-\tilde{k}, 0[\quad \text{for} \quad m \in [\tilde{m}, 1[. \tag{30}$$

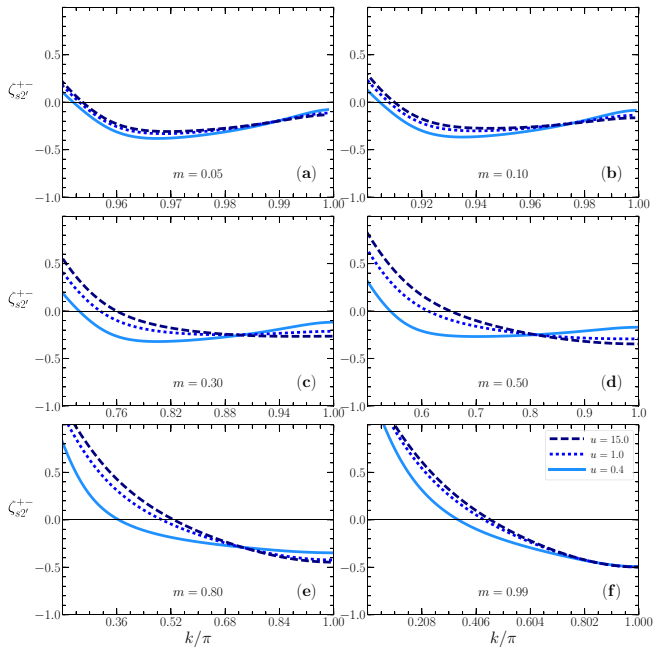

FIG. 10. The same as in Fig. 7 for the $s2'$ branch line. As in Fig. 9, in the case of $S^{xx}(k,\omega)$, the momentum dependent exponent plotted here is valid only for the k intervals of the $s2'$ branch line in Figs. 3 and 4 for which there is a gap between it and the upper threshold of the lower continuum.

TABLE II. The momentum $k > 0$ and s and $s2$ bands number and current number deviations defined in Appendix D for longitudinal spin excitations populated by one $s2$ particle and thus described both real and complex nonreal rapidities in the case of the $s2$ branch line, $\bar{s}$ branch line, $\bar{s}'$ branch line, and $s2'$ branch line that for the momentum intervals given in the text are part of the corresponding gapped lower threshold.

Branch line	k in terms of q	δN_s^F	δJ_s^F	δN_s^{NF}	δJ_{s2}	δN_{s2}
$s2$	$k = k_{F\uparrow} - k_{F\downarrow} + q$	-2	-1	0	0	1
$\bar{s}$	$k = k_{F\uparrow} - q$	-2	$-1/2$	-1	0	1
$\bar{s}'$	$k = k_{F\uparrow} - q$	1	$-1/2$	-1	$-1/2$	1
$s2'$	$k = \pi + q$	-2	0	0	0	1

The corresponding k dependent exponents of general form, Eq. (21), that appear in the expression, $S^{zz}(k,\omega) = C_{zz}^{\Delta}(\omega - \Delta_{\beta}^{zz}(k))^{\zeta_{\beta}^{zz}(k)}$, Eq. (20) for $ab = +-$ and $\beta = s2, \bar{s}, \bar{s}', s2'$, read

$$\zeta_{s2}^{zz}(k) = -1 + \sum_{\iota=\pm 1}\left[-\frac{\iota}{\xi_{s\,s}^{1}} - \xi_{s\,s}^{1} + \Phi_{s,s2}(\iota k_{F\downarrow}, q)\right]^2$$
$$\text{for} \quad q = k - k_{F\uparrow} + k_{F\downarrow} \quad \text{and} \quad k \in]0, (k_{F\uparrow} - k_{F\downarrow})[,$$

$$\zeta_{\bar{s}}^{zz}(k) = -1 + \sum_{\iota=\pm 1}\left[-\frac{\iota}{\xi_{s\,s}^{1}} + \iota\frac{\xi_{s\,s2}^{0}}{2} - \frac{\xi_{s\,s}^{1}}{2} - \Phi_{s,s}(\iota k_{F\downarrow}, q)\right]^2$$
$$\text{for} \quad q = k_{F\uparrow} - k \quad \text{and}$$
$$k \in](k_{F\uparrow} - k_{F\downarrow}), (\pi - \tilde{k})[\quad \text{for} \quad m \in]0, \tilde{m}]$$
$$k \in](k_{F\uparrow} - k_{F\downarrow}), (\pi - \tilde{k})[\quad \text{for} \quad m \in]0, \tilde{m}],$$

$$\zeta_{\bar{s}'}^{zz}(k) = -1 + \sum_{\iota=\pm 1}\left[\frac{\iota}{2\xi_{s\,s}^{1}} + \frac{\xi_{s\,s}^{1}}{2} - \Phi_{s,s}(\iota k_{F\downarrow}, q)\right]^2$$
$$\text{for} \quad q = k_{F\downarrow} - k \quad \text{and}$$
$$k \in](\pi - \tilde{k}), 2k_{F\downarrow}[\quad \text{for} \quad m \in]0, \tilde{m}],$$

$$\zeta_{s2'}^{zz}(k) = -1 + \sum_{\iota=\pm 1}\left[-\frac{\iota}{\xi_{s\,s}^{1}} + \Phi_{s,s2}(\iota k_{F\downarrow}, q)\right]^2$$
$$\text{for} \quad q = k - \pi \quad \text{and}$$
$$k \in]2k_{F\downarrow}, \pi[\quad \text{for} \quad m \in]0, \tilde{m}]$$
$$k \in](\pi - \tilde{k}), \pi[\quad \text{for} \quad m \in [\tilde{m}, 1[. \tag{31}$$

Also in the present case of $S^{zz}(k,\omega)$, the three functionals $\Phi_{\iota}(q)$ in the general expression, Eq. (21), specific to the $s2$, $s2'$ branch lines, $\bar{s}$ branch line, and $\bar{s}'$ branch line are provided in Eqs. (D9), (D10), and (D11), respectively. The corresponding suitable values of the number and current number deviations used in such functionals are though different for the present branch lines. They are given in Table II.

The behaviors of the spin dynamical structure factor $S^{zz}(k,\omega)$ are actually qualitatively different from those of $S^{+-}(k,\omega)$. Except for $\zeta_{\bar{s}'}^{zz}(k)$, the exponents in Eq. (31) are positive for all their k intervals. That $\bar{s}'$ branch line exponent is

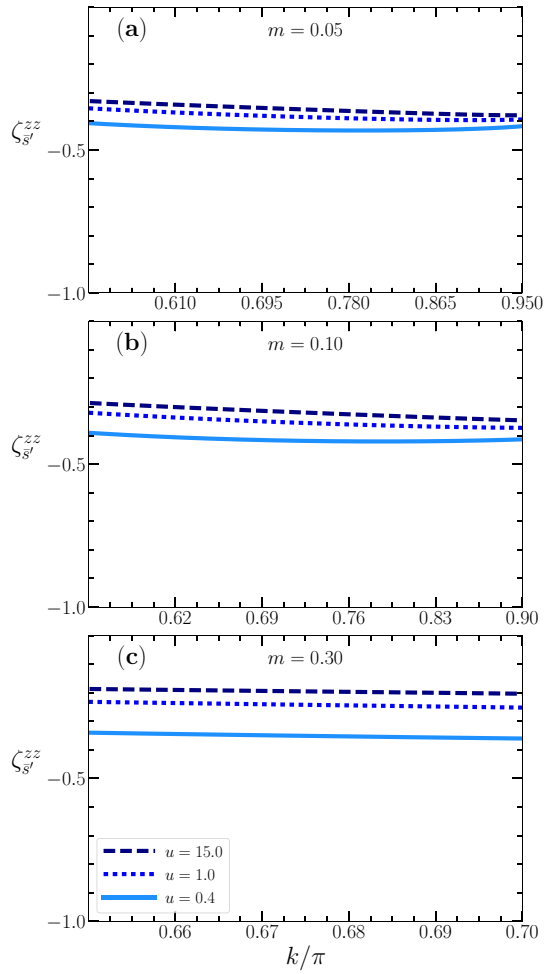

FIG. 11. The same as in Fig. 8 for the $\bar{s}'$ branch line of $S^{zz}(k,\omega)$. For that dynamical structure factor, this exponent is the only that is negative and refers to singularities near the corresponding small momentum intervals of the gapped lower threshold of the spin n-string continuum in Figs. 5 and 6. Such singularities only emerge in $S^{zz}(k,\omega)$ for spin densities $0 < m < \tilde{m}$ where $\tilde{m} = 0$ for $u \to 0$ and $\tilde{m} \approx 0.317$ for $u \gg 1$.

plotted as a function of k in Fig. 11. It is negative for its whole k subinterval, which is part of the k interval of the gapped lower threshold in Fig. 5. The $\bar{s}'$ branch line's m-dependent subinterval is either small or that line is not part of the $S^{zz}(k,\omega)$'s gapped lower threshold at all. Its momentum width decreases upon increasing m up to the spin density $\tilde{m}$. As mentioned above, this spin density decreases upon decreasing u, having the limiting values $\tilde{m} = 0$ for $u \to 0$ and $\tilde{m} \approx 0.317$ for $u \gg 1$. For $\tilde{m} < m < 1$, the $\bar{s}'$ branch line is not part of the $S^{zz}(k,\omega)$'s gapped lower threshold spectrum. This is why for $m = 0.5 > \tilde{m}$ and $m = 0.8 > \tilde{m}$ that line does not appear in the gapped lower threshold plotted in Fig. 6.

Hence, gapped lower threshold's singularities only emerge in $S^{zz}(k,\omega)$ for spin densities $0 < m < \tilde{m}$ at and just above the $\bar{s}'$ branch line, the corresponding line shape reading, $S^{zz}(k,\omega) = C^{\Delta}_{zz}[\omega - \Delta^{zz}_{\bar{s}'}(k)]^{\zeta^{+-}_{\bar{s}'}(k)}$. That branch line k subinterval width though strongly decreases upon increasing m up to $\tilde{m}$.

These behaviors are consistent with the $S^{zz}(k,\omega)$'s spectral weight stemming from spin n-string states decreasing upon increasing the spin density, being negligible for $\tilde{m} < m < 1$. Consistent with the u dependence of the spin density $\tilde{m}$, this spectral weight suppression becomes stronger upon decreasing u. Hence, increasing the spin density m within the interval $m \in]0,\tilde{m}]$ and lowering the u value tends to suppress the contribution of spin n-string states to $S^{zz}(k,\omega)$.

B. The line shape near the lower thresholds

To provide an overall physical picture that accounts for all gapped lower threshold's singularities and lower threshold's singularities in the spin dynamical structure factors, here we shortly revisit their line shape behavior at and just above the lower thresholds of the lower continua in Figs. 1–6. The corresponding contributions are from excited states described by real Bethe-ansatz rapidities. Such lower continua contain most spectral weight of the corresponding spin dynamical structure factors.

In the case of the transverse dynamical structure factor, $S^{xx}(k,\omega) = \frac{1}{4}[S^{+-}(k,\omega) + S^{-+}(k,\omega)]$, we consider the transitions to excited states that determine the line shape in the vicinity of the lower thresholds of both $S^{+-}(k,\omega)$ and $S^{-+}(k,\omega)$, respectively. The spectrum of $S^{xx}(k,\omega)$ at and just above its lower threshold, refers to a superposition of the lower threshold spectra $\omega^{+-}(k)$ and $\omega^{-+}(k)$, Eqs. (B10) and (B11)-(B12), respectively. The (k,ω)-plane lower continuum that results from such a spectra superposition is represented in Figs. 3 and 4.

Similarly to Eq. (20), for spin densities $0 < m < 1$, $u > 0$, and $k \in]0,\pi[$ the line shape of the spin dynamical structure factors $S^{ab}(k,\omega)$ where $ab = +-, -+, xx, zz$ near and just above their lower thresholds has the following general form:

$$S^{ab}(k,\omega) = C_{ab}\big[\omega - \omega^{ab}_{lt}(k)\big]^{\zeta^{ab}_{s}(k)} \quad \text{for} \quad \big[\omega - \omega^{ab}_{lt}(k)\big] \geqslant 0, \quad \text{where} \quad ab = +-, -+, xx, zz. \tag{32}$$

In the case of $S^{xx}(k,\omega)$, this expression can be expressed as

$$S^{xx}(k,\omega) = S^{+-}(k,\omega) \quad \text{for} \quad k \in [0,(k_{F\uparrow} - k_{F\downarrow})[\\ = S^{-+}(k,\omega) \quad \text{for} \quad k \in](k_{F\uparrow} - k_{F\downarrow}),\pi[. \tag{33}$$

The lower thresholds under consideration refer to a single s branch line that except for $S^{-+}(k,\omega)$ has two sections. In Eq. (32), C_{ab} are constants that have a fixed value for the k and ω ranges corresponding to small values of the energy deviation $[\omega - \omega^{ab}_{lt}(k)] \geqslant 0$. The $ab = +-, -+, zz$ lower threshold spectra $\omega^{+-}(k)$, $\omega^{-+}(k)$, and $\omega^{zz}(k)$ in that deviation are given in Eqs. (B10), (B11)-(B12), and (B13)-(B14), respectively.

The k dependent exponents appearing in the spin dynamical factors' expression, Eq. (32), are also of general form, Eq. (21). In the present case, they are given by

$$\zeta^{-+}_{s}(k) = -1 + \sum_{\iota=\pm 1}\left[-\frac{\xi^{1}_{ss}}{2} - \Phi_{s,s}(\iota k_{F\downarrow}, q)\right]^2 \quad \text{for} \quad q = k_{F\uparrow} - k \quad \text{and} \quad k \in](k_{F\uparrow} - k_{F\downarrow}),\pi[,$$

TABLE III. The momentum $k > 0$ intervals and s band number and current number deviations defined in Appendix D for the s branch lines that coincide with the lower thresholds of the $-+$, $+-$, and zz dynamical structure factors lower continua. In the case of $S^{+-}(k,\omega)$ and $S^{zz}(k,\omega)$, such lower continua appear in Figs. 1, 2, 5, and 6, respectively. The lower continua of $S^{xx}(k,\omega)$ displayed in Figs. 3 and 4 are a superposition of those of $S^{+-}(k,\omega)$ and $S^{-,+}(k,\omega)$.

s	$k = k(q)$ intervals	δN_s^F	δJ_s^F	δN_s^{NF}
$-+$	$k = k_{F\uparrow} - q \in](k_{F\uparrow} - k_{F\downarrow}), \pi[$	0	$-1/2$	-1
$+-$	$k = k_{F\uparrow} + q \in [0, (k_{F\uparrow} - k_{F\downarrow})[$	0	$-1/2$	1
$+-$	$k = k_{F\uparrow} - q \in](k_{F\uparrow} - k_{F\downarrow}), \pi[$	2	$-1/2$	-1
zz	$k = k_{F\downarrow} - q \in]0, 2k_{F\downarrow}[$	1	1/2	-1
zz	$k = k_{F\downarrow} + qk \in]2k_{F\downarrow}, \pi]$	-1	1/2	1

$$\zeta_s^{+-}(k) = -1 + \sum_{\iota=\pm 1}\left[-\frac{\xi_{ss}^1}{2} + \Phi_{s,s}(\iota k_{F\downarrow}, q)\right]^2$$
$$\text{for} \quad q = k - k_{F\uparrow} \quad \text{and} \quad k \in]0, (k_{F\uparrow} - k_{F\downarrow})[,$$
$$\zeta_s^{+-}(k) = -1 + \sum_{\iota=\pm 1}\left[\frac{\iota}{\xi_{ss}^1} - \frac{\xi_{ss}^1}{2} - \Phi_{s,s}(\iota k_{F\downarrow}, q)\right]^2$$
$$\text{for} \quad q = k_{F\uparrow} - k \quad \text{and} \quad k \in](k_{F\uparrow} - k_{F\downarrow}), \pi[,$$
$$\zeta_s^{zz}(k) = -1 + \sum_{\iota=\pm 1}\left[\frac{\iota}{2\xi_{ss}^1} + \frac{\xi_{ss}^1}{2} - \Phi_{s,s}(\iota k_{F\downarrow}, q)\right]^2$$
$$\text{for} \quad q = k_{F\downarrow} - k \quad \text{and} \quad k \in]0, 2k_{F\downarrow}[,$$
$$\zeta_s^{zz}(k) = -1 + \sum_{\iota=\pm 1}\left[-\frac{\iota}{2\xi_{ss}^1} + \frac{\xi_{ss}^1}{2} + \Phi_{s,s}(\iota k_{F\downarrow}, q)\right]^2$$
$$\text{for} \quad q = k - k_{F\downarrow} \quad \text{and} \quad k \in]2k_{F\downarrow}, \pi[. \qquad (34)$$

The functional $\Phi_\iota(q)$ in the general exponent expression, Eq. (21), is for the present s branch lines given in Eq. (D12). The suitable specific values of the number and current number deviations used in such a functional to obtain the exponents in Eq. (34) are provided in Table III.

As confirmed by the form of the expressions given in Eqs. (B10) and (B12), one has that $\omega_{lt}^{+-}(k) = \omega_{lt}^{-+}(k)$ for $k \in](k_{F\uparrow} - k_{F\downarrow}), \pi[$. In that k interval, the line shape of $S^{xx}(k,\omega) = \frac{1}{4}[S^{+-}(k,\omega) + S^{-+}(k,\omega)]$ is controlled by the smallest of the exponents $\zeta_s^{-+}(k)$ and $\zeta_s^{+-}(k)$ in Eq. (34), which turns out to be $\zeta_s^{-+}(k)$. Hence, the exponent $\zeta_s^{xx}(k)$ is given by

$$\zeta_s^{xx}(k) = -1 + \sum_{\iota=\pm 1}\left[-\frac{\xi_{ss}^1}{2} + \Phi_{s,s}(\iota k_{F\downarrow}, q)\right]^2 \quad \text{for}$$
$$q = k - k_{F\uparrow} \quad \text{and} \quad k \in]0, (k_{F\uparrow} - k_{F\downarrow})[$$
$$= -1 + \sum_{\iota=\pm 1}\left[-\frac{\xi_{ss}^1}{2} - \Phi_{s,s}(\iota k_{F\downarrow}, q)\right]^2 \quad \text{for}$$
$$q = k_{F\uparrow} - k \quad \text{and} \quad k \in](k_{F\uparrow} - k_{F\downarrow}), \pi[. \qquad (35)$$

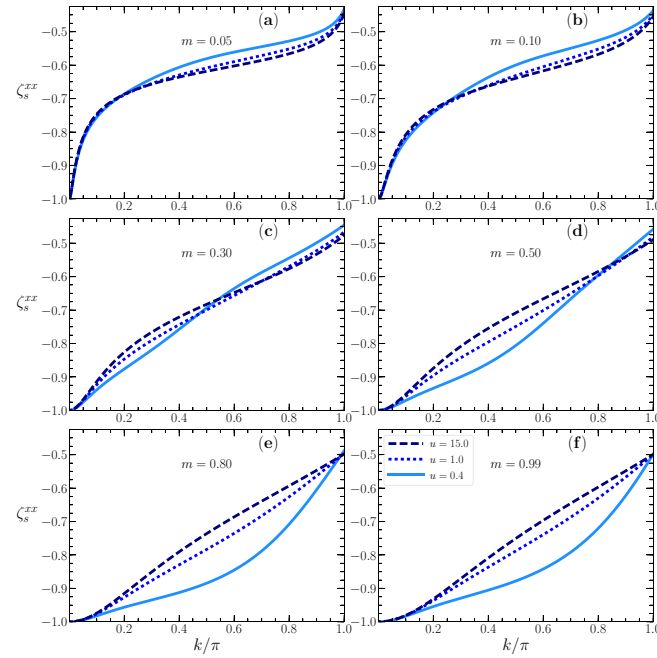

FIG. 12. The momentum dependence of the exponent that controls the $S^{xx}(k,\omega)$'s line shape near and just above the lower threshold of the lower continuum in Figs. 3 and 4 for spin densities m (a) 0.05, (b) 0.1, (c) 0.3, (d) 0.5, (e) 0.8, and (f) 0.99 and $u = 0.4$, 1.0, 15.0. For $k \in]0, (k_{F\uparrow} - k_{F\downarrow})[$ and $k \in](k_{F\uparrow} - k_{F\downarrow}), \pi[$ that exponent corresponds to that of $S^{+-}(k,\omega)$ and $S^{-+}(k,\omega)$, respectively.

This exponent is plotted as a function of k in Fig. 12. The s branch line exponent $\zeta_s^{zz}(k)$ whose expression is given in Eqs. (34) is also plotted as a function of momentum in Fig. 13.

Both such exponents are negative in the whole momentum interval $k \in]0, \pi[$ for spin densities $0 < m < 1$ and $u > 0$. It follows that there are singularities at and just above the corresponding lower thresholds. (Due to a sign error, the minus sign in the quantity $-\xi_{ss}^1/2$ appearing in Eq. (35) was missed in Ref. [17] where the exponent $\zeta_1^{xx}(k)$ is named ξ^t. Its momentum dependence plotted in Fig. 12 corrects that plotted in Fig. 5 of Ref. [17].)

V. LIMITING BEHAVIORS OF THE SPIN DYNAMICAL STRUCTURE FACTORS

Consistent with the relation, Eq. (5), the spin dynamical structure factor $S^{-+}(k,\omega)$ is at $m = 0$ that obtained in the $m \to 0$ limit from $m > 0$ values, whereas $S^{+-}(k,\omega)$ is at $m = 0$ that obtained in the $m \to 0$ limit from $m < 0$ values. One then confirms that $S^{-+}(k,\omega) = S^{+-}(k,\omega)$ at $m = 0$. However, in the $m \to 0$ limit from $m > 0$ values, the $S^{+-}(k,\omega)$ gapped continuum, Eq. (6), becomes a gapless line that coincides with both its $\bar{s}$ and $\bar{s}'$ branch lines and the lower threshold of $S^{-+}(k,\omega) = S^{+-}(k,\omega)$ at $m = 0$.

In the case of the initial ground state referring to $h = 0$ and thus $m = 0$, one has in addition that $S^{zz}(k,\omega) = S^{xx}(k,\omega)$. The selection rules in Eq. (A1) impose that the longitudinal dynamical structure factor is fully controlled by transitions from the $S = S^z = 0$ ground state to spin triplet excited states with spin numbers $S = 1$ and $S^z = 0$. This is different from

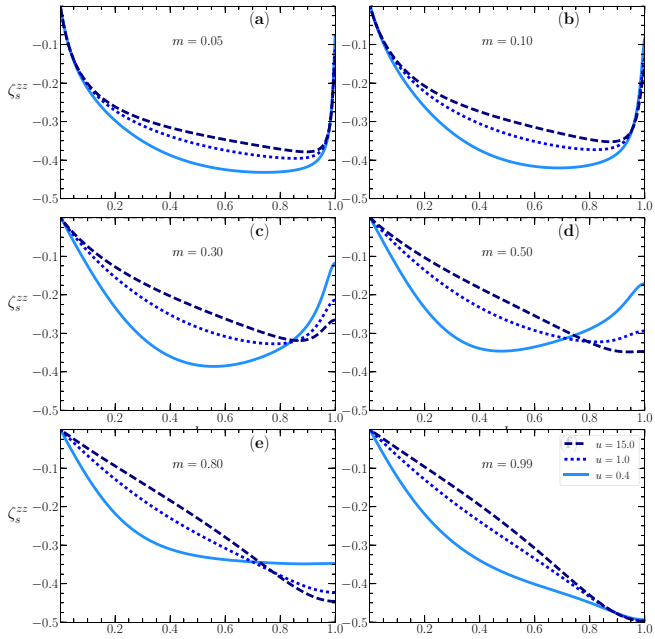

FIG. 13. The momentum dependence of the exponent that controls the $S^{zz}(k,\omega)$ line shape near and just above the lower threshold of the lower continuum in Figs. 5 and 6 for spin densities m (a) 0.05, (b) 0.1, (c) 0.3, (d) 0.5, (e) 0.8, and (f) 0.99 and $u = 0.4$, 1.0, 15.0.

the case when the initial ground state refers to $h \neq 0$ and $m \neq 0$. Then according to the selection rules, Eq. (A2), the longitudinal dynamical structure factor $S^{zz}(k,\omega) \neq S^{xx}(k,\omega)$ is controlled by transitions from the ground state with spin numbers $S^z = S$ or $S^z = -S$ to excited states with the same spin numbers $S^z = S$ or $S^z = -S$, respectively.

In the case of the $h = 0$ and $m = 0$ initial ground state, (i) $S^{zz}(k,\omega)$ and (ii) $S^{+-}(k,\omega)$ and $S^{-+}(k,\omega)$ are fully controlled by transitions to spin triplet $S = 1$ excited states with (i) $S^z = 0$ and (ii) $S^z = \pm 1$, respectively. Their s band two-hole spectrum is obtained in the $m \to 0$ limit from that of $S^{+-}(k,\omega)$ for $m < 0$ and from that of $S^{-+}(k,\omega)$ for $m > 0$ and thus reads

$$\begin{aligned}\omega^{xx}(k) = \omega^{zz}(k) &= -\varepsilon_s(q_1) - \varepsilon_s(q_2),\\ &\text{where } k = \iota\pi - q_1 - q_2 \text{ and } \iota = \pm 1\\ &\text{for } q_1 \in [-\pi/2, \pi/2]\\ &\text{and } q_2 \in [-\pi/2, \pi/2].\end{aligned} \tag{36}$$

Consistent, spin $SU(2)$ symmetry implies that the triplet $S = 1$ and $S^z = 0$ excited states that control $S^{zz}(k,\omega)$ have exactly the same spectrum, Eq. (36), as the triplet $S = 1$ and $S^z = \pm 1$ excited states that control $S^{+-}(k,\omega)$ and $S^{-+}(k,\omega)$.

In spite of the singular behavior concerning the class of excited states that control the longitudinal dynamical structure factor for $m = 0$ and $m > 0$ initial ground states, respectively, one confirms in the following that the same line shape near the spin dynamical structure factors' lower thresholds is obtained at $m = 0$ and in the $m \to 0$ limit, respectively.

A. Behaviors of the spin dynamical structure factors in the $m \to 0$ limit

In the $m \to 0$ limit from $m > 0$ values, the transverse spin structure factor $S^{-+}(k,\omega)$ lower threshold spectrum, Eq. (B10), expands to the whole $k \in [0,\pi]$ interval. The corresponding line shape near the s branch line is then valid for $k \in]0,\pi[$. Since a similar spectrum is obtained for the lower threshold of $S^{-+}(k,\omega)$ in the $m \to 0$ limit from $m < 0$ values, one finds

$$\begin{aligned}\omega_{lt}^{xx}(k) &= -\varepsilon_s(k_F - k), \quad \text{where}\\ k &= \frac{\pi}{2} - q \in]0,\pi[\quad \text{for}\\ q &\in]-\pi/2, \pi/2[.\end{aligned} \tag{37}$$

As reported above, in the $m \to 0$ limit from $m > 0$ values the $S^{+-}(k,\omega)$'s gapped continuum associated with the spectrum, Eq. (6), becomes a gapless line that coincides with both the spectra in Eqs. (23) and (24) of its $\bar{s}$ and $\bar{s}'$ branch lines, respectively, and the lower threshold of $S^{-+}(k,\omega) = S^{+-}(k,\omega)$ at $m = 0$. [In the $m \to 0$ limit from $m < 0$ values, the $\bar{s}$ and $\bar{s}'$ branch lines rather stem from $S^{-+}(k,\omega)$.] Hence, the spectra $\Delta_{\bar{s}'}^{+-}(k) = \Delta_{\bar{s}}^{+-}(k)$ read in that limit,

$$\begin{aligned}\Delta_{\bar{s}'}^{+-}(k) &= \Delta_{\bar{s}}^{+-}(k)\\ &= -\varepsilon_s(\pi/2 - k) \quad \text{where } k = \frac{\pi}{2} - q\\ \text{for } k &\in]0,\pi[\quad \text{for } q \in]-\pi/2, \pi/2[.\end{aligned} \tag{38}$$

It then turns out that the corresponding exponents $\zeta_{\bar{s}'}^{+-}(k)$ and $\zeta_{\bar{s}}^{+-}(k)$, Eq. (26), have in the $m \to 0$ limit exactly the same value. In addition, that value is the same as that of $\zeta_s^{xx}(k)$, Eq. (35), reached in that limit. Indeed, by use of the limiting behaviors $\lim_{m\to 0} \Phi_{s,s}(\pm k_{F\downarrow}, q) = \pm 1/(2\sqrt{2})$ for $q \neq \pm k_{F\downarrow}$, $\lim_{m\to 0} \Phi_{s,s2}(\pm k_F, 0) = \pm 1/\sqrt{2}$, and $\lim_{m\to 0} \xi_{ss}^1 = 1/\sqrt{2}$ reported in Eqs. (E46), (E47), and (E52), one finds that

$$\begin{aligned}\zeta_s^{xx}(k) &= -1 + \sum_{\iota=\pm 1}\left[-\frac{\xi_{ss}^1}{2} - \Phi_{s,s}(\iota\pi/2, q)\right]^2 = -\frac{1}{2},\\ \zeta_{\bar{s}'}^{+-}(k) &= -1 + \sum_{\iota=\pm 1}\left[-\frac{\xi_{ss}^1}{2} - \Phi_{s,s}(\iota\pi/2, q)\right]^2 = -\frac{1}{2},\\ \zeta_{\bar{s}}^{+-}(k) &= -1 + \sum_{\iota=\pm 1}\left[\iota\frac{\xi_{ss2}^0}{2} + \frac{\xi_{ss}^1}{2} - \Phi_{s,s}(\iota\pi/2, q)\right]^2 = -\frac{1}{2}.\end{aligned} \tag{39}$$

The spin $SU(2)$ symmetry obliges as well that at $m = 0$ the results should be similar for the transverse and longitudinal spin structure factors, respectively. In the $m \to 0$ limit, the longitudinal spin structure factor lower threshold spectrum, Eq. (B13), expands to the whole $k \in]0,\pi[$ interval and indeed is similar to that in Eq. (37), as it reads

$$\begin{aligned}\omega_{lt}^{zz}(k) = \omega_s^{zz}(k) &= -\varepsilon_s(\pi/2 - k), \quad \text{where}\\ k = k_F - q &\in]0,\pi[\quad \text{for} \quad q \in]-\pi/2, \pi/2[.\end{aligned} \tag{40}$$

In spite of such a similarity, the longitudinal dynamical structure factor is at $m = 0$ fully controlled by transitions from the ground state to excited states with spin numbers $S = 1$ and

$S^z = 0$. The line shape obtained from such spin triplet excited states is though exactly the same as that obtained in the $m \to 0$ limit from the $S^z = S$ or $S^z = -S$ and $S > 0$ excited states.

However, in the $m \to 0$ limit the $S^{zz}(k,\omega)$'s gapped $\bar{s}$ and $\bar{s}'$ branch line spectra in Eqs. (28) and (29), respectively, become gapless and coincide with both each other and with the lower threshold of the longitudinal spin structure factor, Eq. (40), for whole $k \in]0,\pi[$ interval,

$$\Delta^{zz}_{\bar{s}'}(k) = -\varepsilon_s(\pi/2 - k) \quad \text{and} \quad k = \frac{\pi}{2} - q, \quad \text{where} \quad k \in]0,\pi[\quad \text{for} \quad q \in]-\pi/2,\pi/2[. \tag{41}$$

One then finds that in such a limit, $\zeta^{zz}_{\bar{s}'}(k) < \zeta^{zz}_{\bar{s}}(k)$. Here $\zeta^{zz}_{\bar{s}'}(k)$ and $\zeta^{zz}_{\bar{s}}(k)$ are the corresponding branch line exponents given in Eq. (31). Such an inequality implies that the line shape is controlled by the exponents $\zeta^{zz}_{\bar{s}'}(k)$ and $\zeta^{zz}_{s}(k)$ such that $\zeta^{zz}_{\bar{s}'}(k) = \zeta^{zz}_{s}(k)$ in the $m \to 0$ limit, as given below. Here $\zeta^{zz}_{\bar{s}'}(k)$ is the exponent associated with the spectrum in Eq. (29).

The use of the limiting behaviors reported in Eqs. (E46) and (E52), confirms that the exponent $\zeta^{zz}_{\bar{s}'}(k)$, Eq. (31), equals both the exponent $\zeta^{zz}_{s}(k)$, Eq. (34), and those given in Eq. (39). The former two exponents are found to be given by

$$\zeta^{zz}_{s}(k) = -1 + \sum_{\iota=\pm 1}\left[\frac{\iota}{2\xi^1_{ss}} + \frac{\xi^1_{ss}}{2} - \Phi_{s,s}(\iota\pi/2, q)\right]^2 = -\frac{1}{2},$$
$$\zeta^{zz}_{\bar{s}'}(k) = -1 + \sum_{\iota=\pm 1}\left[\frac{\iota}{2\xi^1_{ss}} + \frac{\xi^1_{ss}}{2} - \Phi_{s,s}(\iota\pi/2, q)\right]^2 = -\frac{1}{2}. \tag{42}$$

Again and in spite of such similarities, the two classes of excited states described by real and complex nonreal rapidities, respectively, that at $m = 0$ contribute to the longitudinal dynamical structure factor have rather spin numbers $S = 1$ and $S^z = 0$. The line shape associated with such spin triplet excited states is though exactly the same as that obtained in the $m \to 0$ limit from the above excited states.

One then concludes that for $u > 0$ and in the $m \to 0$ limit the line shape at and just above the lower threshold of the spin structure factor is of the form,

$$S^{aa}(k,\omega) = C\,[\omega - \omega(k)]^{-1/2} \quad \text{where} \quad \omega(k) = 2t\int_0^\infty d\omega\,\frac{\cos\left(\omega\,\Lambda_s\left(\frac{\pi}{2} - k\right)\right)}{\omega\cosh\omega}\,J_1(\omega), \tag{43}$$

for $]0,\pi[$ and $aa = xx, yy, zz$ where C is a constant that has a fixed value for the k and ω ranges corresponding to small values of the energy deviation $[\omega - \omega(k)]$, $J_1(\omega)$ is a Bessel function, and the s band rapidity function $\Lambda_s(q)$ is defined in terms of its inverse function $q = q_s(\Lambda)$ in Eq. (E23). The exponent $-1/2$ is indeed that known to control the line shape at and just above the lower threshold of $\omega(k)$ [16].

B. Behaviors of the spin dynamical structure factors in the $m \to 1$ limit

The sum rules, Eq. (A3), imply that $\lim_{m\to 1} S^{-+}(k,\omega) = 0$ and $\lim_{m\to 1} S^{zz}(k,\omega) = 0$. It follows that as $m \to 1$ and thus $h \to h_c$, the spin dynamical structure factor is dominated by $S^{xx}(k,\omega)$. Here h_c is the critical field associated with the spin energy scale $2\mu_B h_c$, Eq. (3), at which fully polarized ferromagnetism is achieved.

At $h = h_c$ the power-law expressions of the present dynamical theory involving k dependent exponents are not valid, being replaced by a δ-function-like distribution,

$$S^{xx}(k,\omega) = \frac{\pi}{2}\delta\left(\omega - \omega^{xx}_{lt}(k)\right) \quad \text{where} \quad \omega^{xx}_{lt}(k) = 4t\,(\sqrt{1+u^2} - u) - \frac{2t}{\pi}\int_{-\pi}^{\pi} dk\,\sin k\,\arctan\left(\frac{\sin k - \Lambda_s(\pi - k)}{u}\right), \tag{44}$$

for $[0,\pi]$. Here the s band rapidity function $\Lambda_s(q)$ is defined in terms of its inverse function $q = q_s(\Lambda)$ in Eq. (E32).

VI. DISCUSSION AND CONCLUDING REMARKS

A. Discussion of the results

Our results provide important information about how in 1D Mott-Hubbard insulators electron itinerancy associated in the present model with the transfer integral t affects the spin dynamics: The main effect of increasing t at constant U and thus decreasing the ratio $u = U/4t$ is on the energy bandwidth of the corresponding relevant spectra.

Physically, this is justified by the interplay of kinetic energy and spin fluctuations. However, the matrix elements that control the spectral weights and the related momentum-dependent exponents in the dynamical structure factors' expressions studied in this paper are little affected by decreasing the ratio $u = U/4t$.

The internal degrees of freedom of the s and $s2$ particles refer to one unbound singlet pair of spins $1/2$ and two bound singlet pairs of such spins. The spins $1/2$ in such pairs refer to rotated electrons that singly occupy sites. In the $u \to 0$ limit, the corresponding s and $s2$ energy dispersion's bandwidths reach their maximum values, $\lim_{u\to 0} W_s = 2t[1 + \sin(\frac{\pi}{2}m)]$ and $\lim_{u\to 0} W_{s2} = 4t\sin(\frac{\pi}{2}m)$, respectively, whereas $\lim_{u\to\infty} W_s = \lim_{u\to\infty} W_{s2} = 0$, as given in Eq. (E25). Indeed, for small, intermediate, and large yet finite u values the s particles for all spin densities m and the $s2$ particles for $m > 0$, along with the two and four spins $1/2$ within them, respectively, contribute to the kinetic energy associated with electron itinerancy. However, in the $u \to \infty$ limit *all* spin configurations become degenerate and the spins $1/2$ within the s and $s2$ particles become localized.

Consistently, the kinetic energy, $E_{\rm kin} = t\,\partial\langle\hat{H}\rangle/\partial t$, of all Mott-Hubbard insulator's states decreases from a maximum value reached in the $u \to 0$ limit to zero for $u \to \infty$. Intermediate u values refer to a crossover between these two limiting behaviors. While this applies to all spin densities, for further information on the interplay of kinetic energy and spin fluctuations at $m = 0$, see for instance Sec. IV of Ref. [31] for electronic density $n = 1$.

The dynamical theory used in the studies of this paper refers to a specific case of the general dynamical theory considered in Ref. [17]. The former theory refers to the

Hamiltonian, Eq. (1), acting onto a subspace that includes spin n-string states. It has specific values for the spectral parameters that control the momentum dependent exponents in the spin dynamical structure factors' expressions that have been obtained in this paper for (k, ω)-plane regions at and near well-defined types of spectral features.

As mentioned in Sec. I, the issue of how the branch-line cusp singularities stem from the behavior of matrix elements between the $m > 0$ ground states and specific classes of excited states is shortly discussed in Appendix D. The dynamical theory refers to the thermodynamic limit, in which the matrix elements squares $|\langle \nu|\hat{S}^a_k|GS\rangle|^2$ in Eq. (4) have in terms of the relative weights $a(m_{+1}, m_{-1})$ and lowest peak weights $A^{(0,0)}$ defined in that Appendix the general form given in its Eq. (D7). The theory provides in that Appendix Eq. (D6) the dependence of such weights on the $\iota = \pm 1$ functionals Φ^2_ι that control the cusp singularities exponents.

Unfortunately, it does not provide the precise values of the u and m dependent constant $0 < B_s \leqslant 1$ and u dependent constants $0 < f_l < 1$ where $l = 0, 2, 4$ in the $A^{(0,0)}$ expression under consideration. Those contribute to the coefficients C^{Δ}_{ab} and C_{ab}, respectively, in the spin dynamical structure factors' analytical expressions, Eqs. (20) and (32), which are determined by the lowest peaks spectral weights. In spite of this limitation, our results provide important physical information on such factors.

The possible alternative use of form factors of the $\sigma = \uparrow, \downarrow$ electron creation and annihilation operators involved in the dynamical structure factors studied in this paper remains an unsolved problem for the present 1D Hubbard model.

When $\zeta^{ab}_\beta(k) = -1 + \sum_{\iota=\pm 1} \Phi^2_\iota < 0$, Eq. (21), there are cusp singularities at and just above the corresponding β branch lines. The form of the matrix elements expression, Eq. (D7), reveals both that the occurrence of cusp singularities is controlled by the matrix elements $\langle \nu|\hat{S}^a_k|GS\rangle$ and that $|\langle \nu|\hat{S}^a_k|GS\rangle|^2$ also diverges in the case of the excited states that generate such singularities. This confirms that there is a direct relation between the negativity of the exponents $\zeta^{ab}_\beta(k)$ and the amount of spectral weight at and just above the corresponding β branch lines.

For simplicity, in this paper we have not provided further details of the dynamical theory that are common to those already given in Ref. [17]. The form of both the relative weights and the lowest peak weights considered in the studies of Ref. [25] for the charge degrees of freedom of the 1D Hubbard model for electronic densities $n_e \in [0, 1]$ at spin density $m = 0$ is similar to that of the present relative weights $a(m_{+1}, m_{-1})$ and lowest peak weights $A^{(0,0)}$ for the spin degrees of freedom of the same model for spin densities $m \in [0, 1]$ at electronic density $n_e = 1$. Such studies consider the $u \to \infty$ limit in which for the dynamical correlation function under consideration the values of the lowest peak weights can be calculated. The results of that reference confirm that the cusp singularities correspond to (k, ω)-plane regions with a larger amount of spectral weight.

That the momentum-dependent exponents in Eqs. (20) and (32) and thus the corresponding matrix elements that control the spectral weights, Eq. (D7), are little affected by decreasing the ratio $u = U/4t$ reveals that in the present case of the spin dynamical structure factors of the 1D Hubbard model's Mott-Hubbard insulating phase the relative spectral-weight contributions of different types of excited energy eigenstates is little u dependent. This means that concerning that issue, results for the most known limit of small yet finite t^2/U and thus large u in which the present quantum problem is equivalent to the spin-1/2 XXX chain [4,28] also apply to small and intermediate u values. This applies to the analysis presented in Sec. III, concerning the spectral weight in the gap regions being negligible in the present thermodynamic limit

Our results have focused on the contribution from spin n-string states. This refers to the line shape at and just above the (k, ω)-plane gapped lower threshold's spectra $\Delta^{ab}_\beta(k)$ where $ab = +-, xx, zz$ and β refers to different branch lines. In well-defined m-dependent k subintervals, Eqs. (22)–(25) and (27)–(30), such branch lines coincide with the gapped lower thresholds under consideration. In these physically important (k, ω)-plane regions, the spin dynamical structure factors $S^{ab}(k, \omega)$ have the general analytical expression provided in Eq. (20). In the case of $S^{+-}(k, \omega)$ and $S^{xx}(k, \omega)$, such gapped lower thresholds refer to the n-string states' upper continua shown in the (k, ω)-plane in Figs. 1–4, respectively.

That as justified in Sec. III the spectral weight in the gap regions is negligible in the present thermodynamic limit, is consistent with the amount of that weight existing just below the (k, ω)-plane gapped lower thresholds of the n-string states' spectra shown in Figs. 1–6 being vanishingly small or negligible. This is actually behind the validity at finite magnetic fields $0 < h < h_c$ and in the thermodynamic limit of the analytical expressions of the spin dynamical structure factors of general form, Eq. (20), obtained in this paper.

The momentum dependent exponents that control the spin dynamical structure factors' line-shape in such expressions are given in Eq. (26) for $S^{+-}(k, \omega)$ and $S^{xx}(k, \omega)$ and in Eq. (31) for $S^{zz}(k, \omega)$. In the former case, the exponents associated with the (k, ω)-plane vicinity of the $s2-$, $\bar{s}'-$, $\bar{s}-$, and $s2'$-branch lines are plotted in Figs. 7–10. Such lines refer to different k intervals of the gapped lower threshold of the n-string states' spectra of $S^{+-}(k, \omega)$ and $S^{xx}(k, \omega)$. The solid lines in Figs. 1–4 that belong to that gapped lower threshold correspond to k intervals for which the exponents are negative. In them, singularities occur in the spin dynamical structure factors' expression, Eq. (20), at and above the gapped lower thresholds.

In the case of $S^{xx}(k, \omega)$, the expression given in that equation does not apply for small spin densities in the ranges and corresponding k intervals given in Eqs. (18) and (19). For these spin-density ranges and momentum intervals, there is overlap between the lower continuum and upper n-string states' continuum, as shown in Figs. 3(a)–3(c).

However, consistently with the perturbative arguments provided in Appendix D in terms of the number of elementary processes associated with annihilation of one s particle, the contribution to $S^{zz}(k, \omega)$ from excited states populated by n-strings is much weaker than for $S^{+-}(k, \omega)$ and $S^{xx}(k, \omega)$ and is negligible in the case of $S^{-+}(k, \omega)$. In the case of $S^{zz}(k, \omega)$ it does not lead to a (k, ω)-plane continuum. The gapped lower threshold of such states is shown in Figs. 5 and 6. There the k subinterval associated with the $\beta = \bar{s}'$ branch line is the only one at and above which there are singularities. We have found that out of the four branch-line's exponents whose expressions

are provided in Eq. (31), only that of the $\beta = \bar{s}'$ branch line is indeed negative. That line is represented in the gapped lower threshold of $S^{zz}(k,\omega)$ shown in Figs. 5(a)–5(c) by a solid (green) line. The corresponding exponent is plotted in Fig. 11.

That line's k subinterval is though small. Its momentum width decreases upon decreasing u and/or increasing the spin density within the range $0 < m \leqslant \tilde{m}$. Here $\tilde{m}$ increases from $\tilde{m} = 0$ for $u \to 0$ to $\tilde{m} \approx 0.317$ for large u. For spin densities $\tilde{m} \leqslant m < 1$, that line is not part of the gapped lower threshold, so that the contribution to $S^{zz}(k,\omega)$ from excited states populated by n-strings becomes negligible. Consistent, in Figs. 5(d)–5(f) and 6 that line is lacking.

To to provide an overall physical picture that includes the relative (k,ω)-plane location of all spectra with a significant amount of spectral weight, we also accounted for the contributions from all types of excited energy eigenstates that lead to gapped and gapless lower threshold singularities in the spin dynamical structure factors. This includes excited energy eigenstates described only by real Bethe-ansatz rapidities and thus without n-strings, which are known to lead to most spectral weight of the sum rules, Eq. (A3). Their contribution to $S^{+-}(k,\omega)$, $S^{xx}(k,\omega)$, and $S^{zz}(k,\omega)$ leads to the (k,ω)-plane lower continua shown in Figs. 1–6, respectively.

B. Concluding remarks

Spin n-strings have been identified in experimental studies of $CuCl_2{\cdot}2N(C_5D_5)$ and $Cu(C_4H_4N_2)(NO_3)_2$ [4–6]. In this paper the contribution of spin n-strings to the spin dynamical structure factors of the 1D fermionic Hubbard model with one electron per site in a magnetic field has been studied. That model describes a 1D Mott-Hubbard insulator.

1D Mott-Hubbard insulators are a paradigm for the importance of strong correlations and are known to exhibit a wide variety of unusual physical phenomena. For instance, while in the 1D Hubbard metallic phase increasing the onsite repulsion U reduces the lattice distortion, in its Mott-Hubbard insulating phase Coulomb correlations enhance the lattice dimerization [32]. 1D Mott-Hubbard insulators can be studied within condensed matter by inelastic neutron scattering in spin chains such as for instance chain cuprates, as well as a number of quasi-1D organic compounds [4,5,33].

The theoretical description of the spin degrees of freedom of some of such condensed-matter systems is commonly modeled by the spin-1/2 XXX antiferromagnet [4,5]. As justified in the following, our study indicates that the 1D Hubbard model with one electron per site can alternatively be used to describe the spin dynamical properties of such systems.

Analysis of the spin dynamical structure factors spectra plotted in the (k,ω) plane in Figs. 1–6, reveals that the only effect of decreasing the ratio $u = U/4t$ is to increase such spectra energy bandwidths. (Within the isotropic spin-1/2 XXX chain, this can be achieved by increasing the exchange integral J.)

It is somehow surprising that the 1D Hubbard model with one electron per site for $u = 15$, which is equivalent to a isotropic spin-1/2 XXX chain with $J = 4t^2/U$, and the former model for $u = 0.4$ and $u = 1.0$, lead to spin dynamical structure factors' spectra that except for their energy bandwidth have basically the same form.

However, the type of momentum dependencies of the exponents plotted in Figs. 7–13 that control the (k,ω)-plane line shape of the spin dynamical structure factors in the vicinity of the singularities located in the gapped lower thresholds of the spin n-string states' spectra and lower thresholds of the lower continua represented in Figs. 1–6 is not affected by decreasing u.

That as found in this paper the main effect of increasing t at constant U and thus decreasing the ratio $u = U/4t$ is on the energy bandwidth of the corresponding relevant spectra is an important information about how in 1D Mott-Hubbard insulators electron itinerancy associated in the present model with the transfer integral t affects the spin dynamics.

This seems to confirm that concerning the spin dynamical properties of spin chain compounds in a magnetic field, both the 1D Hubbard model with one electron per site and the spin-1/2 XXX antiferromagnet are suitable model candidates. Consistent, for general Mott-Hubbard insulating materials there is no reason for the on-site repulsion to be much stronger than the electron hopping amplitude t. This situation is realized in the Bechgaard salts [32].

Since the dynamical theory used in our study for the whole $u > 0$ range and the thermodynamic limit only provides the line shape at and near the cusp singularities located at the gapped lower thresholds and lower thresholds, it cannot access other possible peaks, as for instance those due to the Brillouin-zone folding effect. However and as discussed in Sec. VI A, results for the most known limit of small yet finite t^2/U and thus large u in which the present quantum problem is equivalent to the spin-1/2 XXX chain [4] also apply to small and intermediate u values provided that the spectral features energy bandwidths are suitably rescaled. Hence, one can at least confirm that the cusp singularities located at the gapped lower thresholds and lower thresholds predicted by the half-filled 1D Hubbard model are observable in neutron scattering experiments.

In such experiments, the quantity that is observed is proportional to

$$S^{av}(k,\omega) = \tfrac{1}{6}[S^{-+}(k,\omega) + S^{+-}(k,\omega) + 4S^{zz}(k,\omega)]. \quad (45)$$

Upon superposition of the spectra of the spin dynamical structure factors on the right-hand side of this equation, we have checked that *all* cusp singularities at and near both the gapped lower thresholds and lower thresholds found in this paper for the 1D Hubbard model at any of the u values $u = 0.4$, $u = 0.1$, and $u = 15.0$ correspond to peaks shown in Fig. 4 of Ref. [4] for $CuCl_2{\cdot}2N(C_5D_5)$ and in Fig. 5 of that reference for $Cu(C_4H_4N_2)(NO_3)_2$ at the finite values of the magnetic field considered in these figures and suitable transfer integral t values, to reach agreement with the corresponding energy bandwidths. This should obviously apply to $u = 15.0$ at which large u value the spin degrees of freedom of the present model are described by the spin-1/2 XXX chain (with exchange integral $J = 4t^2/U = t/u$) used in the studies of Ref. [4] to theoretically access the cusp singularities under consideration.

That such a correspondence also applies to $u = 0.4$ and $u = 1.0$ is justified by the results of this paper according to which: The dependence on u of the momentum dependence

of the negative exponents that control the spin dynamical structure factors' line shape is rather weak; The main effect of decreasing u on such factors' spectra is merely to increase their energy bandwidth.

The dynamical theory used in our study provides analytical expressions of the spin dynamical structure factors at and just above the (k,ω)-plane gapped lower thresholds and lower thresholds of their spectra with more spectral weight. The use of other methods such as the time-dependent density matrix renormalization group [34–36] to obtain the line shape of such dynamical functions over other (k,ω)-plane regions would provide valuable complementary information.

In the case of 1D Mott-Hubbard insulators, the apparent independence on the u values of the spin dynamics found in this paper, suggests that the suitable values of the interaction for such systems are rather settled by the agreement with experimental results on the charge dynamics and one-particle spectral function at energy scales above the Mott-Hubbard gap.

ACKNOWLEDGMENTS

J.M.P.C. thanks Boston University's Condensed Matter Theory Visitors Program for support and Boston University for hospitality during the initial period of this research. He acknowledges the support from FCT through Grants No. PTDC/FIS-MAC/29291/2017 and No. SFRH/BSAB/142925/2018. J.M.P.C. and T.Č. thank Pedro D. Sacramento for illuminating discussions and they acknowledge the support from FCT through the Grant No. UID/FIS/04650/2013. T.Č. gratefully acknowledges the support by the Institute for Basic Science in Korea (Project No. IBS-R024-D1).

APPENDIX A: USEFUL SELECTION RULES AND SUM RULES

Let $|S,\alpha\rangle$, $|S^z,\beta\rangle$, and $|S,S^z,\gamma\rangle$ denote energy eigenstates where $S\in[0,N/2]$ is their spin, S^z their spin projection, and α, β, and γ represent all other quantum numbers needed to uniquely specify these states, respectively. The selection rules given in the following are derived from the properties of the operators $\hat{S}^z_k$ and $\hat{S}^\pm_k$ by straightforward manipulations involving their operator algebra [28].

At vanishing magnetic field, $h=0$, the following selection rules hold in the thermodynamic limit:

$$\begin{aligned}
&\langle S,\alpha|\hat{S}^a_k|S'\alpha'\rangle = 0 \quad \text{for} \quad S=S'=0 \quad \text{and} \quad a=z,\pm,\\
&\langle S,\alpha|\hat{S}^a_k|S'\alpha'\rangle = 0 \quad \text{for} \quad |S-S'|\neq 0,1 \quad \text{and} \quad a=z,\pm,\\
&\langle S^z,\beta|\hat{S}^\pm_k|S^{z'},\beta'\rangle = 0 \quad \text{for} \quad S^{z'}\neq S^z\pm 1,\\
&\langle S^z,\beta|\hat{S}^z_k|S^{z'},\beta'\rangle = 0 \quad \text{for} \quad S^{z'}\neq S^z. \qquad \text{(A1)}
\end{aligned}$$

However, for finite magnetic fields $0<h<h_c$ the following selection rules are valid in that limit:

$$\begin{aligned}
&\langle S,S,\gamma|\hat{S}^\pm_k|S',S^{z'},\gamma'\rangle = 0\\
&\quad \text{for} \quad S'\neq S\pm 1 \quad \text{and} \quad S^{z'}\neq S\pm 1,\\
&\langle S,S,\gamma|\hat{S}^z_k|S',S^{z'},\gamma'\rangle = 0\\
&\quad \text{for} \quad S'\neq S \quad \text{and} \quad S^{z'}\neq S. \qquad \text{(A2)}
\end{aligned}$$

Finally, the dynamical structure factors satisfy the following sum rules:

$$\begin{aligned}
&\frac{1}{2\pi^2}\int_{-\pi}^{\pi}dk\int_0^\infty d\omega\, S^{+-}(k,\omega) = (1+m),\\
&\frac{1}{2\pi^2}\int_{-\pi}^{\pi}dk\int_0^\infty d\omega\, S^{-+}(k,\omega) = (1-m),\\
&\frac{1}{2\pi^2}\int_{-\pi}^{\pi}dk\int_0^\infty d\omega\, S^{zz}(k,\omega) = \frac{1}{2}(1-m^2). \qquad \text{(A3)}
\end{aligned}$$

APPENDIX B: GAPLESS TRANSVERSE AND LONGITUDINAL CONTINUUM SPECTRA

Within a k extended zone scheme, the $S^{-+}(k,\omega)$'s spectrum $\omega^{-+}(k)$ and the $S^{+-}(k,\omega)$'s spectrum $\omega^{+-}(k)$ associated with the lower continuum in Figs. 1 and 2 read

$$\begin{aligned}
&\omega^{-+}(k) = -\varepsilon_s(q_1)-\varepsilon_s(q_2),\\
&\text{where} \quad k=\iota\pi-q_1-q_2 \quad \text{and} \quad \iota=\pm 1\\
&\text{for} \quad q_1\in[-k_{F\downarrow},k_{F\downarrow}] \quad \text{and} \quad q_2\in[-k_{F\downarrow},k_{F\downarrow}], \qquad \text{(B1)}
\end{aligned}$$

and

$$\begin{aligned}
&\omega^{+-}(k) = \varepsilon_s(q_1)-\varepsilon_s(q_2),\\
&\text{where} \quad k=\iota\pi+q_1-q_2 \quad \text{and} \quad \iota=\pm 1\\
&\text{for} \quad |q_1|\in[k_{F\downarrow},k_{F\uparrow}] \quad \text{and} \quad q_2\in[-k_{F\downarrow},k_{F\downarrow}], \qquad \text{(B2)}
\end{aligned}$$

respectively. Here $\varepsilon_s(q)$ is the s band energy dispersion given in Eq. (E8).

The spectrum $\omega^{xx}(k)$ of the transverse dynamical structure factor $S^{xx}(k,\omega)$ associated with the lower continuum in Figs. 3 and 4 results from combination of the two spectra $\omega^{-+}(k)$ and $\omega^{+-}(k)$ in Eqs. (B1) and (B2), respectively.

However, the spectrum $\omega^{zz}(k)$ associated with the lower continuum in Figs. 5 and 6 is given by

$$\begin{aligned}
&\omega^{zz}(k) = \varepsilon_s(q_1)-\varepsilon_s(q_2),\\
&\text{where} \quad k=q_1-q_2\\
&\text{for} \quad |q_1|\in[k_{F\downarrow},k_{F\uparrow}] \quad \text{and} \quad q_2\in[-k_{F\downarrow},k_{F\downarrow}]. \qquad \text{(B3)}
\end{aligned}$$

The upper thresholds of the two-parametric spectra, Eqs. (B1) and (B2), have the following one-parametric spectra for spin densities $m\in]0,1[$:

$$\begin{aligned}
\omega^{+-}_{ut}(k) &= 2\mu_B\, h-\varepsilon_s(k_{F\downarrow}-k) \quad \text{where} \quad k=k_{F\downarrow}-q\\
&\quad \text{for} \quad k\in[0,k_{F\downarrow}] \quad \text{and} \quad q\in[0,k_{F\downarrow}],\\
&= \varepsilon_s(q_1)-\varepsilon_s(q_2), \quad \text{where} \quad k=\pi+q_1-q_2\\
&\quad \text{for} \quad k\in[k_{F\downarrow},\pi] \quad \text{and} \quad v_s(q_1)=v_s(q_2),\\
&\quad \text{with} \quad q_1\in[-k_{F\uparrow},-k_{F\downarrow}]\\
&\quad \text{and} \quad q_2\in[-k_{F\downarrow},0], \qquad \text{(B4)}
\end{aligned}$$

and

$$\begin{aligned}
\omega^{-+}_{ut}(k) &= -2\varepsilon_s\left(\frac{\pi-k}{2}\right), \quad \text{where} \quad k=\pi-2q\\
&\quad \text{for} \quad k\in[(k_{F\uparrow}-k_{F\downarrow}),\pi]\\
&\quad \text{and} \quad q\in[-k_{F\downarrow},0], \qquad \text{(B5)}
\end{aligned}$$

respectively.

The upper threshold spectrum $\omega_{ut}^{xx}(k)$ of the combined spectra, Eqs. (B1) and (B2), is given by

$$\begin{aligned}\omega_{ut}^{xx}(k) &= \omega_{ut}^{+-}(k) \quad \text{for} \quad k \in \left[0, k_{ut}^{xx}\right] \\ &= \omega_{ut}^{-+}(k) \quad \text{for} \quad k \in \left[k_{ut}^{xx}, \pi\right], \end{aligned} \tag{B6}$$

where the momentum k_{ut}^{xx} is such that $\omega_{ut}^{+-}(k_{ut}^{xx}) = \omega_{ut}^{-+}(k_{ut}^{xx})$.

However, the one-parametric upper threshold spectrum associated with the two-parametric longitudinal spectrum, Eq. (B3), reads for $m \in]0, 1[$

$$\begin{aligned}\omega_{ut}^{zz}(k) &= \varepsilon_s(q_1) - \varepsilon_s(q_2) \quad \text{where} \quad k = q_1 - q_2 \\ &\quad \text{for} \quad v_s(q_1) = v_s(q_2) \quad \text{and} \quad k \in [0, k_{F\uparrow}] \ \text{with} \\ &\quad q_1 \in [k_{F\downarrow}, k_{F\uparrow}] \quad \text{and} \quad q_2 \in [0, k_{F\downarrow}], \\ &= 2\mu_B\, h - \varepsilon_s(k_{F\uparrow} - k) \quad \text{where} \quad k = k_{F\uparrow} - q \\ &\quad \text{for} \quad k \in [k_{F\uparrow}, \pi] \quad \text{and} \quad q \in [-k_{F\downarrow}, 0]. \end{aligned} \tag{B7}$$

At $k = 0, k_{F\downarrow}, \pi$ and $k = 0, k_{F\uparrow} - k_{F\downarrow}, \pi$, the upper threshold spectra, Eqs. (B4) and (B5), respectively, are given by

$$\begin{aligned}\omega_{ut}^{+-}(0) &= W_s^h = 2\mu_B\, h, \\ \omega_{ut}^{+-}(k_{F\downarrow}) &= W_s = 2\mu_B\, h + W_s^p, \\ \omega_{ut}^{+-}(\pi) &= 0, \\ \omega_{ut}^{-+}(k_{F\uparrow} - k_{F\downarrow}) &= 0, \\ \omega_{ut}^{-+}(\pi) &= 2W_s^p. \end{aligned} \tag{B8}$$

At $k = 0, k_{F\uparrow}, \pi$ the upper threshold spectrum $\omega_{ut}^{zz}(k)$ reads

$$\begin{aligned}&\omega_{ut}^{zz}(0) = 0, \quad \omega_{ut}^{zz}(k_{F\uparrow}) = W_s = 2\mu_B\, h + W_s^p, \\ &\omega_{ut}^{zz}(\pi) = W_s^h = 2\mu_B\, h. \end{aligned} \tag{B9}$$

The energy scales $W_s = W_s^p + W_s^h$, W_s^p, and W_s^h are in the above equations the s band energy width, the s particle energy bandwidth, and the s hole energy bandwidth defined by Eqs. (E24)–(E26).

The dynamical theory used in our study provides the spin dynamical structure factors' line shape near the lower thresholds of the spectra, Eqs. (B1), (B2), and (B3). In the case of (i) $S^{-+}(k, \omega)$ and (ii) $S^{+-}(k, \omega)$ and $S^{zz}(k, \omega)$ such lower thresholds refer to (i) a single s branch line and (ii) two sections of a s branch line, respectively.

These lower thresholds spectra can be expressed in terms of the excitation momentum k or of the s band momentum q and are given by

$$\begin{aligned}\omega_{lt}^{-+}(k) &= -\varepsilon_s(k_{F\uparrow} - k) \quad \text{and} \\ &\quad k = k_{F\uparrow} - q, \quad \text{where} \\ &\quad k \in](k_{F\uparrow} - k_{F\downarrow}), \pi[\quad \text{and} \\ &\quad q \in]-k_{F\downarrow}, k_{F\downarrow}[, \end{aligned} \tag{B10}$$

$$\begin{aligned}\omega_{lt}^{+-}(k) &= \varepsilon_s(k - k_{F\uparrow}) \quad \text{and} \\ &\quad k = k_{F\uparrow} + q, \quad \text{where} \\ &\quad k \in]0, (k_{F\uparrow} - k_{F\downarrow})[\quad \text{and} \\ &\quad q \in]-k_{F\uparrow}, -k_{F\downarrow}[, \end{aligned} \tag{B11}$$

$$\begin{aligned}\omega_{lt}^{+-}(k) &= -\varepsilon_s(k_{F\uparrow} - k) \quad \text{and} \\ &\quad k = k_{F\uparrow} - q, \quad \text{where} \\ &\quad k \in](k_{F\uparrow} - k_{F\downarrow}), \pi[\quad \text{and} \\ &\quad q \in]-k_{F\downarrow}, k_{F\downarrow}[, \end{aligned} \tag{B12}$$

$$\begin{aligned}\omega_{lt}^{zz}(k) &= -\varepsilon_s - k_{F\downarrow}[_{F\downarrow} - k) \quad \text{and} \\ &\quad k = k_{F\downarrow} - q, \quad \text{where} \\ &\quad k \in]0, 2k_{F\downarrow}[\text{and} \\ &\quad q \in]-k_{F\downarrow}, k_{F\downarrow}[, \end{aligned} \tag{B13}$$

$$\begin{aligned}\omega_{lt}^{zz}(k) &= \varepsilon_s(k - k_{F\downarrow}) \quad \text{and} \\ &\quad k = k_{F\downarrow} + q, \quad \text{where} \\ &\quad k \in]2k_{F\downarrow}), \pi[\quad \text{and} \\ &\quad q \in]k_{F\downarrow}, k_{F\uparrow}[. \end{aligned} \tag{B14}$$

APPENDIX C: ENERGY GAPS' EXPRESSIONS AND LIMITING VALUES

In this Appendix, the expressions in terms of the s and $s2$ bands energy dispersions and limiting values of the energy gaps $\Delta_{\rm gap}^{+-}(k)$, Eq. (15), $\Delta_{\rm gap}^{xx}(k)$, Eq. (16), and $\Delta_{\rm gap}^{zz}(k)$, Eq. (17), and their values at some specific momenta are provided.

For $m \in [0, \tilde{m}]$ the energy gap $\Delta_{\rm gap}^{+-}(k)$ reads

$$\begin{aligned}\Delta_{\rm gap}^{+-}(k) &= -2\mu_B\, h + \varepsilon_{s2}(k) + \varepsilon_s(k_{F\downarrow} - k) \\ &\quad \text{for} \quad k \in]0, (k_{F\uparrow} - k_{F\downarrow})[, \\ \Delta_{\rm gap}^{+-}(k) &= 2\mu_B\, h - \varepsilon_s(k_{F\uparrow} - k) + \varepsilon_s(k_{F\downarrow} - k) \\ &\quad \text{for} \quad](k_{F\uparrow} - k_{F\downarrow}), \tilde{k}[, \\ \Delta_{\rm gap}^{+-}(k) &= 2\mu_B\, h - W_{s2} \quad \text{for} \quad k \in]\tilde{k}, k_{F\downarrow}[, \\ \Delta_{\rm gap}^{+-}(k) &= 4\mu_B\, h - W_{s2} - \varepsilon_s(k_{F\downarrow} - k) \\ &\quad + \varepsilon_s(q) - \varepsilon_s(k + q - \pi) \\ &\quad \text{for} \quad k \in]k_{F\downarrow}, 2k_{F\downarrow}[\quad \text{and} \\ &\quad q \in]-(k_\bullet - k_{F\uparrow} + k_{F\downarrow}), 0[\\ q_1 &= k + q - \pi \in]-k_{F\uparrow}, -k_\bullet[, \\ \Delta_{\rm gap}^{+-}(k) &= \varepsilon_{s2}(k - 2k_{F\downarrow}) + \varepsilon_s(q) - \varepsilon_s(k + q - \pi) \\ &\quad \text{for} \quad k \in]2k_{F\downarrow}, \pi[\ \text{and} \\ &\quad q \in]-k_{F\downarrow}, -(k_\bullet - k_{F\uparrow} + k_{F\downarrow})[\\ &\quad q_1 = k + q - \pi \in]-k_\bullet, -k_{F\downarrow}[\\ &\quad \text{for} \quad \text{spin densities} \ \ m \in [0, \tilde{m}]. \end{aligned} \tag{C1}$$

For spin densities $m \in [\tilde{m}, 1[$ its expression is

$$\begin{aligned}\Delta_{\rm gap}^{+-}(k) &= -2\mu_B\, h + \varepsilon_{s2}(k) + \varepsilon_s(k_{F\downarrow} - k) \\ &\quad \text{for} \quad k \in]0, \tilde{k}[, \\ \Delta_{\rm gap}^{+-}(k) &= 2\mu_B\, h - W_{s2} \quad \text{for} \quad k \in]\tilde{k}, k_{F\downarrow}[, \\ \Delta_{\rm gap}^{+-}(k) &= 4\mu_B\, h - W_{s2} - \varepsilon_s(k_{F\downarrow} - k) \\ &\quad + \varepsilon_s(q) - \varepsilon_s(k + q - \pi) \\ &\quad \text{for} \quad k \in]k_{F\downarrow}, 2k_{F\downarrow}[\quad \text{and} \end{aligned}$$

$$
\begin{aligned}
&q \in]-(k_\bullet - k_{F\uparrow} + k_{F\downarrow}), 0[\\
&q_1 = k + q - \pi \in]-k_{F\uparrow}, -k_\bullet[, \\
\Delta^{+-}_{\rm gap}(k) &= \varepsilon_{s2}(k - 2k_{F\downarrow}) + \varepsilon_s(q) - \varepsilon_s(k + q - \pi) \\
&\text{for} \quad k \in]2k_{F\downarrow}, \pi[\quad \text{and} \\
&q \in]-k_{F\downarrow}, -(k_\bullet - k_{F\uparrow} + k_{F\downarrow})[\\
&q_1 = k + q - \pi \in]-k_\bullet, -k_{F\downarrow}[\\
&\text{for} \quad \text{spin densities} \quad m \in [\tilde{m}, 1[. \qquad \text{(C2)}
\end{aligned}
$$

The momentum $k_\bullet$ appearing in the above equations satisfies the following equation, expressed in terms of the s band group velocity defined in Eq. (E10):

$$
v_s(k_\bullet) = v_s(k_\bullet - k_{F\uparrow} + k_{F\downarrow}) \quad \text{where} \quad k_\bullet > k_{F\downarrow}. \qquad \text{(C3)}
$$

(The limiting behaviors of the s band group velocity are given in Eqs. (E29), (E30), (E35), (E36), and (E38).)

The energy gap $\Delta^{+-}_{\rm gap}(k)$ is given by $2\mu_B h - W_{s2}$ for the following k values and spin densities:

$$
\begin{aligned}
\Delta^{+-}_{\rm gap}(k) &= 2\mu_B h - W_{s2}, \\
&k = 0 \quad \text{for} \quad m \in]0, 1[, \\
&k = k_{F\uparrow} - k_{F\downarrow} \quad \text{for} \quad m \in [0, 1/3], \\
&k \in]\tilde{k}, k_{F\downarrow}[\quad \text{for} \quad m \in [0, \tilde{m}], \\
&k \in]\tilde{k}, k_{F\downarrow}[\quad \text{for} \quad m \in [\tilde{m}, 1[. \qquad \text{(C4)}
\end{aligned}
$$

Here W_{s2} is the $s2$ band energy width. From the use of results given in Appendix E, one finds that the energy scale $2\mu_B h - W_{s2} \geqslant 0$ in Eq. (C4) has the following limiting values:

$$
\begin{aligned}
&\lim_{u\to 0}(2\mu_B h - W_{s2}) = 0 \quad \text{for} \quad m \in]0, 1[, \\
&\lim_{m\to 0}(2\mu_B h - W_{s2}) = 0 \quad \text{for} \quad u > 0, \\
&\lim_{m\to 1}(2\mu_B h - W_{s2}) = U - (\sqrt{(4t)^2 + (2U)^2} \\
&\qquad - \sqrt{(4t)^2 + U^2}) > 0 \quad \text{for} \quad u > 0 \\
&\qquad \approx U \quad \text{for} \quad u \ll 1 \\
&\qquad \approx \frac{t}{u} = \frac{4t^2}{U} \quad \text{for} \quad u \gg 1. \qquad \text{(C5)}
\end{aligned}
$$

At $k = \pi$ (that in the spectra expressions means the $k \to \pi$ limit) the present gap reads

$$
\Delta^{+-}_{\rm gap}(\pi) = 4\mu_B h \quad \text{for} \quad m \in]0, 1[\text{and} \quad u > 0. \qquad \text{(C6)}
$$

This expression has the following limiting values:

$$
\begin{aligned}
&\lim_{u\to 0} \Delta^{+-}_{\rm gap}(\pi) = 8t \sin\left(\frac{\pi}{2}m\right) \quad \text{for} \quad m \in]0, 1[, \\
&\lim_{m\to 0} \Delta^{+-}_{\rm gap}(\pi) = 0 \quad \text{for} \quad u > 0, \\
&\lim_{m\to 1} \Delta^{+-}_{\rm gap}(\pi) = \sqrt{(4t)^2 + (U)^2} - U > 0 \quad \text{for} \quad u > 0 \\
&\qquad \approx 4t - U \quad \text{for} \quad u \ll 1 \\
&\qquad \approx \frac{2t}{u} = \frac{4t^2}{U} \quad \text{for} \quad u \gg 1. \qquad \text{(C7)}
\end{aligned}
$$

The energy gap $\Delta^{xx}_{\rm gap}(k)$, Eqs. (15) and (16), can be expressed as

$$
\begin{aligned}
\Delta^{xx}_{\rm gap}(k) &= \Delta^{+-}_{\rm gap}(k) \quad \text{for} \quad k \in]0, k^{xx}_{ut}[, \\
\Delta^{xx}_{\rm gap}(k) &= \Delta^{-+}_{\rm gap}(k) \quad \text{for} \quad k \in]k^{xx}_{ut}, \pi[, \qquad \text{(C8)}
\end{aligned}
$$

where $k^{xx}_{ut} > 0$ is the k value at which $\omega^{-+}_{ut}(k^{xx}_{ut}) = \omega^{+-}_{ut}(k^{xx}_{ut})$ and

$$
\Delta^{-+}_{\rm gap}(k) = \Delta^{-+}(k) - \omega^{-+}_{ut}(k). \qquad \text{(C9)}
$$

The gapped lower threshold spectrum $\Delta^{-+}(k)$ in this expression obeys the equality $\Delta^{-+}(k) = \Delta^{+-}(k)$, where $\Delta^{+-}(k)$ is given in Eqs. (13) and (14).

For spin densities $m \in [0, \tilde{m}]$, the energy gap $\Delta^{-+}_{\rm gap}(k)$, Eq. (C9), reads

$$
\begin{aligned}
\Delta^{-+}_{\rm gap}(k) &= \varepsilon_{s2}(k) \quad \text{for} \quad k \in]0, (k_{F\uparrow} - k_{F\downarrow})[, \\
\Delta^{-+}_{\rm gap}(k) &= 4\mu_B h - \varepsilon_s(k_{F\uparrow} - k) + 2\varepsilon_s\left(\frac{\pi - k}{2}\right) \\
&\qquad \text{for} \quad k \in](k_{F\uparrow} - k_{F\downarrow}), \tilde{k}[, \\
\Delta^{-+}_{\rm gap}(k) &= 4\mu_B h - W_{s2} - \varepsilon_s(k_{F\downarrow} - k) + 2\varepsilon_s\left(\frac{\pi - k}{2}\right) \\
&\qquad \text{for} \quad k \in]\tilde{k}, 2k_{F\downarrow}[, \\
\Delta^{-+}_{\rm gap}(k) &= \varepsilon_{s2}(k - 2k_{F\downarrow}) + 2\varepsilon_s\left(\frac{\pi - k}{2}\right) \\
&\qquad \text{for} \quad k \in]2k_{F\downarrow}, \pi[, \qquad \text{(C10)}
\end{aligned}
$$

whereas for $m \in [\tilde{m}, 1[$ it is given by

$$
\begin{aligned}
\Delta^{-+}_{\rm gap}(k) &= \varepsilon_{s2}(k) \quad \text{for} \quad k \in [0, \tilde{k} - \delta\tilde{k}_1], \\
\Delta^{-+}_{\rm gap}(k) &= 4\mu_B h - W_{s2} - \varepsilon_s(k_{F\downarrow} - k) \\
&\qquad \text{for} \quad k \in]\tilde{k}, (k_{F\uparrow} - k_{F\downarrow})[, \\
\Delta^{-+}_{\rm gap}(k) &= 4\mu_B h - W_{s2} - \varepsilon_s(k_{F\downarrow} - k) + 2\varepsilon_s\left(\frac{\pi - k}{2}\right) \\
&\qquad \text{for} \quad k \in](k_{F\uparrow} - k_{F\downarrow}), 2k_{F\downarrow}[, \\
\Delta^{-+}_{\rm gap}(k) &= \varepsilon_{s2}(k - 2k_{F\downarrow}) + 2\varepsilon_s\left(\frac{\pi - k}{2}\right) \\
&\qquad \text{for} \quad k \in]2k_{F\downarrow}, \pi[. \qquad \text{(C11)}
\end{aligned}
$$

At $k = 0, k_{F\uparrow} - k_{F\downarrow}, \pi$ the energy gap $\Delta^{-+}_{\rm gap}(k)$ is given by

$$
\begin{aligned}
\Delta^{-+}_{\rm gap}(0) &= 4\mu_B h - W_{s2} \quad \text{for} \quad m \in]0, 1[, \\
\Delta^{-+}_{\rm gap}(k_{F\uparrow} - k_{F\downarrow}) &= 4\mu_B h \quad \text{for} \quad m \in [0, \tilde{m}], \\
\Delta^{-+}_{\rm gap}(\pi) &= 4\mu_B h - 2W^p_s \\
&\qquad \text{for} \quad m \in]0, 1[. \qquad \text{(C12)}
\end{aligned}
$$

In the k intervals $k \in]\bar{k}_0, \pi[$ and $k \in]\bar{k}_0, \bar{k}_1[$, Eq. (18), for spin densities $m \in]0, \bar{m}_0]$ and $m \in]0, \bar{m}]$, respectively, one has that $\Delta^{xx}_{\rm gap}(k) = \Delta^{-+}_{\rm gap}(k) < 0$. For instance, at $k = \pi$ (and in the $k \to \pi$ limit in the spectra expressions) and for spin densities $m \in]0, 1[$, the energy gap $\Delta^{xx}_{\rm gap}(\pi) = \Delta^{-+}_{\rm gap}(\pi)$ is in the $u \to 0$ limit and for $u \gg 1$

given by

$$\begin{aligned}\Delta^{xx}_{\rm gap}(\pi) &= 12t\left[\sin\left(\frac{\pi}{2}m\right)-\frac{1}{3}\right]\\ &= -4t \quad \text{for} \quad m\to 0\\ &= 0 \quad \text{for} \quad m=\bar{m}_0=\frac{2}{\pi}\arcsin\left(\frac{1}{3}\right)\approx 0.216\\ &= 8t \quad \text{for} \quad m\to 1,\end{aligned} \tag{C13}$$

and

$$\begin{aligned}\Delta^{xx}_{\rm gap}(\pi) &= -\frac{\pi t}{u}=-\frac{4\pi t^2}{U} \quad \text{for} \quad m\to 0\\ &= 0 \quad \text{for} \quad m=\bar{m}_0\approx 0.239\\ &= \frac{4t}{u}=\frac{16t^2}{U} \quad \text{for} \quad m\to 1,\end{aligned} \tag{C14}$$

respectively.

Finally, the energy gap $\Delta^{zz}_{\rm gap}(k)$, Eqs. (15) and (17), is for spin densities $m\in]0,\tilde{m}]$ and $m\in[\tilde{m},1[$ given by

$$\begin{aligned}\Delta^{zz}_{\rm gap}(k) &= \varepsilon_{s2}(k-(k_{F\uparrow}-k_{F\downarrow}))\\ &\quad \text{for} \quad k\in]0,(k_{F\uparrow}-k_{F\downarrow})[\\ &= 4\mu_B h - W_{s2}-\varepsilon_s(k_{F\uparrow}-k)\\ &\quad \text{for} \quad k\in](k_{F\uparrow}-k_{F\downarrow}),(\pi-\tilde{k})[\\ &= 4\mu_B h-\varepsilon_s(k_{F\downarrow}-k)\\ &\quad \text{for} \quad k\in](\pi-\tilde{k}),2k_{F\downarrow}[\\ &= \varepsilon_{s2}(k-\pi) \quad \text{for} \quad k\in]2k_{F\downarrow},\pi[\\ &\quad \text{when} \quad m\in[0,\tilde{m}],\end{aligned} \tag{C15}$$

and

$$\begin{aligned}\Delta^{zz}_{\rm gap}(k) &= \varepsilon_{s2}(k-(k_{F\uparrow}-k_{F\downarrow})) \quad \text{for} \quad k\in(0,(k_{F\uparrow}-k_{F\downarrow}))\\ &= 4\mu_B h - W_{s2}-\varepsilon_s(k_{F\uparrow}-k)\\ &\quad \text{for} \quad k\in](k_{F\uparrow}-k_{F\downarrow}),(\pi-\tilde{k})[\\ &= \varepsilon_{s2}(k-\pi) \quad \text{for} \quad k\in](\pi-\tilde{k}),\pi[\\ &\quad \text{when} \quad m\in[\tilde{m},1[,\end{aligned} \tag{C16}$$

respectively.

APPENDIX D: MATRIX ELEMENTS FUNCTIONALS AND CUSP SINGULARITIES

The ground state at a given spin density m is populated by $N_s=N_\downarrow$ s particles that fill a s band Fermi sea $q\in[-k_{F\downarrow},k_{F\downarrow}]$, where $k_{F\downarrow}$ is given in Eq. (E7) and by a full c band $q\in[-\pi,\pi]$ populated by $N_c=N$ c particles that do not participate in the spin dynamical properties. Within the present thermodynamic limit, we have here ignored corrections of $1/L$ order to these bands momentum limiting values. There are no $s2$ particles in the ground state.

However, the following number and current number deviations under transitions from the ground state to excited energy eigenstates are associated with momentum deviations $1/L$ corrections that must be accounted for even in the thermodynamic limit,

$$\begin{aligned}&\delta N^F_{s,\iota} \quad \text{for} \quad \iota=1,-1 \quad (\text{right, left}) \quad s \text{ particles,}\\ &\delta N^F_s=\sum_{\iota=\pm 1}\delta N^F_{s,\iota} \quad \text{and} \quad \delta J^F_s=\frac{1}{2}\sum_{\iota=\pm 1}\iota\,\delta N^F_{s,\iota},\\ &\delta J_{s2}=\frac{\iota}{2}\delta N_{s2}(q)|_{q=\iota(k_{F\uparrow}-k_{F\downarrow})},\\ &\delta J^F_c=\frac{1}{2}\sum_{\iota=\pm 1}\iota\,\delta N^F_{c,\iota}, \quad \text{where}\\ &\delta N^F_{c,\iota}=-\delta N^F_{c,-\iota}.\end{aligned} \tag{D1}$$

Under the transitions from the ground state to the excited energy eigenstates that span the spin subspaces of the quantum problem studied in this paper, the number of s particles may change. This leads to number deviations δN_s. The specific number deviations $\delta N^F_{s,\iota}$ in Eq. (D1) refer only to changes of the s particles numbers at the left ($\iota=-1$) or right ($\iota=1$)s band Fermi points. The same information is contained in the two Fermi points number deviations $\delta N^F_{s,\iota}$ and in the corresponding Fermi points number deviations $\delta N^F_s=\sum_{\iota=\pm 1}\delta N^F_{s,\iota}$ and current number deviations $\delta J^F_s=\frac{1}{2}\sum_{\iota=\pm 1}\iota\,\delta N^F_{s,\iota}$.

The overall s particles number deviation δN_s can be expressed as

$$\delta N_s=\delta N^F_s+\delta N^{NF}_s. \tag{D2}$$

Here δN^{NF}_s refers to changes in the number of s particles at s band momenta other than at the Fermi points.

For the spin subspaces under consideration, the $s2$ band number deviations only read $\delta N_{s2}=0$ or $\delta N_{s2}=1$. In the latter case, the $s2$ particle can be created at any $s2$ band momentum $q\in[-(k_{F\uparrow}-k_{F\downarrow}),(k_{F\uparrow}-k_{F\downarrow})]$. Only when the $s2$ particle is created at the $s2$ band limiting values $q=-(k_{F\uparrow}-k_{F\downarrow})$ or $q=(k_{F\uparrow}-k_{F\downarrow})$ that process leads to a current number deviation $\delta J_{s2}=-1/2$ and $\delta J_{s2}=1/2$, respectively.

The dynamical structure factors are within the dynamical theory used in the studies of this paper expressed as a sum of s-band spectral function terms $B_s(k,\omega)$ (denoted by $B_Q(k,\omega)$ in Ref. [17]), each associated with a reference energy eigenstate whose s-band Fermi sea changes from occupancy one to zero at the $\iota=+1$ right and $\iota=-1$ left Fermi points $q_{Fs,\iota}=q^0_{Fs,\iota}+\pi\delta N^F_{s,\iota}/L$. Here $q^0_{Fs,\iota}$ refers to the ground state and the $\iota=\pm 1$ number deviations $\delta N^F_{s,\iota}$ are those in Eq. (D1).

In the subspaces of our study, that reference state corresponds to fixed $\iota=\pm 1$ deviations $\delta N^F_{s,\iota}$ and can have no holes within the s-band Fermi sea, one hole at a fixed s-band momentum q, or two holes at fixed s-band momenta q an q', all inside that Fermi sea and away from the Fermi points. In addition, that state can have no s particles or a single s particle at a fixed s-band momentum q outside the s-band Fermi sea and away from its Fermi points. It can also have no $s2$ particles or one $s2$ particle at a fixed momentum $q''\in[-(k_{F\uparrow}-k_{F\downarrow}),(k_{F\uparrow}-k_{F\downarrow})]$.

Besides the reference state, each term $B_s(k,\omega)$ involves sums that run over $m_\iota=1,2,3,...$ elementary particle-hole processes of $\iota=\pm 1$ momenta $\iota 2\pi/L$ around the corresponding Fermi points $q_{Fs,\iota}$ that generate a tower of excited states

upon that reference state. It reads [17]

$$B_s(k,\omega) = \frac{L}{2\pi}\sum_{m_{+1};m_{-1}} A^{(0,0)}\, a(m_{+1},\, m_{-1}) \times \delta\left(\omega - \epsilon - \frac{2\pi}{L}\, v_s \sum_{\iota=\pm 1}(m_\iota + \Phi_\iota^2/4)\right) \times \delta\left(k - \frac{2\pi}{L}\sum_{\iota=\pm 1}\iota\,(m_\iota + \Phi_\iota^2/4)\right). \quad \text{(D3)}$$

Here $v_s = v_s(k_{F\downarrow})$ where $v_s(q)$ is the s-band group velocity, Eq. (E10), and the *lowest peak weight* $A^{(0,0)}$ and the weights $A^{(0,0)}\, a(m_{+1},\, m_{-1})$ refer to the matrix elements square $|\langle\nu|\hat{S}^a_k|GS\rangle|^2$ in Eq. (4) between the ground state and the $m_\iota = 0$ reference excited state and the corresponding $m_\iota > 0$ tower excited states. For the present subspaces, the $\iota = \pm 1$ functionals Φ_ι and the spectrum ϵ in Eq. (D3) have the general form

$$\begin{aligned}\Phi_\iota = {} & \frac{\iota\,\delta N_s^F}{2\xi^1_{ss}} + \xi^1_{ss}\left(\delta J_s^F - 2\delta J_{s2}\right) + \Phi_{s,s}(\iota k_{F\downarrow}, q)\delta N_s(q) \\ & - \Phi_{s,s}(\iota k_{F\downarrow}, q')\delta N_s(q') \\ & + (1 - \delta_{|q''|,(k_{F\uparrow}-k_{F\downarrow})})\,\Phi_{s,s2}(\iota k_{F\downarrow}, q'')\delta N_{s2}(q''), \\ & \text{where} \\ & \epsilon = \varepsilon_s(q)\delta N_s(q) + \varepsilon_s(q')\delta N_s(q') + \varepsilon_{s2}(q'')\delta N_{s2}(q'') \\ \delta N_s(q) = 0, \pm 1\,; \quad & \delta N_s(q') = 0, -1 \quad \text{and} \\ \delta N_{s2}(q'') = 0,\, 1. & \end{aligned} \quad \text{(D4)}$$

Here the deviations δN_s^F, δJ_s^F, and δJ_{s2} are given in Eq. (D1), the $\iota = \pm 1$ phase shifts $\Phi_{s,s}(\iota k_{F\downarrow}, q)$ and $\Phi_{s,s2}(\iota k_{F\downarrow}, q)$ in units of 2π are defined by Eq. (E43), the phase-shift related parameter ξ^1_{ss} is defined in Eq. (E50), and the energy dispersions $\varepsilon_s(q)$ and $\varepsilon_{s2}(q)$ are given in Eqs. (E8) and (E9), respectively.

The relative weights $a(m_{+1},\, m_{-1})$ in Eq. (D3) can be expressed in terms of the γ function as [17]

$$a(m_{+1}, m_{-1}) = \prod_{\iota=\pm 1} a_\iota(m_\iota), \quad \text{where}$$
$$a_\iota(m_\iota) = \frac{\Gamma\left(m_\iota + \Phi_\iota^2\right)}{\Gamma(m_\iota + 1)\,\Gamma\left(\Phi_\iota^2\right)}. \quad \text{(D5)}$$

In the present thermodynamic limit, the matrix elements weights have the following asymptotic behavior [17]:

$$A^{(0,0)} = \left(\frac{1}{L\,B_s}\right)^{-1+\sum_{\iota=\pm 1}\Phi_\iota^2} \prod_{\iota=\pm 1} e^{-f_0 + f_2(2\tilde{\Phi}_\iota)^2 - f_4(2\tilde{\Phi}_\iota)^4},$$
$$a(m_{+1}, m_{-1}) = \prod_{\iota=\pm 1} \frac{\left(m_\iota + \Phi_\iota^2/4\right)^{-1+\Phi_\iota^2}}{\Gamma\left(\Phi_\iota^2\right)}. \quad \text{(D6)}$$

Here $\tilde{\Phi}_\iota = \Phi_\iota - \iota\delta N^F_{s,\iota}$, the constant $0 < B_s \leqslant 1$ and the constants $0 < f_l < 1$ where $l = 0, 2, 4$ depends on u and m and depend only on u, respectively, and are independent of L. Importantly, in that limit the matrix elements square in Eq. (4) then read

$$\begin{aligned}|\langle\nu|\hat{S}^a_k|GS\rangle|^2 = {} & \left(\frac{1}{L\,B_s}\right)^{-1+\sum_{\iota=\pm 1}\Phi_\iota^2} \\ & \times \prod_{\iota=\pm 1} \frac{e^{-f_0 + f_2(2\tilde{\Phi}_\iota)^2 - f_4(2\tilde{\Phi}_\iota)^4}}{\Gamma\left(\Phi_\iota^2\right)}\left(m_\iota + \Phi_\iota^2/4\right)^{-1+\Phi_\iota^2} \\ = {} & \left(\frac{1}{L\,B_s}\right)^{-1+\sum_{\iota=\pm 1}\Phi_\iota^2} \prod_{\iota=\pm 1} \frac{e^{-f_0 + f_2(2\tilde{\Phi}_\iota)^2 - f_4(2\tilde{\Phi}_\iota)^4}}{\Gamma\left(\Phi_\iota^2\right)} \\ & \times\left[\frac{L}{4\pi\, v_s}(\omega - \epsilon + \iota\, v_s\, k)\right]^{-1+\Phi_\iota^2}. \end{aligned} \quad \text{(D7)}$$

Here the equality $m_\iota = \frac{L}{4\pi\, v_s}(\omega - \epsilon + \iota\, v_s\, k) - \Phi_\iota^2/4$ imposed by the δ-functions in Eq. (D3) has been used.

In the general case in which the two $\iota = \pm 1$ functionals Φ_ι are finite the s-particle spectral function $B_s(k,\omega)$, Eq. (D3), can be written as [17]

$$B_s(k,\omega) = \frac{1}{4\pi\, B_s\, v_s}\prod_{\iota=\pm 1}\Theta(\omega - \epsilon + \iota\, v_s\, k) \times \frac{e^{-f_0 + f_2(2\tilde{\Phi}_\iota)^2 - f_4(2\tilde{\Phi}_\iota)^4}}{\Gamma\left(\Phi_\iota^2\right)}\left(\frac{\omega - \epsilon + \iota\, v_s\, k}{4\pi\, B_s\, v_s}\right)^{-1+\Phi_\iota^2}. \quad \text{(D8)}$$

To reach the second expression, which in the thermodynamic limit is exact, Eqs. (D6) and (D7) were used.

The summation of the terms $B_s(k,\omega)$ that lead to expressions for the dynamical structure factors can be performed and reach several kinds of contributions.

When $\delta N_s(q) = \delta N_s(q') = 0$ and $\delta N_{s2}(q'') = 0$ or $\delta N_{s2}(q'') = 1$ at $q'' = 0$ in Eq. (D4), such summations lead to $S^{ab}(k,\omega) \propto (\omega - \omega_0)^{\zeta^{ab}}$ for $(\omega - \omega_0) \neq \pm v_s\,(k - k_0)$, where $\omega_0 = 0$ and $\omega_0 = 4\mu_B\, h$ for $\delta N_{s2}(q'') = 0$ and $\delta N_{s2}(0) = 1$, respectively, $k_0 = 2k_{F\downarrow}\,\delta J_s^F$, and $\zeta^{ab} = -2 + \sum_{\iota=\pm 1}\Phi_\iota^2$. Moreover, they lead to an alternative behavior $B(k,\omega) \propto (\omega - \omega_0 \mp v_s\,(k - k_0))^{\zeta^{ab}_\pm}$ for $(\omega - \omega_0) \approx \pm v_s\,(k - k_0)$ where $\zeta^{ab}_\pm = -1 + \Phi_\pm^2$. These behaviors are only valid in very small (k,ω)-plane regions associated with very small values of ω or $(\omega - 4\mu_B\, h)$ and of $(k - k_0)$ and lead to cusp singularities when $\zeta^{ab} < 0$ and/or $\zeta^{ab}_\pm < 0$ [17].

When *only one* of the deviations $\delta N_s(q)$, $\delta N_s(q')$, and $\delta N_{s2}(q'')$ in Eq. (D4) reads 1 (or -1) the summation of terms $B_s(k,\omega)$ gives the line shape of the dynamical structure factors in the (k,ω)-plane vicinity of branch lines associated with the lower thresholds, Eqs. (20) and (32). The form of the exponents $\zeta^{ab}_\beta(k) = -1 + \sum_{\iota=\pm 1}\Phi_\iota^2$, Eq. (21), in these expressions is fully determined by the square matrix elements, Eq. (D7).

When several of the deviations $\delta N_s(q)$, $\delta N_s(q')$, and $\delta N_{s2}(q'')$ in Eq. (D4) are given by 1 (or -1), the summation of terms $B_s(k,\omega)$ leads to a line shape without cusp singularities.

The results of this paper focus on the line shape near the branch lines associated with the lower thresholds, Eqs. (20) and (32). They rely on the specific form that the functional, Eq. (D4), has for the $s2$, $s2'$ branch lines, $\bar{s}$ branch lines, and $\bar{s}'$ branch lines that are part of the gapped lower thresholds.

In the case of the $s2$ and $s2'$ branch lines, that spectral functional's form is

$$\Phi_\iota(q) = \iota\,\xi^0_{ss}\frac{\delta N^F_s}{2} + \xi^1_{ss}\,\delta J^F_s + \Phi_{s,s2}(\iota k_{F\downarrow}, q)$$
$$= \frac{\iota\,\delta N^F_s}{2\xi^1_{ss}} + \xi^1_{ss}\,\delta J^F_s + \Phi_{s,s2}(\iota k_{F\downarrow}, q)$$
$$\text{for} \quad s2 \quad \text{and} \quad s2' \quad \text{branch lines.} \qquad \text{(D9)}$$

For the excited energy eigenstates that contribute to the singularities at and above the $s2$ and $s2'$ branch lines, the maximum interval of the $s2$ band momentum q in Eq. (D9) is $q \in [0, (k_{F\uparrow} - k_{F\downarrow})[$ or $q \in]-(k_{F\uparrow} - k_{F\downarrow}), 0]$.

For $\bar{s}$ and $\bar{s}'$ branch lines, the spectral functionals are different and have the form

$$\Phi_\iota(q) = \iota\,\xi^0_{ss}\frac{\delta N^F_s}{2} + \frac{\iota\,\xi^0_{ss2}}{2} + \xi^1_{ss}\,\delta J^F_s - \Phi_{s,s}(\iota k_{F\downarrow}, q)$$
$$= \frac{\iota\,\delta N^F_s}{2\xi^1_{ss}} + \frac{\iota\,\xi^0_{ss2}}{2} + \xi^1_{ss}\,\delta J^F_s - \Phi_{s,s}(\iota k_{F\downarrow}, q)$$
$$\text{for} \quad \bar{s} \quad \text{branch lines,} \qquad \text{(D10)}$$

and

$$\Phi_\iota(q) = \iota\,\xi^0_{ss}\frac{\delta N^F_s}{2} + \xi^1_{ss}\left(\delta J^F_s - 2\delta J_{s2}\right) - \Phi_{s,s}(\iota k_{F\downarrow}, q)$$
$$= \frac{\iota\,\delta N^F_s}{2\xi^1_{ss}} + \xi^1_{ss}\left(\delta J^F_s - 2\delta J_{s2}\right) - \Phi_{s,s}(\iota k_{F\downarrow}, q)$$
$$\text{for} \quad \bar{s}' \quad \text{branch lines,} \qquad \text{(D11)}$$

respectively. Here the maximum interval of the s band momentum is $q \in]-k_{F\downarrow}, k_{F\downarrow}[$, $\xi^0_{ss} = 1/\xi^1_{ss}$ at one electron per site and we accounted for the phase shift $\Phi_{s,s2}[\iota k_{F\downarrow}, \pm(k_{F\uparrow} - k_{F\downarrow})]$ reading $\mp\xi^1_{ss}$ [see Eq. (E53)].

The values of the s and $s2$ bands number and current number deviations that in the case of the transverse and longitudinal spin excitations are used in Eqs. (D9)–(D11) are provided in Tables I and II, respectively.

Finally, the momentum dependent exponents that control the line shape near the s branch lines that refer to parts of the lower thresholds of the combined spectra, Eqs. (B1) and (B2) of Appendix B, and of the spectrum, Eq. (B3), involve spectral functionals of general form

$$\Phi_\iota(q) = \frac{\iota\,\delta N^F_s}{2\xi^1_{ss}} + \xi^1_{ss}\,\delta J^F_s \mp \Phi_{s,s}(\iota k_{F\downarrow}, q),$$
$$\text{where}$$
$$- \rightarrow \quad \text{maximum interval} \quad q \in]-k_{F\downarrow}, k_{F\downarrow}[$$
$$+ \rightarrow \quad \text{maximum interval} \quad |q| \in]k_{F\downarrow}, k_{F\uparrow}]$$
$$\text{for} \quad s \quad \text{branch lines.} \qquad \text{(D12)}$$

Here $-$ and $+$ is the phase-shift sign in $\mp\Phi_{s,s}(\iota k_{F\downarrow}, q)$ suitable to s branch lines involving s band hole and s particle creation, respectively, at a q belonging to the given maximum intervals.

The values of the s band number and current number deviations that are used in Eq. (D12) are provided in Table III.

In terms of many-electron processes, the quantum problem studied in this paper is not perturbative. However, in terms of the fractionalized particles that naturally emerge from the rotated-electrons degrees of freedom separation it is perturbative. (In the subspace of the present quantum problem, rotated-electron operators are expressed in terms of corresponding fractionalized particles operators as given in Eq. (80) of Ref. [17].)

The case of most interest for the studies of this paper refers to the gapped excited energy eigenstates populated by one $s2$ particle. For the $+-$, xx, and zz spin dynamical structure factors, such states are behind the (k, ω)-plane spectral weight located above the gapped lower thresholds shown in Figs. 1–6. For such $+-$, zz, and $-+$ factors the s-particle number deviations, $\delta N_s = \delta N^F_s + \delta N^{NF}_s$, Eq. (D2), are given by $\delta N_s = -1$, $\delta N_s = -2$, and $\delta N_s = -3$, respectively. That $\sum_{\iota=\pm1}\Phi^2_\iota(q)$ increases upon increasing $|\delta N_s|$ is behind both a decreasing amount of spectral weight above the corresponding gapped lower threshold and an increase of the momentum-dependent exponents, Eqs. (20) and (32).

APPENDIX E: SOME USEFUL QUANTITIES

In this Appendix a set of quantities needed for our study are defined and corresponding useful limiting behaviors are provided.

The quantum problem described by the 1D Hubbard model with one electron per site in a magnetic field acting in the spin subspaces considered in this paper involves a subset of Bethe ansatz equations.

The equation associated with the s band of the classes of excited energy eigenstates that span such spin subspaces is given by

$$q_j = \frac{2}{L}\sum_{j'=1}^{L}\arctan\left(\frac{\Lambda_s(q_j) - \sin k(q_{j'})}{u}\right)$$
$$- \frac{2}{L}\sum_{j'=1}^{N_\uparrow} N_s(q_{j'})\arctan\left(\frac{\Lambda_s(q_j) - \Lambda_s(q_{j'})}{2u}\right)$$
$$- \frac{2}{L}\sum_{j'=1}^{N_\uparrow - N_\downarrow + N_{s2}} N_{s2}(q_{j'})\left\{\arctan\left(\frac{\Lambda_s(q_j) - \Lambda_{s2}(q_{j'})}{u}\right)\right.$$
$$\left. + \arctan\left(\frac{\Lambda_s(q_j) - \Lambda_{s2}(q_{j'})}{3u}\right)\right\},$$
$$\text{where} \quad j = 1, ..., N_\uparrow. \qquad \text{(E1)}$$

That associated with the $s2$ band reads

$$q_j = \frac{2}{L}\sum_{j'=1}^{L}\arctan\left(\frac{\Lambda_{s2}(q_j) - \sin k(q_{j'})}{2u}\right)$$
$$- \frac{2}{L}\sum_{j'=1}^{N_\uparrow} N_s(q_{j'})\{\arctan\left(\frac{\Lambda_{s2}(q_j) - \Lambda_s(q_{j'})}{u}\right)$$
$$+ \arctan\left(\frac{\Lambda_{s2}(q_j) - \Lambda_s(q_{j'})}{3u}\right)\},$$
$$\text{where} \quad j = 1, ..., N_\uparrow - N_\downarrow + N_{s2}$$
$$\text{and} \quad N_{s2} = 0, 1. \qquad \text{(E2)}$$

In these equations, $N_s(q_{j'}) = 1$ and $N_{s2}(q_{j'}) = 1$ for occupied $q_{j'}$ and $N_s(q_{j'}) = 0$ and $N_{s2}(q_{j'}) = 0$ for unoccupied $q_{j'}$.

For the spin subspaces spanned by excited states populated by $N_s = N_\downarrow - 2s$ particles and one $s2$ particle, the Bethe-ansatz equation, Eq. (E2), does not include the third term that involves the spin rapidity differences $\Lambda_{s2}(q_j) - \Lambda_{s2}(q_{j'})$. Indeed, it vanishes for $q_j = q_{j'}$.

The s band Bethe ansatz rapidity is real and associated with the rapidity function $\Lambda_s(q_j)$. The $s2$ band rapidity function $\Lambda_{s2}(q_j)$ that appears in Eqs. (E1) and (E2) is the real part of the following two Bethe ansatz complex rapidities associated with a spin n-string of length $n = 2$,

$$\Lambda_{s2}(q_j) \pm i\,u. \tag{E3}$$

The rapidity function $k(q_j)$ that appears in the above equations is associated with the c band that in the present subspaces is full with a constant occupancy of N c particles and thus is not dynamically active. That function is defined by the following equation:

$$k(q_j) = q_j - \frac{2}{L}\sum_{j'=1}^{N_\uparrow} N_s(q_{j'}) \arctan\left(\frac{\sin k(q_j) - \Lambda(q_{j'})}{u}\right) - \frac{2}{L}\sum_{j'=1}^{N_\uparrow - N_\downarrow + N_{s2}} N_{s2}(q_{j'}) \arctan\left(\frac{\sin k(q_j) - \Lambda_{s2}(q_{j'})}{2u}\right), \quad \text{where} \quad j = 1, ..., N. \tag{E4}$$

In the above equations,

$$q_j = \frac{2\pi}{L} I_j^\beta \quad \text{for} \quad \beta = c, s, s2, \tag{E5}$$

where the quantum numbers I_j^β are either integers or half-odd integers according to the following boundary conditions [10]:

$$\begin{aligned} I_j^c &= 0, \pm 1, \pm 2, ... \quad \text{for } N_s + N_{s2} \text{ even} \\ &= \pm 1/2, \pm 3/2, \pm 5/2, ... \quad \text{for } N_s + N_{s2} \text{ odd}, \\ I_j^s &= 0, \pm 1, \pm 2, ... \quad \text{for } N_\uparrow \text{ odd} \\ &= \pm 1/2, \pm 3/2, \pm 5/2, ... \quad \text{for } N_\uparrow \text{ even}, \\ I_j^{s2} &= 0, \pm 1, \pm 2, ... \quad \text{for } N_{s2} = 1. \end{aligned} \tag{E6}$$

In the thermodynamic limit, we often use continuous momentum variables q that replace the discrete s and $s2$ bands momenta q_j such that $q_{j+1} - q_j = 2\pi/L$. They read $q \in [-k_{F\uparrow}, k_{F\uparrow}]$ and $q \in [-(k_{F\uparrow} - k_{F\downarrow}), (k_{F\uparrow} - k_{F\downarrow})]$, respectively. In that limit the momenta $k_{F\downarrow}$ and $k_{F\uparrow}$ rare given by

$$k_{F\downarrow} = \frac{\pi}{2}(1 - m); \quad k_{F\uparrow} = \frac{\pi}{2}(1 + m); \quad k_F = \frac{\pi}{2}, \tag{E7}$$

for the spin-density interval, $m \in]0, 1[$ where $k_F = \lim_{m\to 0} k_{F\downarrow} = \lim_{m\to 0} k_{F\uparrow}$.

The energy dispersions $\varepsilon_s(q)$ and $\varepsilon_{s2}(q)$ that appear in the spectra of the spin excitations are defined as follows:

$$\varepsilon_s(q) = \bar{\varepsilon}_s(\Lambda_s(q)) \quad \text{for} \quad q \in [-k_{F\uparrow}, k_{F\uparrow}], \quad \text{where}$$
$$\bar{\varepsilon}_s(\Lambda) = \int_B^\Lambda d\Lambda'\, 2t\, \eta_s(\Lambda'), \tag{E8}$$

and

$$\varepsilon_{s2}(q) = 4\mu_B h + \varepsilon_{s2}^0(q) \quad \text{for} \quad q \in [-(k_{F\uparrow} - k_{F\downarrow}), (k_{F\uparrow} - k_{F\downarrow})], \quad \text{where}$$
$$\varepsilon_{s2}^0(q) = \bar{\varepsilon}_{s2}^0(\Lambda_{s2}(q)) \quad \text{and}$$
$$\bar{\varepsilon}_{s2}^0(\Lambda) = \int_\infty^\Lambda d\Lambda'\, 2t\, \eta_{s2}(\Lambda'), \tag{E9}$$

respectively.

The corresponding s and $s2$ bands group velocities are given by

$$v_s(q) = \frac{\partial \varepsilon_s(q)}{\partial q} \quad \text{and} \quad v_{s2}(q) = \frac{\partial \varepsilon_{s2}(q)}{\partial q}. \tag{E10}$$

The distribution $2t\,\eta_s(\Lambda)$ appearing in Eq. (E8) is coupled to a distribution $2t\,\eta_c(k)$ through the following integral equations:

$$2t\,\eta_c(k) = 2t \sin k + \frac{\cos k}{\pi\, u}\int_{-B}^{B} d\Lambda\, \frac{2t\,\eta_s(\Lambda)}{1 + \left(\frac{\sin k - \Lambda}{u}\right)^2}, \tag{E11}$$

and

$$2t\,\eta_s(\Lambda) = \frac{1}{\pi\, u}\int_{-\pi}^{\pi} dk\, \frac{2t\,\eta_c(k)}{1 + \left(\frac{\Lambda - \sin k}{u}\right)^2} - \frac{1}{2\pi\, u}\int_{-B}^{B} d\Lambda'\, \frac{2t\,\eta_s(\Lambda')}{1 + \left(\frac{\Lambda - \Lambda'}{2u}\right)^2}. \tag{E12}$$

The distribution $2t\,\eta_{s2}(\Lambda)$ appearing in Eq. (E9) is given by

$$2t\,\eta_{s2}(\Lambda) = \frac{1}{2\pi\, u}\int_{-\pi}^{\pi} dk\, \frac{2t\,\eta_c(k)}{1 + \left(\frac{\Lambda - \sin k}{2u}\right)^2} - \frac{1}{\pi\, u}\int_{-B}^{B} d\Lambda'\, \frac{2t\,\eta_s(\Lambda')}{1 + \left(\frac{\Lambda - \Lambda'}{u}\right)^2} - \frac{1}{3\pi\, u}\int_{-B}^{B} d\Lambda'\, \frac{2t\,\eta_s(\Lambda')}{1 + \left(\frac{\Lambda - \Lambda'}{3u}\right)^2}, \tag{E13}$$

where the distributions $2t\,\eta_c(k)$ and $2t\,\eta_s(\Lambda)$ are the solutions of Eqs. (E11) and (E12).

The rapidity distribution function $\Lambda_s(q)$ where $q \in [-k_{F\uparrow}, k_{F\uparrow}]$ in the argument of the auxiliary dispersion $\bar{\varepsilon}_s$ in Eq. (E8) is defined in terms of the s band inverse function $q = q_s(\Lambda)$ where $\Lambda \in [-\infty, \infty]$. The latter is defined by the equation

$$q = q_s(\Lambda) = \frac{1}{\pi}\int_{-\pi}^{\pi} dk\, 2\pi\,\rho(k) \arctan\left(\frac{\Lambda - \sin k}{u}\right) - \frac{1}{\pi}\int_{-B}^{B} d\Lambda'\, 2\pi\,\sigma(\Lambda') \arctan\left(\frac{\Lambda - \Lambda'}{2u}\right) \quad \text{for} \quad \Lambda \in [-\infty, \infty]. \tag{E14}$$

The rapidity distribution function $\Lambda_{s2}(q)$ where $q \in [-(k_{F\uparrow} - k_{F\downarrow}), (k_{F\uparrow} - k_{F\downarrow})]$ is also defined in terms of the $s2$ band inverse function $q = q_{s2}(\Lambda)$ where $\Lambda \in [-\infty, \infty]$ as follows:

$$q = q_{s2}(\Lambda) = \frac{1}{\pi}\int_{-\pi}^{\pi} dk\, 2\pi\,\rho(k) \arctan\left(\frac{\Lambda - \sin k}{2u}\right)$$

$$-\frac{1}{\pi}\int_{-B}^{B} d\Lambda'\, 2\pi\sigma(\Lambda')\arctan\left(\frac{\Lambda-\Lambda'}{u}\right)$$
$$-\frac{1}{\pi}\int_{-B}^{B} d\Lambda'\, 2\pi\sigma(\Lambda')\arctan\left(\frac{\Lambda-\Lambda'}{3u}\right)$$
$$\text{for}\quad \Lambda\in[-\infty,\infty]. \tag{E15}$$

Here the distributions $2\pi\rho(k)$ and $2\pi\sigma(\Lambda)$ are the solution of the following coupled integral equations:

$$2\pi\rho(k)=1+\frac{\cos k}{\pi\, u}\int_{-B}^{B} d\Lambda\,\frac{2\pi\sigma(\Lambda)}{1+\left(\frac{\sin k-\Lambda}{u}\right)^2}, \tag{E16}$$

and

$$2\pi\sigma(\Lambda)=\frac{1}{\pi\, u}\int_{-\pi}^{\pi} dk\,\frac{2\pi\rho(k)}{1+\left(\frac{\Lambda-\sin k}{u}\right)^2}$$
$$-\frac{1}{2\pi\, u}\int_{-B}^{B} d\Lambda'\,\frac{2\pi\sigma(\Lambda')}{1+\left(\frac{\Lambda-\Lambda'}{2u}\right)^2}. \tag{E17}$$

Such distributions obey the sum rules

$$\frac{1}{\pi}\int_{-\pi}^{\pi} dk\, 2\pi\rho(k)=2\quad\text{and}\quad\frac{1}{\pi}\int_{-B}^{B} d\Lambda\, 2\pi\sigma(\Lambda)=(1-m). \tag{E18}$$

The parameter $B=\Lambda_s(k_{F\downarrow})$ appearing in the above equations has the limiting behaviors

$$B=\Lambda_s(k_{F\downarrow}),\quad\text{with}$$
$$\lim_{m\to 0} B=\infty\quad\text{and}\quad\lim_{m\to 1} B=0. \tag{E19}$$

Other $\Lambda_s(q)$ and $\Lambda_{s2}(q)$ values are

$$\Lambda_s(0)=0\quad\text{and}\quad\Lambda_s(\pm k_{F\uparrow})=\pm\infty,$$
$$\Lambda_{s2}(0)=0\quad\text{and}\quad\Lambda_{s2}[\pm(k_{F\uparrow}-k_{F\downarrow})]=\pm\infty. \tag{E20}$$

The s band dispersion,

$$\varepsilon_s^0(q)=\bar{\varepsilon}_s^0[\Lambda_s(q)],\quad\text{where}$$
$$\bar{\varepsilon}_s^0(\Lambda)=\int_{\infty}^{\Lambda} d\Lambda'\, 2t\,\eta_s(\Lambda'), \tag{E21}$$

whose zero-energy level is for $0<m<1$ shifted relative to that of $\varepsilon_s(q)$ defines the spin density curve, as given in Eq. (3).

In the $m\to 0$ limit, the $s2$ band does not exist in the ground state. In that limit, it reduces to $q=0$ with $\varepsilon_{s2}(0)=0$ when $N_{s2}=1$. In the same limit, the s band energy dispersion can be written as,

$$\varepsilon_s(q)=\bar{\varepsilon}_s[\Lambda_s(q)]\quad\text{for}\quad q\in\left[-\frac{\pi}{2},\frac{\pi}{2}\right],\quad\text{where}$$
$$\bar{\varepsilon}_s(\Lambda)=-2t\int_0^{\infty} d\omega\,\frac{\cos(\omega\,\Lambda)}{\omega\cosh(\omega\, u)}J_1(\omega), \tag{E22}$$

and the rapidity function $\Lambda_s(q)$ is defined in terms of its inverse function $q=q_s(\Lambda)$, where $\Lambda\in[-\infty,\infty]$ as

$$q=q_s(\Lambda)=\int_0^{\infty} d\omega\,\frac{\sin(\omega\,\Lambda)}{\omega\cosh(\omega\, u)}J_0(\omega). \tag{E23}$$

In these equations $J_0(\omega)$ and $J_1(\omega)$ are Bessel functions.

The s and $s2$ band energy dispersions $\varepsilon_s(q)$ and $\varepsilon_{s2}(q)$, Eqs. (E8) and (E9), respectively, have limiting values,

$$\varepsilon_s(0)=-W_s^p,\quad\varepsilon_s(\pm k_{F\downarrow})=0,$$
$$\varepsilon_s(\pm k_{F\uparrow})=W_s^h=2\mu_B\, h,$$
$$\varepsilon_{s2}(0)=4\mu_B\, h-W_{s2},$$
$$\varepsilon_{s2}[\pm(k_{F\uparrow}-k_{F\downarrow})]=4\mu_B\, h, \tag{E24}$$

where

$$\lim_{u\to 0} W_s^p=2t\left[1-\sin\left(\frac{\pi}{2}\,m\right)\right],$$
$$\lim_{u\to 0} W_s^h=\lim_{u\to 0} 2\mu_B\, h=4t\sin\left(\frac{\pi}{2}\,m\right),$$
$$\lim_{u\to 0} W_s=W_s^p+W_s^h=2t\left[1+\sin\left(\frac{\pi}{2}\,m\right)\right],$$
$$\lim_{u\to\infty} W_s=W_s^p+W_s^h=0,$$
$$\lim_{u\to 0} W_{s2}=4t\sin\left(\frac{\pi}{2}\,m\right),$$
$$\lim_{u\to\infty} W_{s2}=0, \tag{E25}$$

for spin densities $m\in]0,1[$ and

$$\lim_{m\to 1} W_s=W_s^h=2\mu_B\, h_c=\sqrt{(4t)^2+U^2}-U,$$
$$\lim_{m\to 1} W_{s2}=\sqrt{(4t)^2+(2U)^2}-2U, \tag{E26}$$

for all $u>0$ values.

In the $u\to 0$ limit, the s band energy dispersions have for spin densities $m\in]0,1[$ the following expressions:

$$\varepsilon_s(q)=\varepsilon_s^0(q)-\varepsilon_s^0(k_{F\downarrow})=-2t(\cos q-\cos k_{F\downarrow})$$
$$=2t\sin\left(\frac{\pi}{2}\,m\right)-2t\cos q,$$
$$\varepsilon_s^0(q)=-2t(\cos q-\cos k_{F\uparrow})$$
$$=-2t\sin\left(\frac{\pi}{2}\,m\right)-2t\cos q$$
$$\text{for}\quad q\in[-k_{F\uparrow},k_{F\uparrow}]. \tag{E27}$$

The $s2$ band energy dispersions have for $u\to 0$ and spin densities $0<m<1$ the following expressions:

$$\varepsilon_{s2}(q)=4\mu_B\, h-2t[\cos(|q|+k_{F\downarrow})-\cos k_{F\uparrow}]$$
$$=8t\sin\left(\frac{\pi}{2}\,m\right)-2t\left[\cos(|q|+k_{F\downarrow})+\sin\left(\frac{\pi}{2}\,m\right)\right]$$
$$=6t\sin\left(\frac{\pi}{2}\,m\right)-2t\cos(|q|+k_{F\downarrow}),$$
$$\varepsilon_{s2}^0(q)=-2t(\cos(|q|+k_{F\downarrow})-\cos k_{F\uparrow})$$
$$=-2t\sin\left(\frac{\pi}{2}\,m\right)-2t\cos(|q|+k_{F\downarrow})$$
$$\text{for}\quad q\in[-(k_{F\uparrow}-k_{F\downarrow}),(k_{F\uparrow}-k_{F\downarrow})]. \tag{E28}$$

In the $u \to 0$ limit, the corresponding group velocities, Eq. (E10), read

$$\begin{aligned} v_s(q) &= 2t \sin q \quad \text{for} \quad q \in [-k_{F\uparrow}, k_{F\uparrow}], \\ v_{s2}(q) &= \text{sgn}\{q\}\, 2t \sin(|q| + k_{F\downarrow}) \quad \text{for} \\ &\quad q \in [-(k_{F\uparrow} - k_{F\downarrow}), (k_{F\uparrow} - k_{F\downarrow})], \end{aligned} \tag{E29}$$

respectively, so that

$$v_s(k_{F\downarrow}) = v_{s2}(k_{F\uparrow} - k_{F\downarrow}) = 2t \cos\left(\frac{\pi}{2} m\right). \tag{E30}$$

In the $m \to 1$ spin density limit, the s band energy dispersions are for all $u > 0$ values given by the following integrals:

$$\begin{aligned} \varepsilon_s(q) &= -\frac{2t}{\pi} \int_{-\pi}^{\pi} dk \sin k \arctan\left(\frac{\sin k - \Lambda_s(q)}{u}\right) \\ &\quad + \sqrt{(4t)^2 + U^2} - U \\ \varepsilon_s^0(q) &= -\frac{2t}{\pi} \int_{-\pi}^{\pi} dk \sin k \arctan\left(\frac{\sin k - \Lambda_s(q)}{u}\right) \\ &\quad \text{for} \quad q \in [-\pi, \pi], \end{aligned} \tag{E31}$$

where the rapidity function $\Lambda_s(q)$ is defined by its inverse function as

$$q = q_s(\Lambda) = \frac{1}{\pi} \int_{-\pi}^{\pi} dk \arctan\left(\frac{\Lambda - \sin k}{u}\right). \tag{E32}$$

In the same $m \to 1$ limit, the $s2$ band energy dispersions are for all $u > 0$ values given by the integrals

$$\begin{aligned} \varepsilon_{s2}(q) &= -\frac{2t}{\pi} \int_{-\pi}^{\pi} dk \sin k \arctan\left(\frac{\sin k - \Lambda_s(q)}{2u}\right) \\ &\quad + \sqrt{(8t)^2 + (2U)^2} - 2U, \\ \varepsilon_{s2}^0(q) &= -\frac{2t}{\pi} \int_{-\pi}^{\pi} dk \sin k \arctan\left(\frac{\sin k - \Lambda_{s2}(q)}{2u}\right) \\ &\quad \text{for} \quad q \in [-\pi, \pi], \end{aligned} \tag{E33}$$

where the rapidity function $\Lambda_{s2}(q)$ is again defined by its inverse function as

$$q = q_{s2}(\Lambda) = \frac{1}{\pi} \int_{-\pi}^{\pi} dk \arctan\left(\frac{\Lambda - \sin k}{2u}\right). \tag{E34}$$

For $u \gg 1$, one can derive analytical expressions for the s and $s2$ band energy dispersions and the corresponding group velocities, Eq. (E10), for spin densities m in the limits $m \to 0$ and $(1 - m) \ll 1$. For $u \gg 1$ and in the $m \to 0$ limit, the behaviors of the s band energy dispersions and group velocity are

$$\begin{aligned} \varepsilon_s(q) &= -\frac{\pi t}{2u} \cos q \quad \text{and} \quad \varepsilon_s^0(q) = \varepsilon_s(q), \\ v_s(q) &= \frac{\pi t}{2u} \sin q \\ &\quad \text{for} \quad q \in [-\pi/2, \pi/2] \quad \text{and} \quad m \to 0. \end{aligned} \tag{E35}$$

For $u \gg 1$ and $(1 - m) \ll 1$, the s band energy dispersions and group velocity, Eq. (E10), behave as

$$\begin{aligned} \varepsilon_s(q) &= -\frac{t}{u}(\cos q - 1) + \frac{t}{u}(1 - m) \sin q \\ &\quad \times \arctan\left(\frac{1}{2} \tan\left(\frac{q}{2}\right)\right), \\ \varepsilon_s^0(q) &= -\frac{2t}{u} + \varepsilon_s(q) \\ &= -\frac{t}{u}(\cos q + 1) \\ &\quad + \frac{t}{u}(1 - m) \sin q \arctan\left(\frac{1}{2} \tan\left(\frac{q}{2}\right)\right), \\ v_s(q) &= \frac{t}{u} \sin q + \frac{t}{u}(1 - m) \frac{\sin q}{1 + 3\cos^2\left(\frac{q}{2}\right)} \\ &\quad + \frac{t}{u}(1 - m) \cos q \arctan\left(\frac{1}{2} \tan\left(\frac{q}{2}\right)\right) \\ &\quad \text{for} \quad q \in \left[-\frac{\pi}{2}(1 + m), \frac{\pi}{2}(1 + m)\right] \\ &\quad \text{and} \quad (1 - m) \ll 1. \end{aligned} \tag{E36}$$

For $u \gg 1$ and in the $m \to 0$ limit, the $s2$ band energy dispersion and group velocity vanish, consistent with the momentum and energy widths of the $s2$ band vanishing. For $u \gg 1$ and $(1 - m) \ll 1$, they behave as

$$\begin{aligned} \varepsilon_{s2}(q) &= \frac{4t}{u} - \frac{t}{2u}(1 + \cos q) \\ &\quad + \frac{t}{2u}(1 - m) \sin q \Bigg\{ \arctan\left(2 \tan\left(\frac{q}{2}\right)\right) \\ &\quad + \arctan\left(\frac{2}{3} \tan\left(\frac{q}{2}\right)\right) \Bigg\}, \\ \varepsilon_{s2}^0(q) &= \varepsilon_{s2}(q) - \frac{4t}{u}, \\ v_{s2}(q) &= \frac{t}{2u} \sin q + \frac{t}{2u}(1 - m) \sin q \Bigg\{ \frac{1}{1 + 3\sin^2\left(\frac{q}{2}\right)} \\ &\quad + \frac{3}{4 + 5\cos^2\left(\frac{q}{2}\right)} \Bigg\} \\ &\quad + \frac{t}{2u}(1 - m) \cos q \Bigg\{ \arctan\left(2 \tan\left(\frac{q}{2}\right)\right) \\ &\quad + \arctan\left(\frac{2}{3} \tan\left(\frac{q}{2}\right)\right) \Bigg\} \quad \text{for} \\ &\quad q \in [-\pi m, \pi m] \quad \text{and} \quad (1 - m) \ll 1. \end{aligned} \tag{E37}$$

For $u \gg 1$ and $(1 - m) \ll 1$, the following equality holds:

$$v_s(k_{F\downarrow}) = v_{s2}(k_{F\uparrow} - k_{F\downarrow}) = \frac{\pi t}{2u}(1 - m). \tag{E38}$$

The phase shifts play an important role in the spin dynamical properties. They are given by

$$\begin{aligned} 2\pi\, \Phi_{s,\beta}(q, q') &= 2\pi\, \bar{\Phi}_{s,\beta}(r, r'), \\ \text{where} \quad r &= \frac{\Lambda_s(q)}{u} \quad \text{and} \quad r' = \frac{\Lambda_\beta(q')}{u}. \end{aligned} \tag{E39}$$

In the case of the excited energy eigenstates involved in the studies of this paper, $\beta = s, s2$. The rapidity phase shifts $2\pi\,\bar{\Phi}_{s,\beta}(r,r')$ on the right-hand side of the above equality are functions of the rapidity-related variables $r = \Lambda/u$ of the s and $s2$ branches. They are defined by the following integral equations:

$$\bar{\Phi}_{s,s}(r,r') = \frac{1}{\pi}\arctan\left(\frac{r-r'}{2}\right) + \int_{-B/u}^{B/u} dr''\, G(r,r'')\,\bar{\Phi}_{s,s}(r'',r'), \quad \text{(E40)}$$

and

$$\bar{\Phi}_{s,s2}(r,r') = \frac{1}{\pi}\arctan(r-r') + \frac{1}{\pi}\arctan\left(\frac{r-r'}{3}\right) + \int_{-B/u}^{B/u} dr''\, G(r,r'')\,\bar{\Phi}_{s,s2}(r'',r'). \quad \text{(E41)}$$

The kernel $G(r,r')$ in Eqs. (E40) and (E41) is for $u > 0$ given by

$$G(r,r') = -\frac{1}{2\pi}\left\{\frac{1}{1+[(r-r')/2]^2}\right\}. \quad \text{(E42)}$$

The phase shifts that appear in the expressions of the branch line exponents read

$$\Phi_{s,s}(\iota k_{F\downarrow},q) = \bar{\Phi}_{s,s}\left(\iota\frac{B}{u},\frac{\Lambda_s(q)}{u}\right)$$
$$\Phi_{s,s2}(\iota k_{F\downarrow},q) = \bar{\Phi}_{s,s2}\left(\iota\frac{B}{u},\frac{\Lambda_{s2}(q)}{u}\right), \quad \text{where} \quad \iota = \pm 1. \quad \text{(E43)}$$

In the $m \to 0$ limit, the phase shift $\Phi_{s,s}(q,q')$ in units of 2π can be written as

$$\Phi_{s,s}(q,q') = \bar{\Phi}_{s,s}(\Lambda_s(q),\Lambda(q')), \quad \text{where}$$
$$\bar{\Phi}_{s,s}(\Lambda,\Lambda') = \frac{1}{\pi}\int_0^\infty d\omega\,\frac{\sin(\omega\,(\Lambda-\Lambda'))}{\omega(1+e^{2\omega u})}, \quad \text{(E44)}$$

and the rapidity function $\Lambda_s(q)$ is defined in terms of its inverse function in Eq. (E23). The integral in Eq. (E44) can be solved for $u > 0$, with the result

$$\bar{\Phi}_{s,s}(\Lambda,\Lambda') = \frac{i}{2\pi}\,\ln\left\{\frac{\Gamma\left(\frac{1}{2}+i\frac{(\Lambda-\Lambda')}{4u}\right)\Gamma\left(1-i\frac{(\Lambda-\Lambda')}{4u}\right)}{\Gamma\left(\frac{1}{2}-i\frac{(\Lambda-\Lambda')}{4u}\right)\Gamma\left(1+i\frac{(\Lambda-\Lambda')}{4u}\right)}\right\}$$
$$\text{for} \quad \Lambda \neq \iota\infty \quad \text{where} \quad \iota = \pm 1$$
$$= \frac{\iota}{2\sqrt{2}} \quad \text{for} \quad \Lambda = \iota\infty \quad \text{and} \quad \Lambda' \neq \iota\infty$$
$$= \iota\left(\frac{3}{2\sqrt{2}}-1\right) \quad \text{for} \quad \Lambda = \Lambda' = \iota\infty, \quad \text{(E45)}$$

where $\Gamma(x)$ is the usual γ function.

The use of Eq. (E45) leads to the following expressions for the phase shift $\Phi_{s,s}(\iota k_F,q) = \lim_{m\to 0}\Phi_{s,s}(\iota k_{F\downarrow},q)$ in the $m \to 0$ limit for $u > 0$,

$$\lim_{m\to 0}\Phi_{s,s}(\iota k_{F\downarrow},q) = \Phi_{s,s}(\iota\pi/2,q)$$
$$= \frac{\iota}{2\sqrt{2}} \quad \text{for} \quad q \neq \iota k_{F\downarrow}$$
$$= \iota\left(\frac{3}{2\sqrt{2}}-1\right) \quad \text{for} \quad q = \iota k_{F\downarrow}$$
$$\text{for} \quad u > 0 \quad \text{where} \quad \iota = \pm 1. \quad \text{(E46)}$$

In the $m \to 0$ limit and for $u > 0$, the phase shift $\Phi_{s,s2}(\iota k_F,0) = \lim_{m\to 0}\Phi_{s,s2}(\iota k_{F\downarrow},q)$ has in units of 2π the following value:

$$\Phi_{s,s2}(\iota k_F,0) = \frac{\iota}{\sqrt{2}}. \quad \text{(E47)}$$

For $u \gg 1$ and in the $m \to 1$ limit, the phase shifts $\Phi_{s,s}(\iota k_{F\downarrow},q)$ and $\Phi_{s,s2}(\iota k_{F\downarrow},q)$ behave as

$$\lim_{m\to 1}\Phi_{s,s}(\iota k_{F\downarrow},q) = \Phi_{s,s}(0,q) = -\frac{1}{\pi}\arctan\left(\frac{1}{2}\tan\left(\frac{q}{2}\right)\right),$$
$$\lim_{m\to 1}\Phi_{s,s2}(\iota k_{F\downarrow},q) = \Phi_{s,s2}(0,q) = -\frac{1}{\pi}\arctan\left(2\tan\left(\frac{q}{2}\right)\right) - \frac{1}{\pi}\arctan\left(\frac{2}{3}\tan\left(\frac{q}{2}\right)\right). \quad \text{(E48)}$$

The s band Fermi-points phase-shift parameters ξ^j_{ss}, where $j = 0, 1$ are given by

$$\xi^j_{ss} = 1 + \sum_{\iota=\pm 1}(\iota)^j\,\Phi_{s,s}(k_{F\downarrow},\iota k_{F\downarrow}). \quad \text{(E49)}$$

They play an important role in both the spectral and static properties. For one electron per site, the equality $\xi^0_{ss} = 1/\xi^1_{ss}$ holds, so that only one of these two parameters is needed, for instance ξ^1_{ss}, which is a diagonal entry of the 1D Hubbard model dressed charge matrix [37,38].

From manipulations of the phase-shift integral equation, Eq. (E40), one finds that the latter parameter is given by

$$\xi^1_{ss} = \xi^1_{ss}(B/u). \quad \text{(E50)}$$

The function $\xi^1_{ss}(r)$ on the right-hand side of this equation at $r = B/u$ is the solution of the integral equation

$$\xi^1_{ss}(r) = 1 + \int_{-B/u}^{B/u} dr'\, G(r,r')\,\xi^1_{ss}(r'). \quad \text{(E51)}$$

The kernel $G(r,r')$ appearing here is given in Eq. (E42).

For $u > 0$, the parameter ξ^1_{ss} continuously increases from $\xi^1_{ss} = 1/\sqrt{2}$ as $m \to 0$ to $\xi^1_{ss} = 1$ for $m \to 1$, so that its limiting values are

$$\lim_{m\to 0}\xi^1_{ss} = \frac{1}{\sqrt{2}} \quad \text{and} \quad \lim_{m\to 1}\xi^1_{ss} = 1. \quad \text{(E52)}$$

The parameter ξ^1_{ss} is also related to the phase shift $\Phi_{s,s2}(k_{F\downarrow},q)$ in Eq. (E43) as follows:

$$\xi^1_{ss} = -\Phi_{s,s2}(\pm k_{F\downarrow},(k_{F\uparrow}-k_{F\downarrow})) = \Phi_{s,s2}(\pm k_{F\downarrow},-(k_{F\uparrow}-k_{F\downarrow})). \quad \text{(E53)}$$

Finally, the parameter ξ^0_{ss2} that also appears in the momentum dependent exponents is given by

$$\xi^0_{ss2} = 2\Phi_{s,s2}(k_{F\downarrow}, 0), \tag{E54}$$

where the phase shift $\Phi_{s,s2}(k_{F\downarrow}, q)$ is defined in Eq. (E43). At $q = 0$ it is such that $\Phi_{s,s2}(\iota k_{F\downarrow}, 0) = \iota\, \Phi_{s,s2}(k_{F\downarrow}, 0)$. This justifies why $\iota\, \xi^0_{ss2} = 2\Phi_{s,s2}(\iota k_{F\downarrow}, 0) = \iota\, 2\Phi_{s,s2}(k_{F\downarrow}, 0)$ for $\iota = \pm 1$.

The parameter ξ^0_{ss2} continuously decreases from $\xi^0_{ss2} = \sqrt{2}$ as $m \to 0$ to $\xi^0_{ss2} = 0$ for $m \to 1$. Consitent, it follows from Eqs. (E47) and (E48) that

$$\lim_{m\to 0} \xi^0_{ss2} = \sqrt{2} \quad \text{and} \quad \lim_{m\to 1} \xi^0_{ss2} = 0. \tag{E55}$$

[1] Z. Wang, M. Schmidt, A. Loidl, J. Wu, H. Zou, W. Yang, C. Dong, Y. Kohama, K. Kindo, D. I. Gorbunov, S. Niesen, O. Breunig, J. Engelmayer, and T. Lorenz, Phys. Rev. Lett. **123**, 067202 (2019).

[2] A. K. Bera, J. Wu, W. Yang, R. Bewley, M. Boehm, J. Xu, M. Bartkowiak, O. Prokhnenko, B. Klemke, A. T. M. N. Islam, J. M. Law, Z. Wang, and B. Lake, Nat. Phys. **16**, 625 (2020).

[3] Z. Wang, J. Wu, W. Yang, A. K. Bera, D. Kamenskyi, A. T. M. N. Islam, S. Xu, J. M. Law, B. Lake, C. Wu, and A. Loidl, Nature **554**, 219 (2018).

[4] M. Kohno, Phys. Rev. Lett. **102**, 037203 (2009).

[5] M. B. Stone, D. H. Reich, C. Broholm, K. Lefmann, C. Rischel, C. P. Landee, and M. M. Turnbull, Phys. Rev. Lett. **91**, 037205 (2003).

[6] I. U. Heilmann, G. Shirane, Y. Endoh, R. J. Birgeneau, and S. L. Holt, Phys. Rev. B **18**, 3530 (1978).

[7] E. H. Lieb and F. Y. Wu, Phys. Rev. Lett. **20**, 1445 (1968).

[8] E. H. Lieb and F. Y. Wu, Physica A **321**, 1 (2003).

[9] M. J. Martins and P. B. Ramos, Nucl. Phys. B **522**, 413 (1998).

[10] M. Takahashi, Prog. Theor. Phys. **47**, 69 (1972).

[11] J. M. P. Carmelo and P. D. Sacramento, Phys. Rep. **749**, 1 (2018).

[12] J. M. P. Carmelo, S. Nemati, and T. Prosen, Nucl. Phys. B **930**, 418 (2018).

[13] J. M. P. Carmelo and T. Čadež, Nucl. Phys. B **914**, 461 (2017).

[14] H. Benthien and E. Jeckelmann, Phys. Rev. B **75**, 205128 (2007).

[15] M. J. Bhaseen, F. H. L. Essler, and A. Grage, Phys. Rev. B **71**, 020405(R) (2005).

[16] F. H. L. Eßler and V. E. Korepin, Phys. Rev. B **59**, 1734 (1999).

[17] J. M. P. Carmelo and T. Čadež, Nucl. Phys. B **904**, 39 (2016); **961**, 115233 (2020), Corrigendum.

[18] J. M. P. Carmelo, P. Horsch, D. K. Campbell, and A. H. Castro Neto, Phys. Rev. B **48**, 4200(R) (1993).

[19] J. M. P. Carmelo, K. Penc, and D. Bozi, Nucl. Phys. B **725**, 421 (2005); **737**, 351(E) (2006).

[20] J. M. P. Carmelo, D. Bozi, and K. Penc, J. Phys.: Condens. Matter **20**, 415103 (2008).

[21] A. Imambekov and L. I. Glazman, Science **323**, 228 (2009).

[22] A. Imambekov, T. L. Schmidt, and L. I. Glazman, Rev. Mod. Phys. **84**, 1253 (2012).

[23] J. M. P. Carmelo and P. D. Sacramento, Ann. Phys. **369**, 102 (2016).

[24] K. Penc, K. Hallberg, F. Mila, and H. Shiba, Phys. Rev. Lett. **77**, 1390 (1996).

[25] K. Penc, K. Hallberg, F. Mila, and H. Shiba, Phys. Rev. B **55**, 15475 (1997).

[26] S. Sorella and A. Parola, Phys. Rev. Lett. **76**, 4604 (1996).

[27] S. Sorella and A. Parola, Phys. Rev. B **57**, 6444 (1998).

[28] G. Müller, H. Thomas, H. Beck, and J. C. Bonner, Phys. Rev. B **24**, 1429 (1981).

[29] S.-J. Caux and R. Hagemans, J. Stat. Mech. (2006) P12013.

[30] J.-S. Caux and J. M. Maillet, Phys. Rev. Lett. **95**, 077201 (2005).

[31] J. Carmelo and D. Baeriswyl, Phys. Rev. B **37**, 7541 (1988).

[32] D. Baeriswyl, J. Carmelo, and K. Maki, Synth. Met. **21**, 271 (1987).

[33] M. Raczkowski, F. F. Assaad, and L. Pollet, Phys. Rev. B **91**, 045137 (2015).

[34] S. R. White and A. E. Feiguin, Phys. Rev. Lett. **93**, 076401 (2004).

[35] U. Schollwöck, Ann. Phys. **326**, 96 (2011).

[36] A. Moreno, A. Muramatsu, and J. M. P. Carmelo, Phys. Rev. B **87**, 075101 (2013).

[37] H. Frahm and V. E. Korepin, Phys. Rev. B **42**, 10553 (1990).

[38] J. M. P. Carmelo and A. H. Castro Neto, Phys. Rev. Lett. **70**, 1904 (1993).